AD-A147 548 INLET PROCESSES AT EEL POND FALMOUTH MASSACHUSETTS(U) 1/2
COASTAL ENGINEERING RESEARCH CENTER VICKSBURG MS
A E DEWALL ET AL. OCT 84 CERC-MP-84-9
UNCLASSIFIED F/G 8/3 NL

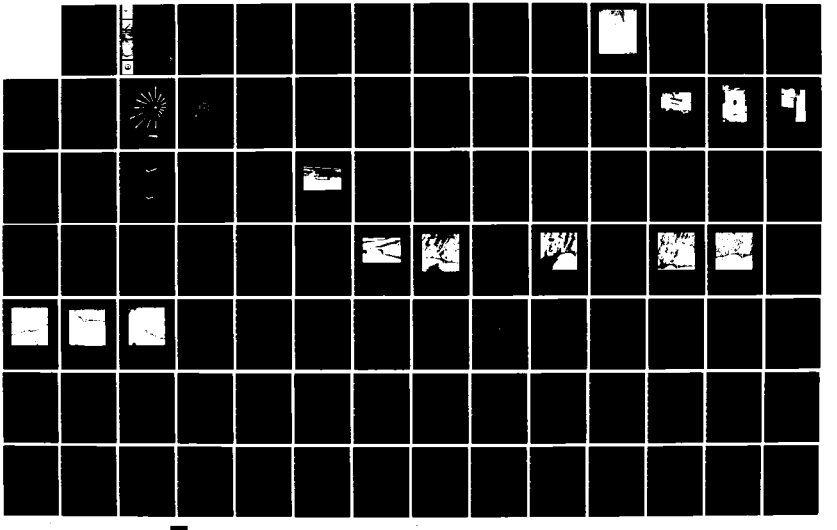

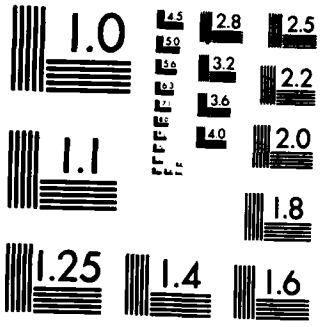
1.0
1.1
1.25
1.4
1.6
1.8
2.0
2.2
2.5
2.8
3.2
3.6
4.0
4.5
5.0
5.6
6.3

US Army Corps of Engineers

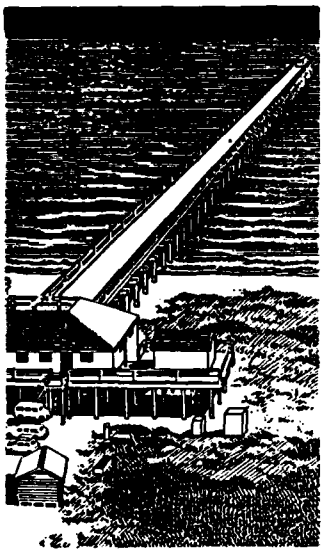

MISCELLANEOUS PAPER CERC-84-9

INLET PROCESSES AT EEL POND FALMOUTH, MASSACHUSETTS

by

Allan E. DeWall, Joan A. Tarnowski,
Bruce Danielson, Lee L. Weishar

Coastal Engineering Research Center

DEPARTMENT OF THE ARMY
Waterways Experiment Station, Corps of Engineers
PO Box 631
Vicksburg, Mississippi 39180-0631

October 1984
Final Report

Prepared for

US Army Engineer Division, New England
424 Trapelo Road
Waltham, Massachusetts 02154

Unclassified

SECURITY CLASSIFICATION OF THIS PAGE (When Data Entered)

REPORT DOCUMENTATION PAGE		READ INSTRUCTIONS BEFORE COMPLETING FORM
1. REPORT NUMBER Miscellaneous Paper CERC-84-9	2. GOVT ACCESSION NO. AD-A147548	3. RECIPIENT'S CATALOG NUMBER
4. TITLE (and Subtitle) INLET PROCESSES AT EEL POND, FALMOUTH, MASSACHUSETTS		5. TYPE OF REPORT & PERIOD COVERED Final report 6. PERFORMING ORG. REPORT NUMBER
7. AUTHOR(s) Allan E. DeWall, Joan A. Tarnowski, Bruce Danielson, Lee L. Weishar		8. CONTRACT OR GRANT NUMBER(s)
9. PERFORMING ORGANIZATION NAME AND ADDRESS US Army Engineer Waterways Experiment Station Coastal Engineering Research Center PO Box 631, Vicksburg, Mississippi 39180-0631		10. PROGRAM ELEMENT, PROJECT, TASK AREA & WORK UNIT NUMBERS
11. CONTROLLING OFFICE NAME AND ADDRESS US Army Engineer Division, New England 424 Trapelo Road Waltham, Massachusetts 02154		12. REPORT DATE October 1984 13. NUMBER OF PAGES 124
14. MONITORING AGENCY NAME & ADDRESS(if different from Controlling Office)		15. SECURITY CLASS. (of this report) Unclassified 15a. DECLASSIFICATION/DOWNGRADING SCHEDULE

16. DISTRIBUTION STATEMENT (of this Report)

Approved for public release; distribution unlimited.

17. DISTRIBUTION STATEMENT (of the abstract entered in Block 20, if different from Report)

18. SUPPLEMENTARY NOTES

Available from National Technical Information Service, 5285 Port Royal Road, Springfield, Virginia 22161.

19. KEY WORDS (Continue on reverse side if necessary and identify by block number)

Inlets--Massachusetts (LC)
Hydraulic measurements (LC)
Sediment transport--Eel Pond (Falmouth, Mass.) (LC)
Eel Pond (Falmouth, Mass.) (LC)
Harbors--Massachusetts (LC)

20. ABSTRACT (Continue on reverse side if necessary and identify by block number)

This report describes a combined office and field study designed to define the causes of a shoaling problem at the entrance to a small craft harbor. The office study consisted of an evaluation of the history of inlet development and an analysis of available wind, current, and wave data. In addition, a one-dimensional numerical model was used to predict stability with varying inlet geometry and the addition of stabilizing structures. Field measurements used in model calibration included water level, current velocity, beach and

(Continued)

DD FORM 1 JAN 73 1473 EDITION OF 1 NOV 65 IS OBSOLETE

Unclassified

SECURITY CLASSIFICATION OF THIS PAGE (When Data Entered)

20. ABSTRACT (Continued).

nearshore sediment samples, bathymetric surveys, and bedform measurements. Inlet hydraulics were found to be dominated by flood tidal flow through Eel Pond into the adjoining Waquoit Bay, causing the pond to act as a sediment sink. Several modifications to the inlet geometry are proposed for reducing inlet shoaling rates.

PREFACE

The work described in this report was conducted during 1980-1983 by the US Army Corps of Engineers Coastal Engineering Research Center (CERC), in cooperation with the US Army Engineer Division, New England (NED). On 1 July 1983, CERC became part of the US Army Engineer Waterways Experiment Station (WES).

Mr. Allan E. DeWall conducted the investigation and prepared this report, with the assistance of Ms. Joan A. Tarnowski and Mr. Bruce Danielson, all formerly of the Coastal Processes Branch, and Dr. Lee L. Weishar, Coastal Processes Branch, Research Division, CERC. The work was under the general direction of Dr. Robert M. Sorensen, former Chief, Coastal Processes and Structures Branch, Mr. Rudolph P. Savage, former Chief, Research Division, and Dr. Robert W. Whalin, Chief, CERC. Project Engineers at NED were Ms. Lydia Wood and Mr. Mark Habel.

The authors gratefully acknowledge field assistance provided by Mr. Mike Dickey, Ms. Martha Hayes, Ms. Carter Laing, Mr. Lin Tornese, Dr. Todd Walton, and Ms. Lydia Wood. Mr. Hank Madden, Falmouth Harbormaster, was especially helpful in providing logistical support during field operations and also collected daily littoral environment observations during the study. Mr. William N. Seelig wrote the INLET2 computer program used to model inlet hydrodynamics.

Commander and Director of WES during the publication of this report was COL Robert C. Lee, CE. Mr. F. R. Brown was Technical Director.

CONTENTS

CONVERSION FACTORS, INCH-POUND TO METRIC (SI) UNITS OF MEASUREMENT

Inch-pound units of measurement used in this report can be converted to metric (SI) units as follows:

Multiply	By	To Obtain
cubic feet per second	0.02831685	cubic metres per second
cubic feet	0.0283168	cubic metres
cubic yards	0.7645549	cubic metres
feet	0.3048	metres
feet per second	0.3048	metres per second
inches	25.4	millimetres
miles per hour	1.609344	kolometres per hour

INLET PROCESSES AT EEL POND
FALMOUTH, MASSACHUSETTS

I. INTRODUCTION

The purpose of this report is to summarize an investigation to determine the cause of a shoaling problem at the entrance to Eel Pond, a small craft harbor located in Falmouth, Massachusetts (Figure 1). Since its formation, resulting from a hurricane in 1938, the inlet has been artificially closed, reopened by another storm and stabilized, to some degree, through natural processes and through placement of structures and dredging efforts. Although the inlet throat is relatively deep (18 to 20 feet*), shoals have accumulated at both ends resulting in hazardous navigation conditions during low water conditions.

This report describes a combined office and field study designed to define the causes of the shoaling problem and to recommend potential solutions. The office study consisted of an evaluation of the history of inlet development made from available reports, surveys, and aerial photographs and an analysis of available wind, current, and wave data. In addition, a one-dimensional numerical model was used to evaluate inlet stability under existing conditions, and to predict stability with various changes to the inlet geometry and with the addition of stabilizing structures. The field study included concurrent tide measurements on either side of the inlet, current velocity measurements within the inlet and in Nantucket sound, beach and nearshore sediment samples, and bedform measurements.

1. Previous Work

A cooperative Beach Erosion Control report, covering the beach between Nobska Point and the entrance to Waquoit Bay, was published by the U.S. Army Engineer Division, New England (NED) in 1962. This study did not address the hydraulics of the navigable inlets in the area, but did include an analysis of shoreline and nearshore contour change rates. The report documents shoreline erosion rates of between 1 and 6 feet per year during the interval 1845 - 1961 in the vicinity of Eel Pond. Following the reopening of Eel Pond inlet in 1944, the erosion rate of the Western Spit of Washburn Island - immediately east of the inlet - increased to 26 feet per year.

A small-boat navigation project reconnaissance report on Eel Pond was prepared by NED in 1978. This report details the recurring shoaling problem in the entrance channel to Eel Pond and lists three dredging efforts (1956 (?), 1967, and 1968) which were undertaken to maintain the channel at an acceptable depth for navigation. Unfortunately, quantities of material dredged are not documented. In a study of sand waves generated by tidal currents, Southard (1981) documented a net counter-clockwise circulation pattern in Vineyard Sound, with the northern (mainland) side dominated by ebb flow, and the southern side dominated by flood flow. Southard documented ebb velocities

* A table of factors for converting inch-pound units of measurement to metric (SI) units is presented on page 4.

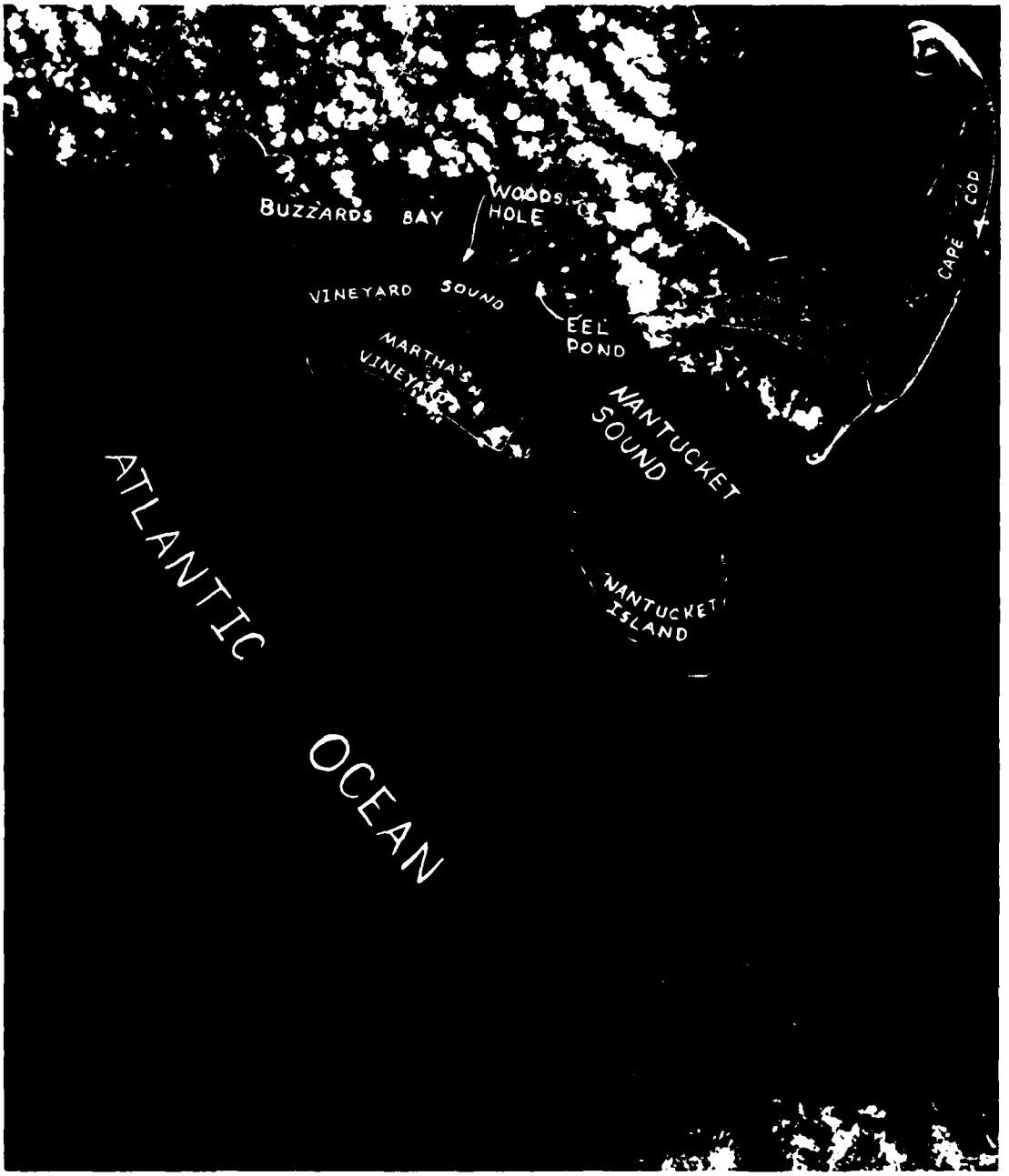

Figure 1. Location of study site

(to southwest) reaching 2.8 knots and flood velocities (to northeast) reaching 3.9 knots. He found that the predominant southwest winds tend to enhance flood velocities, but that these winds also result in a local setup of water elevation. This condition ultimately results in increased ebb velocities and reduced flood velocities after winds have abated. Southard found helical flow in sand wave troughs to be an important mechanism for moving sediment in a direction parallel to sand wave crests. He documented sand wave migration rates averaging 0 to 40 meters per year, with a net displacement toward the southwest in the Middle Ground Shoals area, southwest of Woods Hole.

Aubrey and Gaines (1982) have summarized historic shoreline changes at Popponesset Beach, located five miles to the east (Figure 2). This study, which included the analysis of 43 sets of aerial photographs and 92 historical charts, documented a landward migration of Popponesset. Migration rates range from 4.3 to 11.5 feet per year since 1938. Despite this migration, the average width of the spit was found to remain relatively unchanged. The direction of longshore sediment transport was found to undergo reversals seasonally as well as spatially. Longshore transport was found to be generally directed northward in April and southward in October and November. Directions were variable during other months. The net transport direction was found to converge near the mouth of Cotuit Bay.

A landscape analysis of Washburn Island was prepared by the Massachusetts Department of Environmental Management (1980). This report documents the initial formation of Eel Pond inlet during the 1938 hurricane, its artificial closure by the Army in 1942, and its reopening in a 1944 storm.

A draft environmental impact report prepared by Skidmore, Owings, and Merrill (1982) included a discussion of the geology, soils, and coastal processes of the study area. The report included the results of chemical analyses of sediment and water samples taken from the northeastern arm of Eel Pond. The chemical analyses of the sediments indicate that they are uncontaminated materials and that they meet the category 1 standards specified by the Commonwealth of Massachusetts Water Resources Commission. Follow-up "split-spoon" test borings were made at three sites located in the vicinity of the previous surface samples (Mr. Andrew Magee, Jason M. Cortell and Associates, Personal Communication). These borings indicate a mixture of fine to coarse sand, with traces of silt and gravel to a sediment depth of 10 feet.

2. Study Area

Eel Pond is located on the southwest shore of Cape Cod, at the junction of Vineyard Sound and Nantucket Sound. The site is on an east - west trending reach extending between Nobska Point (Woods Hole) and Succonnesset Point. There are a total of seven inlets presently open in this reach, although only five are considered to be navigable (U. S. Dept of Commerce 1982). Eel Pond inlet is the most recently formed of these five.

Cape Cod, itself, is a recent landform having formed late in the Pleistocene Epoch, in the final stages of the Wisconsin stage - approximately 50 to 70 thousand years ago (Strahler 1966). Most of the sediments in the area represent outwash material from the Cape Cod Bay glacial lobe, and form

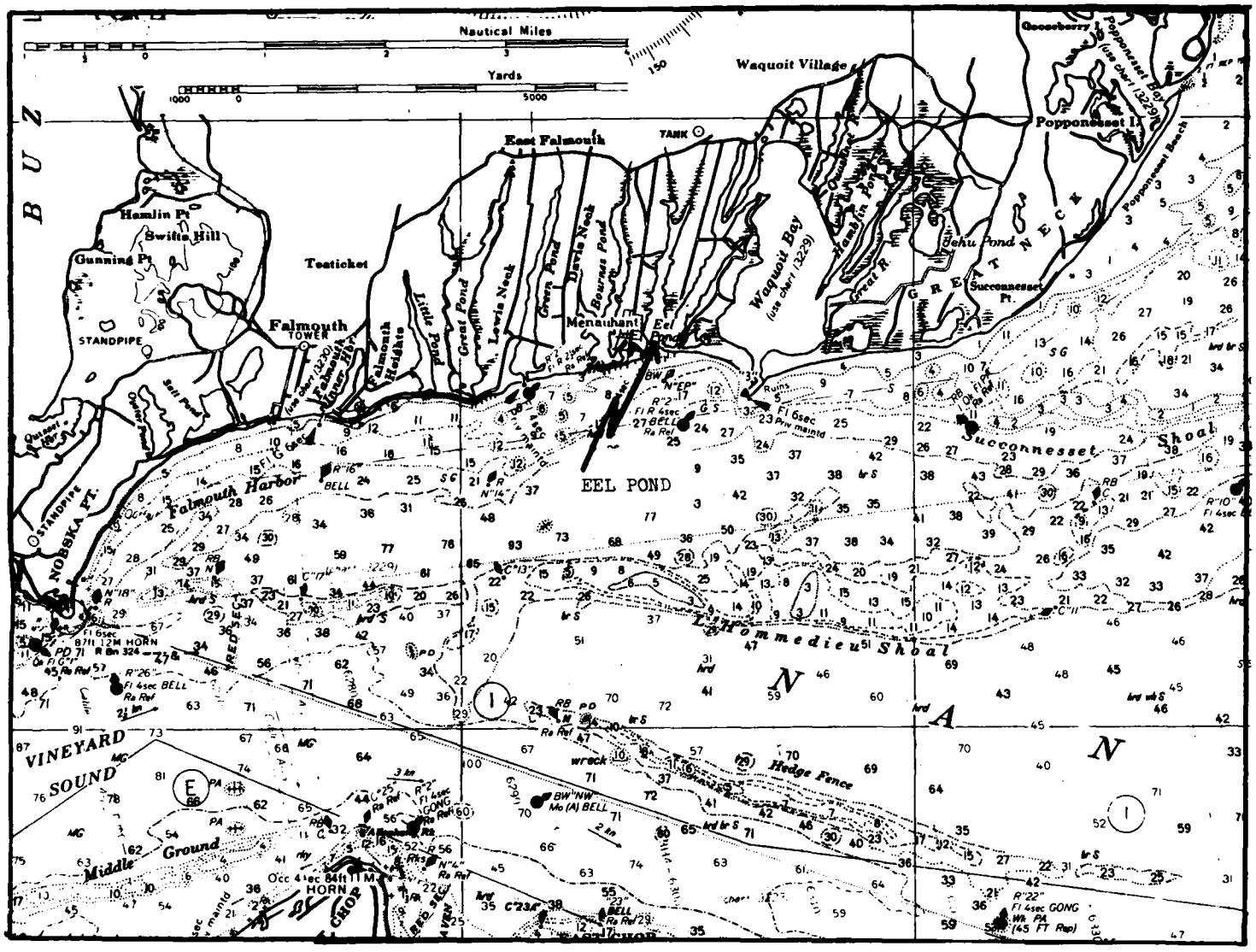

Figure 2. Loca[illegible]n

part of the Mashpee Pitted outwash plain deposits. It is uncertain how far south and east this plain extended, but evidence indicates that during maximum glaciation, so much of the earth's water was tied up in the icecap, that the local shoreline was on the order of 100 miles seaward of its present position. With warming climate and melting ice, sea level gradually rose until it approached its present elevation approximately 5,000 years ago. As the kettle holes and furrows left in front of the receding glacier were flooded, the loose, unconsolidated sediments of the outwash plain were then reworked by the encroaching waves and currents. Baymouth bars were built into barriers, such as the spit that connected Menauhant with what is now Washburn Island - forming Eel Pond. Higher water elevations, which occur during storm surges, periodically wash over these spits and occasionally cause them to breach, connecting the ponds with Vineyard and Nantucket Sounds. Frequently these breaches reclose naturally, resealing the ponds. Examples of this process can be seen at Oyster Pond and Salt Pond, in the western part of the study area, and until relatively recently at Eel Pond.

The earliest documented opening of an inlet directly connecting Eel Pond with Nantucket Sound was during a hurricane in 1938. Prior to this time, the only connection between Eel Pond and Vineyard Sound was through the Seapit River and Waquoit Bay. Shoreline maps compiled by the Beach Erosion Board (U.S. Army Corps of Engineers, 1962) showed a continuous barrier connecting Menauhant with what is now Washburn Island in 1846 and 1888. Aerial photographs in November 1938 show a breach of this barrier adjacent to the Menauhant side of Eel Pond. The U.S. Army reportedly closed the inlet in 1942 (Massachusetts Department of Environmental Management, 1980). A hurricane in 1944 reopened the inlet somewhat east of its earlier position, and it has remained open since that time.

At present, the inlet opens at the southwest end of Eel Pond, adjacent to the Menauhant Yacht Club. At its narrowest constriction, directly in front of the club, the inlet is approximately 100 feet wide and 19 feet deep (Figure 3). A hydrographic survey conducted by NED in April and May 1981 shows sand shoals at either end of the inlet that reduce MLW depths to approximately 4-1/2 feet. The U.S. Coast Pilot (U.S. Department of Commerce, 1982) reports a controlling depth of 3 feet (MLW) as of August 1981.

3. Longshore Transport

The erosion of the glacial moraine deposits, forming Nobska Point at Woods Hole and the sea cliffs at Falmouth Heights, supplies the material for the formation and maintenance of the baymouth barrier beaches. The exposure to an essentially unlimited fetch to the southwest through Vineyard Sound results in a net west to east sediment transport direction, although there is evidence of seasonal and local reversals in direction. Martha's Vineyard, Nantucket Island, and the extensive shoals in Nantucket Sound provide substantial protection from waves approaching from the south through east sectors.

A sand shelf, defined by the 12-foot depth contour, extends from the shoreline, where the contour nearly touches the beach, to the southwest where the shelf widens to 3/4 of a mile (Figures 2 and 27). In many aerial photographs this shelf is a clearly discernible feature with superimposed, nearly shore-normal sand waves. These bedforms indicate an active zone of sediment transport in an essentially longshore direction west of Eel Pond.

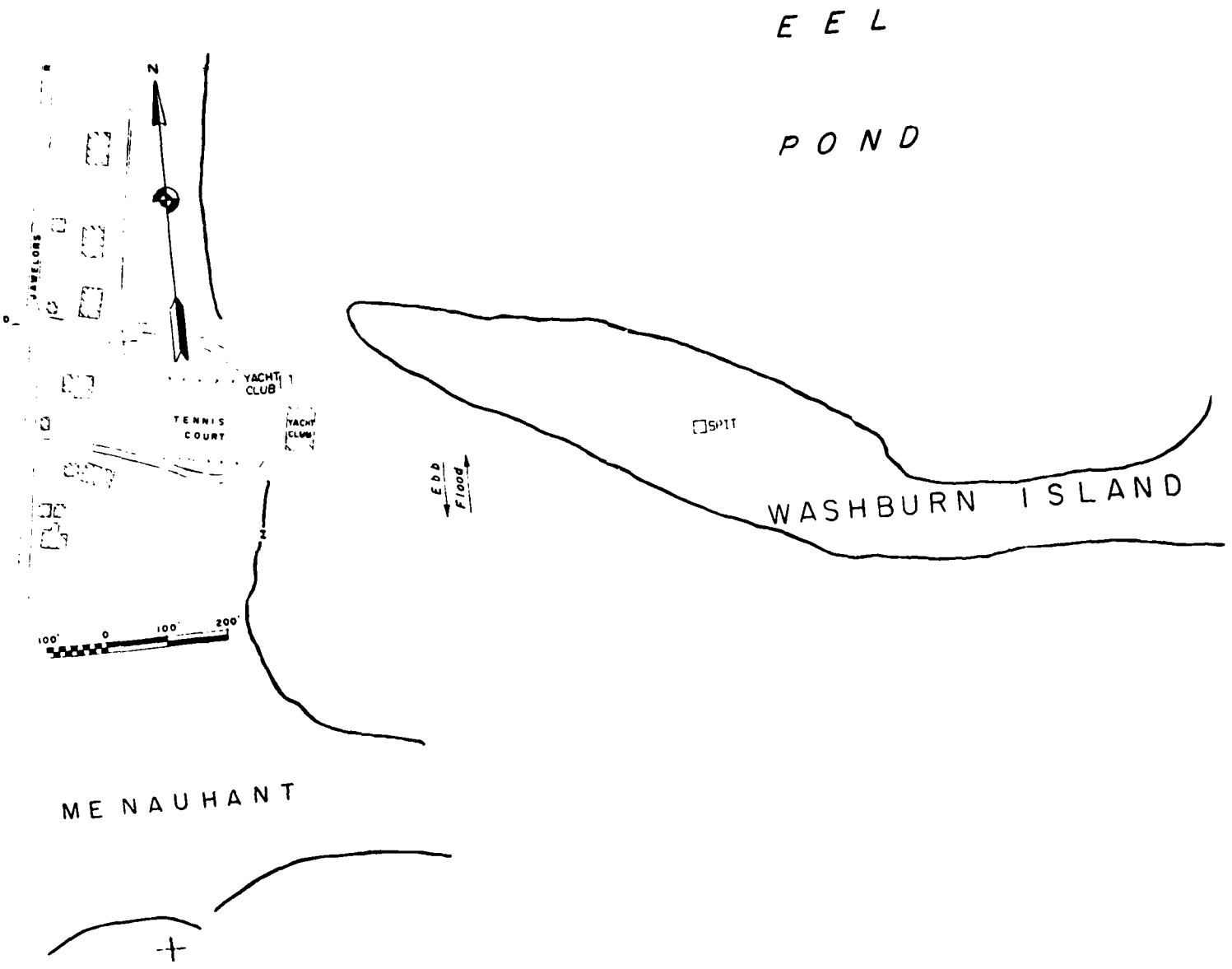

Figure 3. Bathymetry at Eel Pond inlet, based on NED survey in April-May 1979

Due to a local change in shoreline orientation east of Eel Pond, however, this sediment transport would be in an on-off shore direction with reference to the orientation of the Washburn Island shoreline.

Geomorphic indicators of longshore transport direction in the study area are conflicting. Strahler (1966) has suggested that a null point of divergence exists at Succonnesset Point, with transport directed from east to west in the vicinity of Waquoit Bay. The orientation of Bournes Pond inlet and the tendency of inlets (including Eel Pond) to migrate from east to west tend to support this interpretation. However, virtually every aerial photograph and most detailed maps examined in this study strongly suggest a net west to east sediment transport direction in the general vicinity of Eel Pond. Primary indicators are fillet development on the west side of the Waquoit inlet jetties and on the west side of the groin field along the Menauhant shorefront and the barrier beach at Bournes Pond. A local reversal east of Eel Pond is suggested by the landward migrating sand spit and the resulting shoreline offset on either side of the inlet (see Figure 3).

4. Winds

The wind rose in Figure 4a summarizes a 10-year data set from the Nantucket Island Airport. These data show that the prevailing winds are strongly directed from the southwest and west-southwest. An analysis of an earlier 9-year data set from Nantucket (Figure 4b) (U.S. Army Corps of Engineers, 1962) showed that winds with a continuous duration of at least 4 hours and speeds of 30 miles per hour, or greater, occur from the north through east-northeast sectors.

5. Tides

The tides in the study region are mixed, but almost completely diurnal (Redfield, 1980). The mean tide range at Succonnesset Point (3 miles east of Eel Pond) is 1.9 feet and the spring range is 2.3 feet. At Falmouth Heights (3 miles west of Eel Pond) the mean and spring ranges are 1.3 and 1.6 feet (U.S. Department of Commerce, 1982).

Redfield (1980) attributes the behavior of the tide in the area predominantly to the interference between tides entering the strait (formed by Vineyard and Nantucket Sounds) from opposite ends. This interference results in a phase difference between the two progressive waves causing a double high water (see Figure 5). A node occurs in the vicinity of Falmouth Heights which causes the tide to be mainly diurnal. Redfield reports that east of Falmouth the duration of the falling tide tends to be much shorter than that of the rising tide, while west of Falmouth the reverse is true.

The tidal phase difference is also evident from the times of predicted high and low water at Falmouth Heights and Succonnesset Point. High water occurs 1 hour and 10 minutes later at Succonnesset Point; low water occurs 48 minutes later.

The highest recorded tide occurred during the September 1944 hurricane and was 12.7 feet above mean low water (MLW) at Falmouth. Other significant

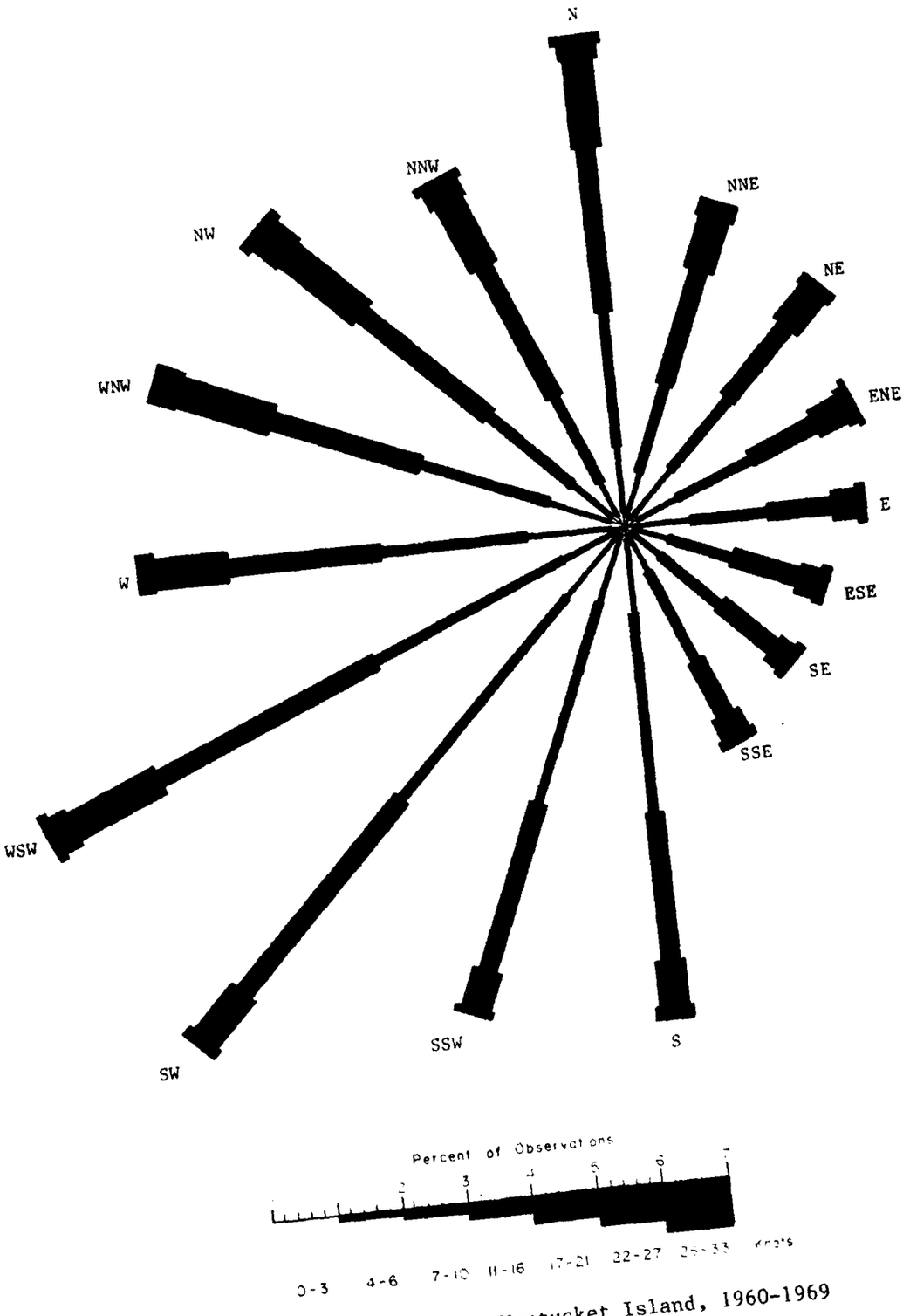

Figure 4a. Wind rose from Nantucket Island, 1960-1969

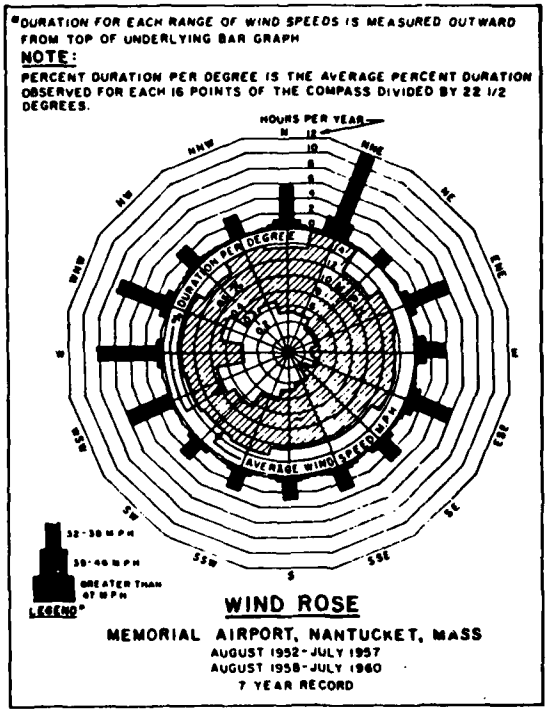

Figure 4b. Wind rose from Nantucket Island, 1952-1960 (from NED, 1962)

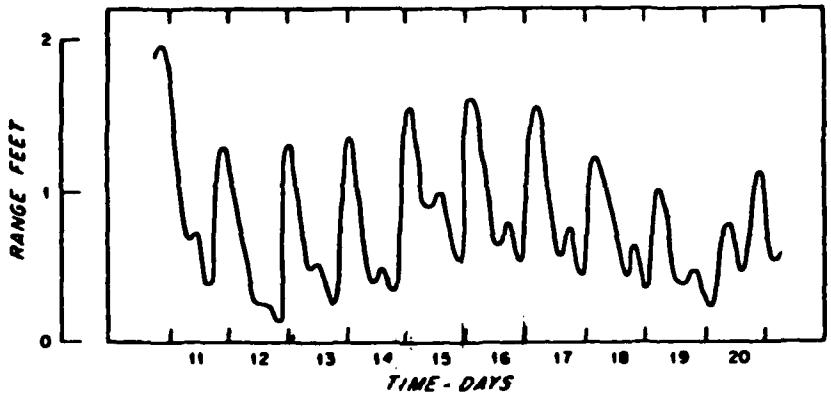

Figure 5. Sample tide record from Bournes Pond illustrating a mixed, almost completely diurnal tide, 11-20 May 1972 (from Redfield, 1980)

high tides have been observed in August 1954 (+9.5 feet, MLW) and September 1938 (+8.6 feet, MLW). Tides of 3 feet above MLW can be expected on the average of once per year (NED 1962).

Hicks, Debaugh, and Hickman (1983) reported an apparent rise in sea level, relative to land, of 0.01 foot per year, as determined from tide records collected between 1933 and 1978 at Woods Hole. Superimposed on this long-term trend, a seasonal variation has been documented for the region, with mean sea level being about 0.6 foot higher in September than it is in February. Redfield (1980) has suggested that this effect might be attributed to the increase in volume of the upper layer of water by warming during this summer. However, Harris (1963) has concluded that this phenomenon is a reflection of the higher frequency of tropical storm activity characteristic of late summer.

Tidal currents flowing through Vineyard and Nantucket Sounds are quite strong, with velocities of 2.3 knots (4 feet per second) reported at maximum ebb and flood flows within 1 mile of shore in the vicinity of Eel Pond (U.S. Department of Commerce, 1982). Although these values represent velocity at the surface, it is clear that tidal currents are sufficiently strong to move large quantities of sediment in the nearshore zone.

6. Waves

As stated earlier, the shoreline at Eel Pond is protected from ocean swell by Nantucket Island, Martha's Vineyard, and extensive shoals offshore. As a result, most of the waves are locally generated by winds blowing across the sounds.

Direct measurements of wave height, period, and direction are not available for Eel Pond. A study is presently being conducted of the coastal processes at Popponesset Beach, which will include directional wave data (D. H. Aubrey, WHOI, personal communication).

Visual wave observations were made at Eel Pond by personnel from the Falmouth Harbor Master's Office, from January through September 1979. A total of 189 near-daily observations of breaker height, period, and direction were made as part of the CERC Littoral Environment Observation Program (Schneider, 1981). A summary of the height and period information is presented in Figure 6. The mean breaker height for all observations was 0.54 foot, with a maximum monthly mean height of 1.5 occurring in September and a minimum monthly mean of 0.3 occurring in July. The highest observed breakers occurred during a storm on 6 September 1979, when a height of 6 feet was recorded. A concurrent wind speed of 55 miles per hour, from the southwest, was measured on the beach. Mean wave period for the 9 months was determined to be 3.76 seconds. The direction of observed wave approach was predominantly from the southwest.

The U.S. Coast Pilot (U.S. Department of Commerce, 1982) reports that in severe winters ice covers much of Nantucket Sound for periods of as much as 6 weeks. Ice conditions would significantly reduce wind-wave generation in the sound and attenuate most wave energy entering from the Atlantic. Ice also has the effect of armoring the beaches against wave attack.

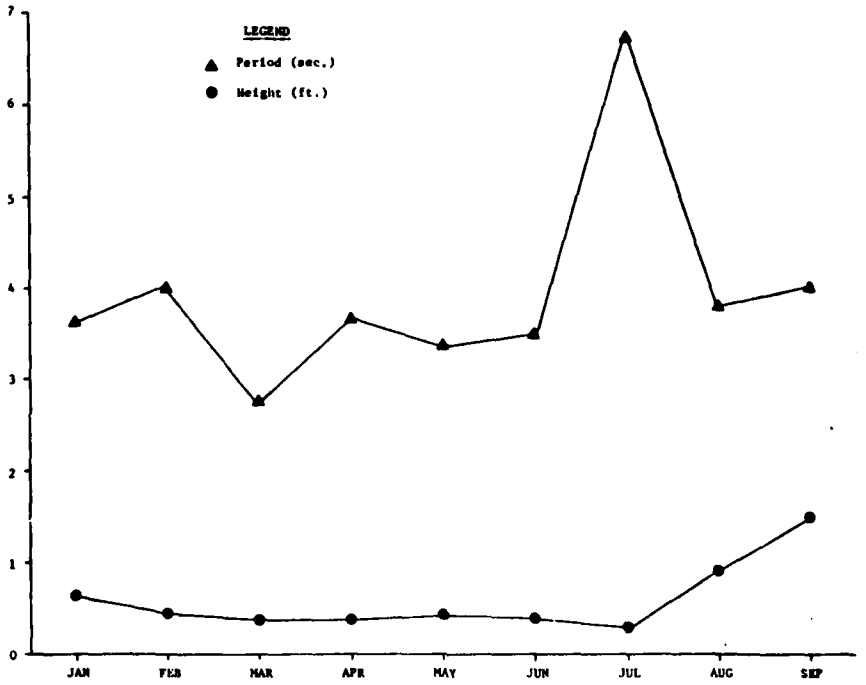

Figure 6. Visually observed breaker height and period from Eel Pond, January-September 1979

7. Civil Works

Documented attempts at stabilizing the shoreline in the vicinity of Eel Pond date to 1918, with the construction of the east jetty at the entrance to Waquoit Bay (U.S. Army Corps of Engineers, 1962). The west jetty was initially constructed in 1937. Both jetties have been lengthened and raised several times since then. A stone structure, described by the U.S. Army Corps of Engineers (1962) as a groin, was built at Menauhant by the state in 1937 and can be seen functioning essentially as a jetty on the west side of the new entrance to Eel Pond in a November 1938 air photo (see Figure 24). Additional structures were built during the 1940's, notably a field of four groins extending eastward from the existing structure. These groins protected a roadbed that ran along the then-continuous barrier bar shown in a June 1943 air photo (Figure 25). Following the subsequent rebreaching of the barrier, the westernmost of these four groins was lengthened in a northerly direction, and functions as a jetty on the west side of the inlet. As the barrier beach migrated landward, the remaining three groins were flanked and are now stranded 300 to 450 feet offshore.

Dredging and beach fill projects in the area are not well documented. An undocumented quantity of sand was dredged from the flood tidal delta, adjacent to the Menauhant Yacht Club, in 1942, and used to repair the breach in the barrier. Borrow pit dimensions, estimated from aerial photographs, were approximately 500 feet by 600 feet. An unknown quantity of material was removed from Eel Pond and placed on the beach to the west of Eel Pond Inlet in 1953 and in 1956 (U.S. Army Corps of Engineers, 1962). The 1956 dredging project was designed to deepen the navigation channel and anchorage to a depth of 6 feet. The channel and anchorage areas were redredged to a depth of 7 feet in 1968. The only other dredging documented in Eel Pond occurred in 1967 when local interests dredged the area around a pier at the Menauhant Yacht Club, just inside the inlet. Volume estimates of these projects are not available.

II. FIELD STUDIES

Three visits were made to the project site in conjunction with this study - two reconnaissance visits and a week-long field trip designed to document tidal-cycle flow characteristics and sediment size distribution trends. A reconnaissance inspection was made on 21 October 1980. During this visit a set of preliminary tidal flow measurements was made at the throat of Eel Pond Inlet, in the Seapit River, and at the throat of Waquoit Bay Inlet. Measurement sites are shown in Figure 7 and data are presented in Table 1. These measurements were taken during the last hour of the predicted flood tide at Eel Pond, and do not represent conditions of maximum flow. The measurements at the Seapit River confirm that the larger tidal prism within Waquoit Bay controls the flow through this connecting channel, with the flow being directed from Eel Pond to Waquoit Bay.

The second reconnaissance visit was on 19 August 1981. The purposes of this visit were to confirm the locations of bench marks, triangulation stations, launching and mooring facilities for the survey boat; to secure permission for use of potential structures selected as tide gage locations; and to discuss logistics and coordination with the Falmouth Harbor Master.

During the week of 14-19 September 1981, a major field trip was made to

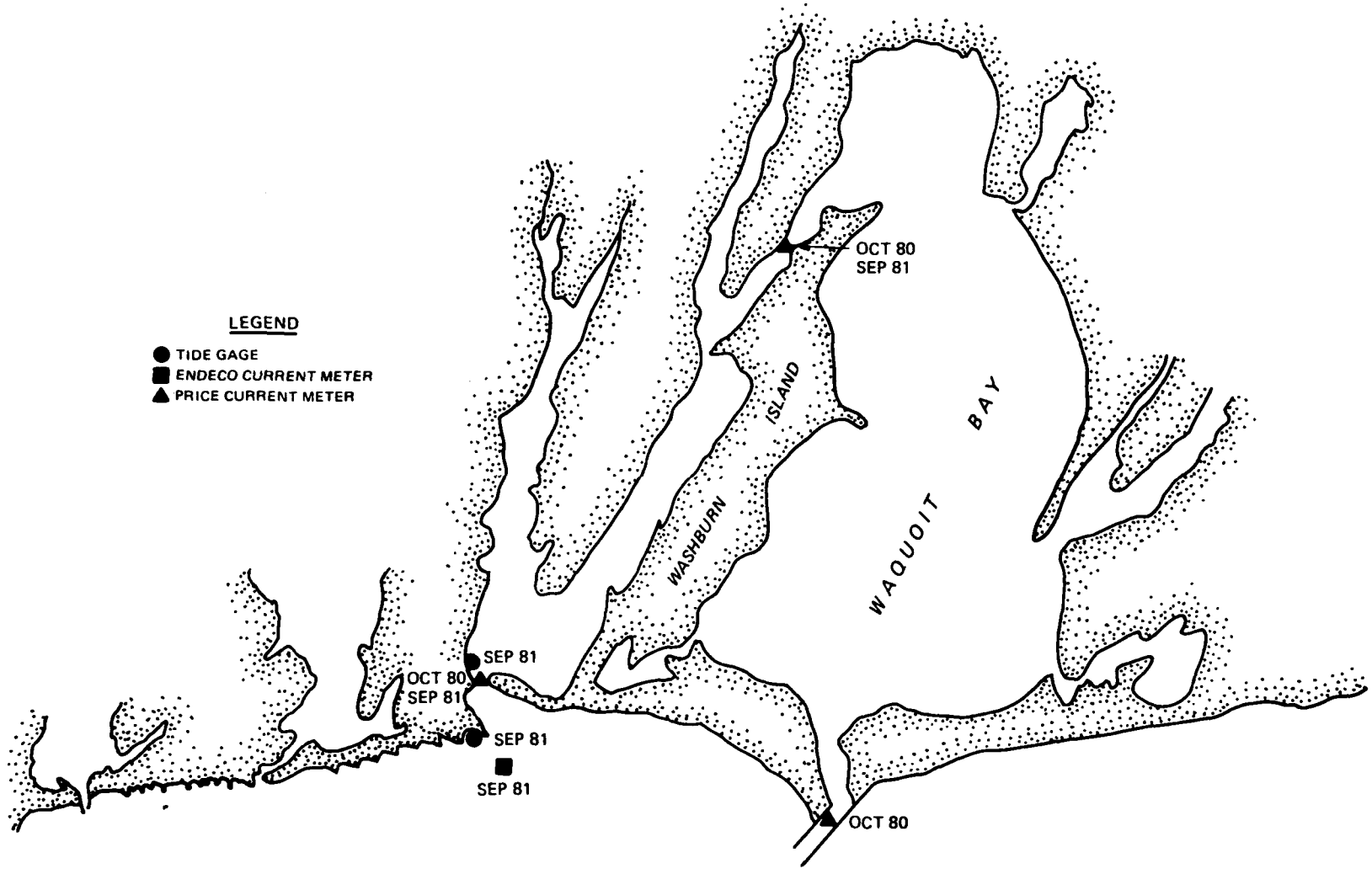

Figure 7. Location of instrumentation sites

Table 1. Eel Pond Velocity Measurements, 21 Oct 80

Eel Pond Inlet

Time (EDT)	Depth (Ft)	Velocity (Fps)	
0945	-4	1.06	(flood)
0947	-6	1.19	"
	-8	1.29	"
	-10	1.21	"
0951	-12	1.30	"
0952	-14	1.11	"
0954	-14	1.08	"
0956	-12	1.29	"
	-10	1.34	"
0959	-8	1.34	"
1000	-6	1.41	"
	-4	1.67	"
	-10	1.60	"

Seapit River

1021	-2	1.06	(to NE)
1024	-4	0.95	"
1025	-6	0.86	"
1026	-7	0.52	"
1029	-6	1.08	"
	-4	1.04	"
1032	-2	1.01	"

Waquoit Bay Inlet

1047	-2	0.97	(flood)
1049	-4	0.73	"
1050	-6	0.99	"
1052	-8	0.73	"
1053	-10	0.86	"
1056	-8	0.87	"
1059	-6	0.78	"
1100	-4	0.78	"
1102	-2	0.77	"

the study site. The purposes of this trip were to measure water elevation differences between Vineyard Sound and Eel Pond, and flow velocities through a full spring tidal cycle. Additionally, an inlet throat cross-section, representative sediment samples, and bedform measurements were collected.

1. Tidal Measurements

Two self-recording tide gages were installed, as indicated in Figure 7. The ocean-side gage was a Bristol bubbler-type. The orifice (sensor) was secured to a 1/2-inch pipe, 1.5 feet above the bottom at a distance 150 feet from shore. Water depth at this point was approximately 6 feet, MLW. The strip chart recorder was installed in a weatherproof box on top of the sand dune west of the jetty (Figures 8-10). The inside tide gage was mounted on the end of a private dock immediately north of the Menauhant Yacht Club (Figure 11). This gage consisted of a stilling - well strapped to a pile with a float/cable system running up the well to a Stevens strip chart recorder. A tide staff was nailed to an adjacent pile. Staff readings were made twice daily and annotated, along with time and date information, to the strip chart for gage calibration. Installation of the tide gages was completed on 14 and 15 September 1981. Gage elevations were referenced to a common, local datum, using survey control established by NED (third-order accuracy). The gages were removed on the afternoon of 17 September (Stevens) and 18 September (Bristol). The complete records are shown in Figure 12.

The maximum tidal range measured was 3.0 feet on the ocean side and 2.45 feet in Eel Pond. For the record obtained, 15-17 September 1981, there was no significant lag at high or low water between the ocean side and pond side of the inlet. The average time of high water occurred 1 hour after the time of predicted high water at Falmouth Harbor while the average time of low water occurred essentially at the same time as predicted (U.S. Department of Commerce, 1981).

2. Current Measurements

On 15 September 1981, an Endeco, model 105, self-recording current meter was installed approximately 1400 feet seaward of the inlet entrance at a 10-foot (MLW) depth. The mooring was located 100 feet southwest of navigation buoy "EP." The current meter tether was attached 4 feet above the ocean bottom and allowed the instrument to move freely with any oscillatory wave motion, so that only net current velocity was recorded (Figure 13). The meter was set up to record new speed and direction at 30-minute intervals. It was operated through 17 September. Velocity data are tabulated in Appendix A and are presented as a rose diagram and as a progressive-vector plot in Figures 14 and 15. These data show a flood current strongly directed to the northeast and an ebb current strongly directed to the northwest suggesting that, even this close to shore, tidal flow through Vineyard Sound plays an important role in sediment transport. The peak velocities, averaging 0.91 fps, were associated with ebb flow. The average peak flood velocity was 0.74 fps. The duration of flood flow exceeded that of ebb flow by approximately 1 hour, resulting in a net flood - directed vector. This is illustrated by Figure 15, where the resultant vector from 15 - 17 September 1981 is directed toward the northeast. With the exception of four measurements made between 1630 and 1800 (EDT) on 15 September 1981, the ENDECO

Photo 11. Five-ton military truck after breaking through soil

Figure 10. Bristol tide gage

Figure 11. Stilling well and housing for Stevens tide gage used in Eel Pond

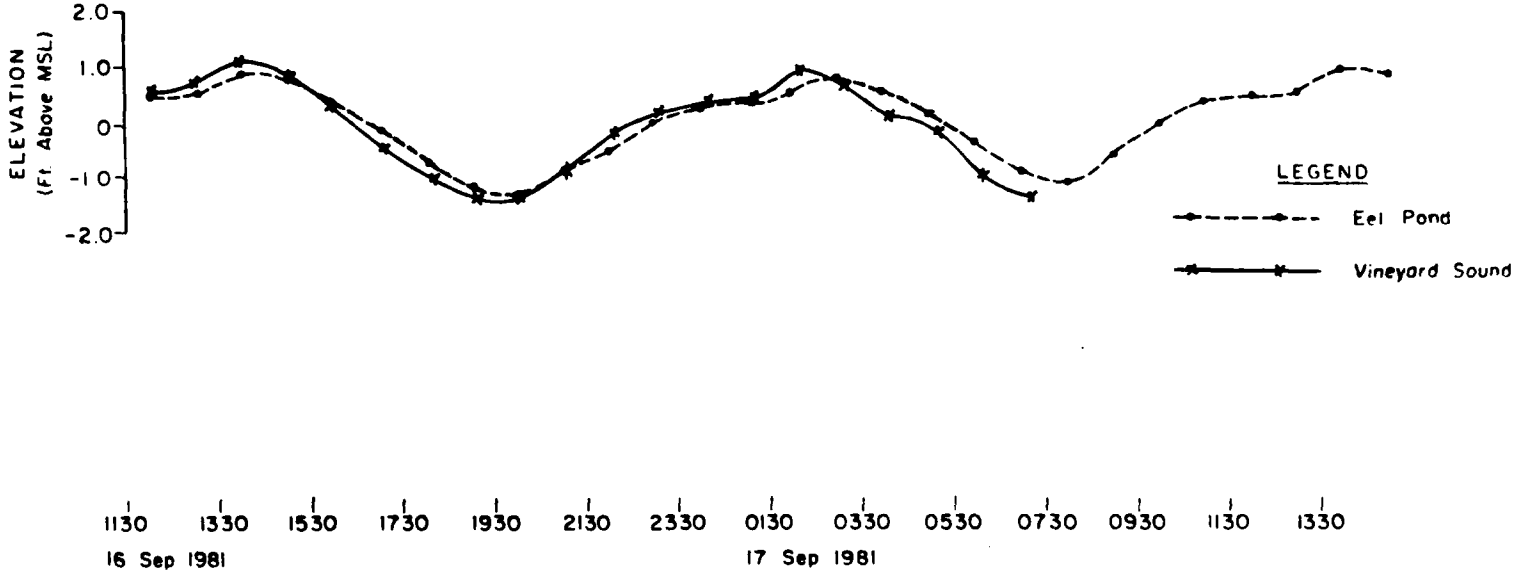

Figure 12. Tide records from Vineyard Sound and Eel Pond, 16-17 September 1981 (EDT)

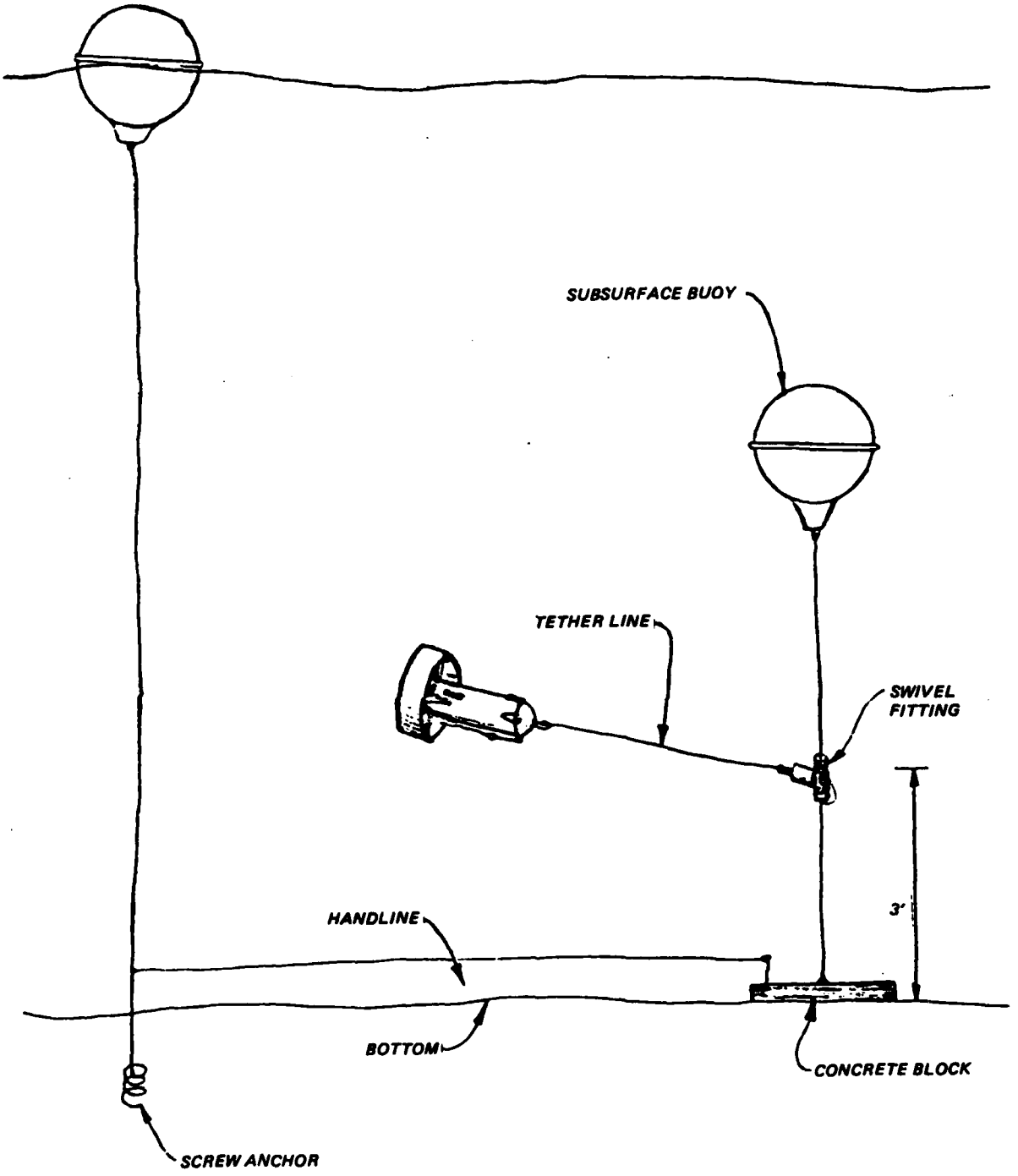

Figure 13. Mooring system used for Endeco 105 current meter

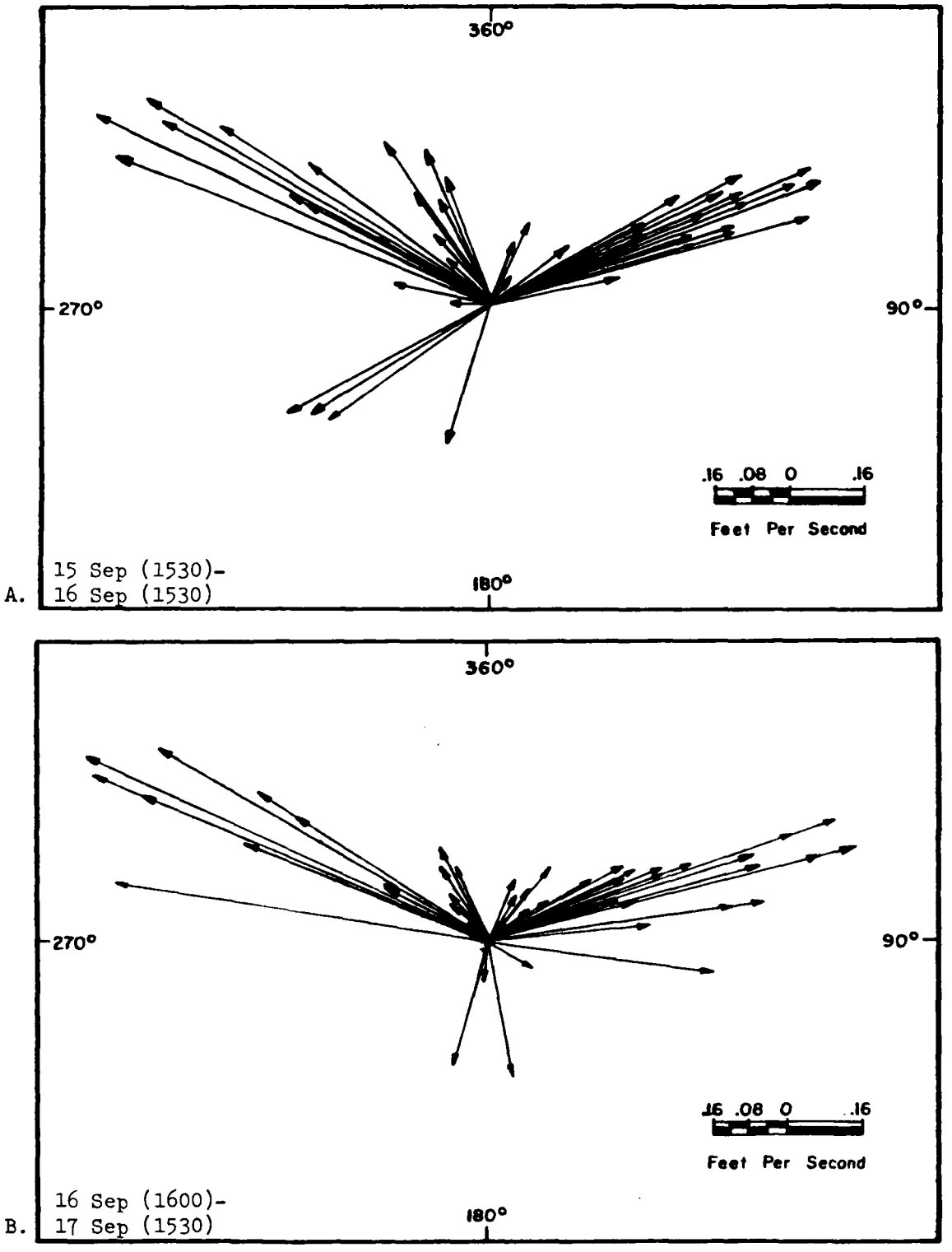

Figure 14. Current rose diagrams from Vineyard Sound at Eel Pond inlet, 15-17 Sep 81

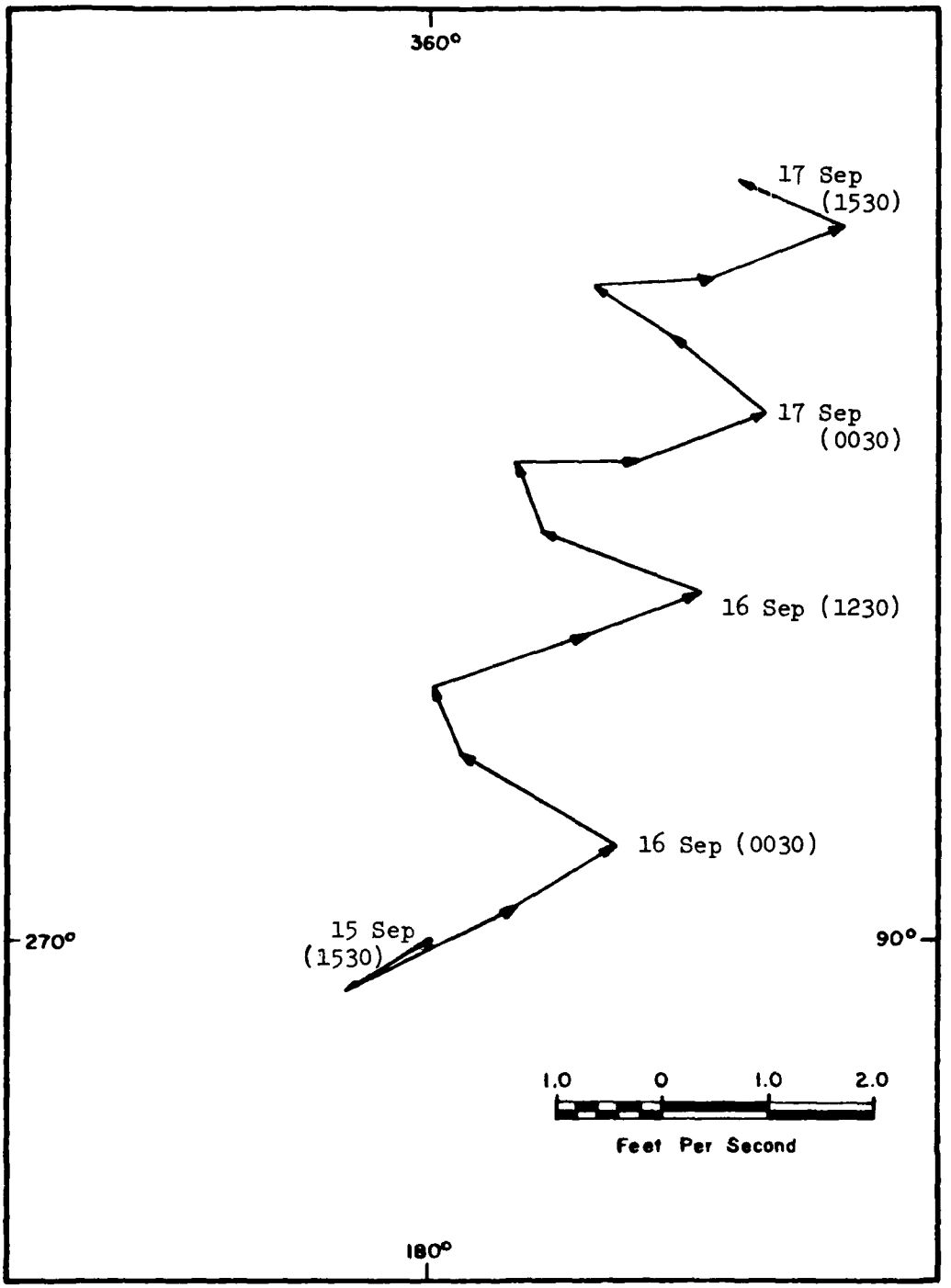

Figure 15. Progressive current vectors from Vineyard Sound at Eel Pond inlet, 15-17 September (3-hour intervals)

current meter did not appear to be located within the track of the expected ebb-oriented "jet" flow. The four measurements on 15 September were directed between 200° and 243° true north (TN). A jet flowing directly out of the inlet would have an expected direction of about 165° TN, indicating a significant deflection to the west by ebb flow through Vineyard Sound.

Starting at 1130, 16 September and continuing through 1230, 17 September current velocity profiles were measured hourly across the inlet throat. Current speed was measured using a Price, model 667, current meter suspended from the bow of the survey boat (Figure 16). Speeds were measured at three depths at each of three stations across the inlet throat. Direction was noted as either "ebb" or "flood" from visual observation at the surface. Positioning was accomplished using a pre-marked cable stretched across the inlet throat. The cable was weighted and dropped to the bottom between measurement sets to allow passage of boat traffic. The measurement technique restricted inlet traffic for approximately one-half hour each hour. Pre-test publicity and concurrent Coast Guard broadcasts over marine radio minimized traffic conflicts. In addition, the survey boat and cable were marked with flashing lights during hours of darkness.

Measurement procedure was as follows: At each hour the cable was pulled taut using an electric power-winch. The survey boat would approach the cable from the down-current side (unless conditions were such that it was necessary to approach from the down-wind side in order to maintain position). The bow line was secured to a block on the cable and the boat was positioned at station "A" (Figure 17). The current meter was then lowered to the bottom using a bow-mounted winch and davit. Total depth was recorded from the pre-marked meter wire. A depth reading was also recorded from the fathometer. The current meter was held at depths equal to 0.8, 0.6, and 0.2 times the total water depth. The actual measurement consisted of the number of revolutions made by the rotor in 1 minute at each depth. This number was later converted to a speed value in feet per second using a calibration curve that was derived for the instrument in the laboratory. The procedure was then repeated at stations "B" and "C."

Inlet throat velocity data are plotted in Figure 18 and Table 2. Individual measurements are tabulated in Appendix B. Maximum velocity was measured on the ebb at 4.3 fps and occurred approximately 3.5 hours after high water. The maximum flood velocity was 3.75 fps occurring 4 hours before high water. In general, the flood current was strongest on the east side of the channel (Station C). Slack water conditions were observed to occur simultaneously with high water and 30 to 45 minutes after low water. A "false" slack water also occurred 1.5 hours before HW on the morning of 17 September.

Weather conditions during the tidal-cycle measurements were characterized by heavy rain and moderate winds (17-22 mph) from the northeast. Total precipitation on 15 and 16 September, as recorded at WHOI, amounted to 1.98 inches. It is expected that the combination of offshore winds and large runoff volume significantly augmented ebb flow velocities and reduced flood flow velocities.

3. Inlet Cross Section

On 18 September a survey of the inlet-throat cross section was made during

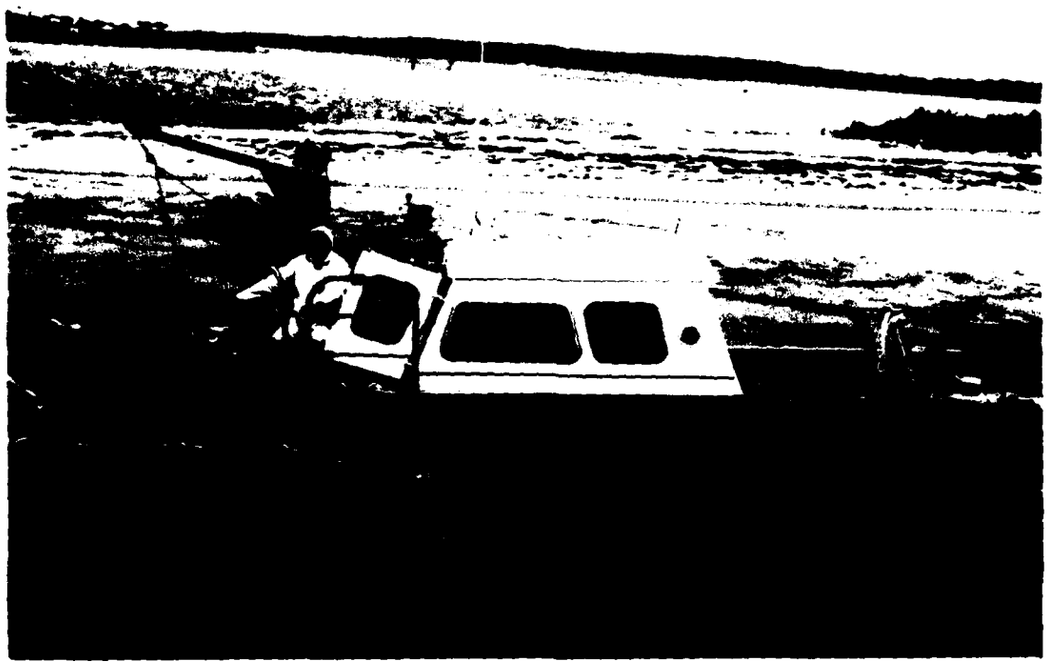

Figure 16. Obtaining hourly current measurement at station C, during peak ebb flow, 16 September 1981

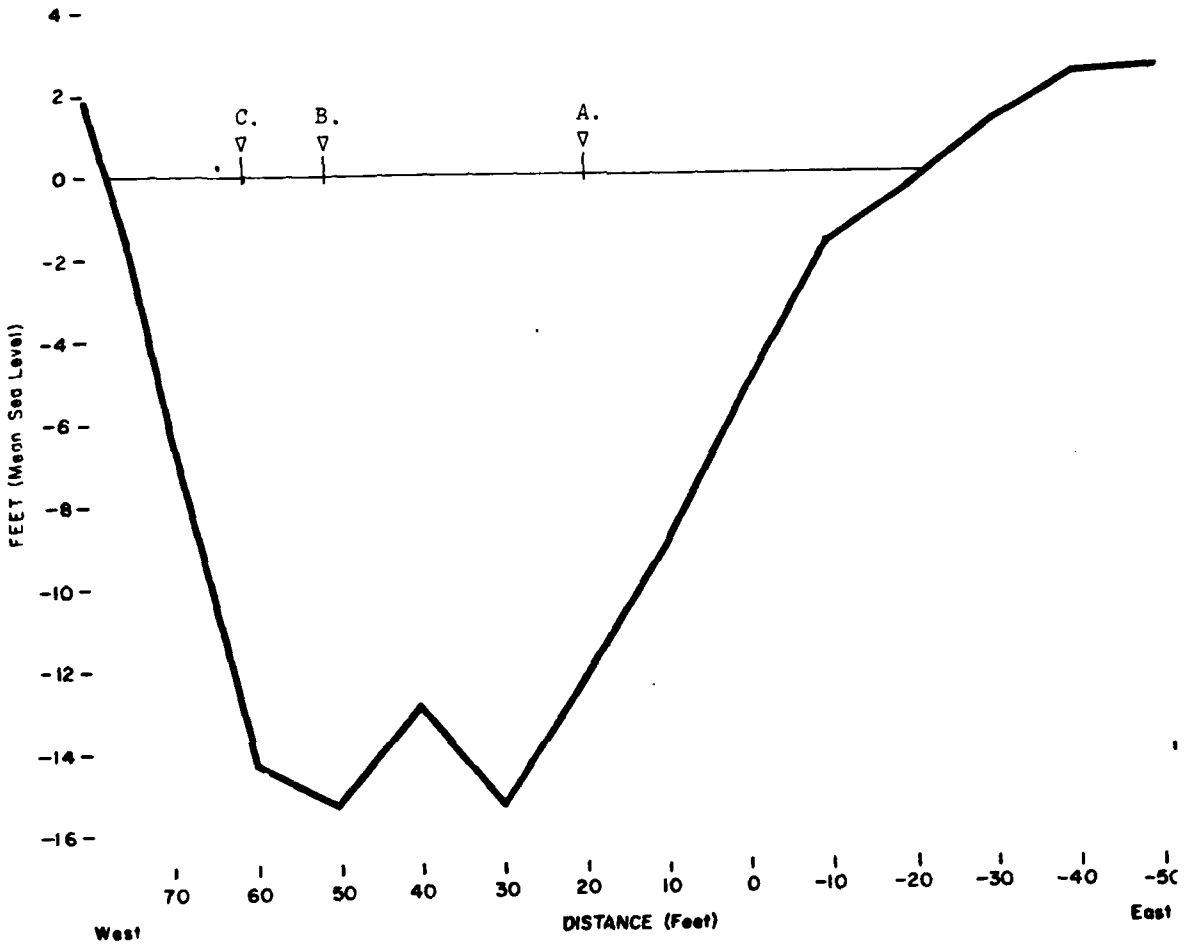

Figure 17. Cross-section and current meter stations at Eel Pond, 18 September 1981

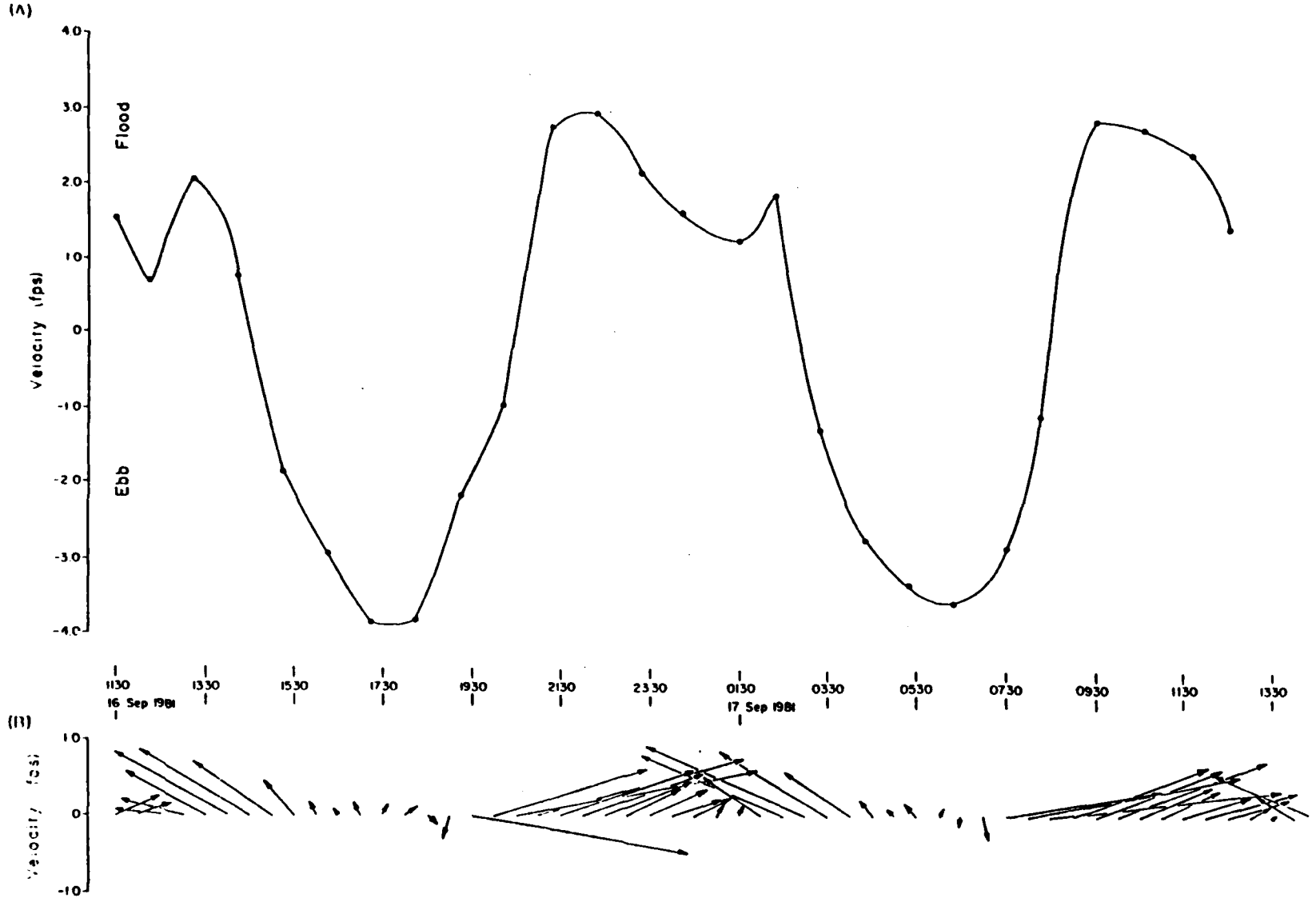

Figure 18. Current velocity measurements in Eel Pond inlet (A) and Vineyard Sound (B), 16-17 September 81 (EDT)

Table 2. Eel Pond Current Data[1]

Date	Time (EDT)	Speed (fps)	Direction
16 Sep 81	1130	1.52	Flood
	1215	0.70	Flood
	1315	2.06	Flood
	1415	0.77	Flood
	1515	1.84	Ebb
	1615	2.93	Ebb
	1715	3.84	Ebb
	1815	3.82	Ebb
	1915	2.17	Ebb
	2015	0.96	Ebb
	2120	2.76	Flood
	2220	2.94	Flood
	2320	2.17	Flood
17 Sep 81	0015	1.62	Flood
	0130	1.26	Flood
	0220	1.87	Flood
	0320	1.29	Ebb
	0420	2.71	Ebb
	0520	3.32	Ebb
	0620	3.59	Ebb
	0730	2.83	Ebb
	0815	1.09	Ebb
	0930	2.87	Flood
	1035	2.75	Flood
	1140	2.42	Flood
	1230	1.44	Flood

Seapit River Current Data[2]

Date	Time (EDT)	Depth (ft)	Speed (fps)	Direction
17 Sep 81	1140	5.6	0.81	NE
		4.0	1.06	NE
		1.4	1.69	NE
	1145	5.6	1.06	NE
		4.0	1.39	NE
		1.4	1.50	NE

[1] Each value represents the average of nine measurements made over an approximate 15-minute interval along a profile line across the inlet throat at Menauhant Yacht Club.

[2] Measurements made in mid-channel, off Commercial Shellfish Dock in 7-ft water depth.

slack water, using a level and rod. Depths were determined along the cable used for the current measurements. The profile is plotted in Figure 17.

4. Sediment Samples

A representative set of beach, pond, and ocean-bottom sediment samples was obtained during the 14-19 September 1981 field trip. Beach sediment was collected as surface grab samples while bottom sediment was sampled by divers using a short (24-inch) piston-coring device. Positioning was accomplished using a sextant with three-point fixes determined from known landmarks. Sample locations are shown in Figure 19.

In the laboratory, a split of each sample was analyzed for grain size distribution. Sample splits with an obvious silt fraction were initially wet-sieved to determine the percentage finer than 62 microns (4 ϕ). The remainder was then dry-sieved at quarter-phi intervals. The sample mean grain size and standard deviation were computed using the method of moments technique (Folk, 1965). These data are listed in Table 3.

Mean grain size was highly variable, reflecting the wide range of sizes available from local till deposits. Cobble- and boulder-sized material lined the inlet throat while silt dominated much of the bottom sediments found within Eel Pond and the Childs River. Beach sediments to the west of Eel Pond inlet ranged from 0.9 to 1.6 mm and ranged from well-sorted (0.37 ϕ) to poorly sorted (1.5 ϕ). Beach sediments to the east ranged from 1.5 to 3.7 mm with sorting values ranging from moderately well sorted (0.7 ϕ) to very poorly sorted (2.18 ϕ) at the base of an eroding glacial bluff. Beach-face sediments along the ocean side of Washburn Island were observed to increase in mean grain size and become more poorly sorted progressing in an easterly direction from the inlet to the eroding bluff--a distance of 2000 feet. Although there were not enough samples to confirm a trend east of the bluff, there was an indication of decreasing sediment size and improved sorting progressing toward Waquoit Bay inlet. Offshore sediments were moderately well sorted to poorly sorted sands, mixed with gravel and cobbles. Mean grain sizes ranged from 0.3 to 0.8 mm. Sediments within Eel Pond were generally silty sands except in the restricted channels of the Childs River and Seapit River where poorly sorted coarse sand with gravel was found. Sediment size coarsened along the southern portion of Eel Pond where the mean grain size was 0.6 mm, suggesting that sand was coming from the Washburn Island sand spit either by overwash, eolian transport, or through an inlet-trapping mechanism.

At the time of sampling a general description of the bottom conditions was also noted, including bedform type and orientation, if present. These observations are included in Table 3.

III. OFFICE STUDIES

The main elements of the office studies included (1) an interpretation of shoreline changes and processes as recorded in available aerial photographs and charts; (2) the computation of potential eolian transport and calibration of a numerical model to predict tides, currents, and ultimate stability of the inlet/bay under various conditions of channel geometry and structural control.

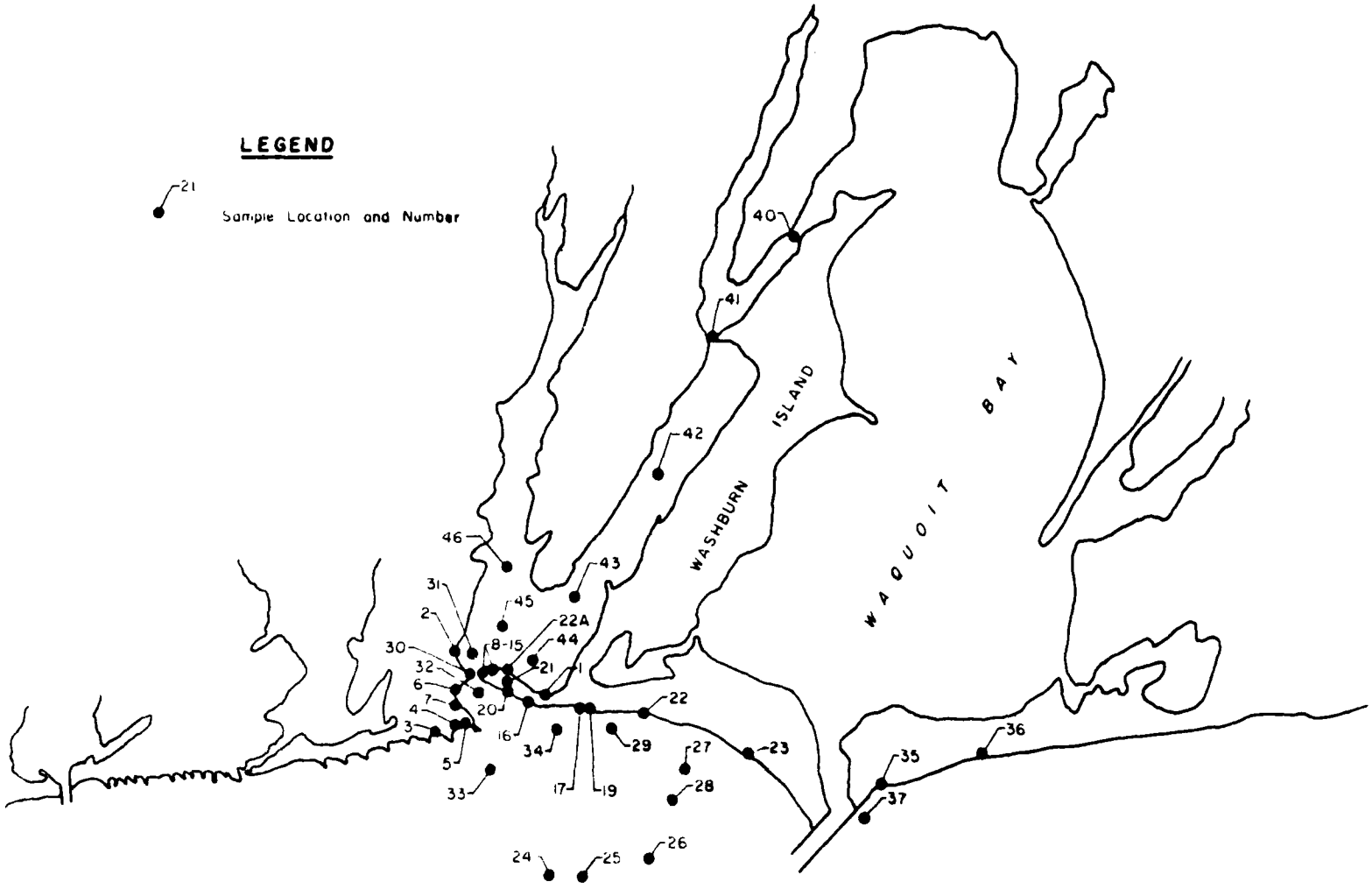

Figure 19. Sediment sample locations, 14-19 September 1981

Table 3. Eel Pond, Massachusetts, Sand Sample Summary
14-19 September 1981

Sample No.	Location	Mean Grain Size (mm)	Mean Grain Size (phi)	Standard Deviation (phi)	Remarks[1]
EP-1	Beach Face	0.74	0.43	1.16	Bay shore, Washburn I.
EP-2	Beach Face	0.80	0.32	0.58	North of Yacht Club
EP-3	Beach Face	1.57	-0.65	1.49	Ocean shoreline, between Groins Nos. 78 and 79[2]
EP-4	Beach Face	0.88	0.18	0.37	East of Groin No. 79
EP-5	Beach Face	0.91	0.14	1.10	West of Jetty No. 80
EP-6	Beach Face	0.89	0.18	1.24	West shore of inlet
EP-7	Dune	0.53	0.92	0.51	West of shore inlet
EP-8	Beach Face	0.63	0.66	0.74	End of spit, Washburn I.
EP-9	Beach Face	0.61	0.72	0.53	2.0 ft. below surface (at water table)
EP-10	Beach Face	1.36	-0.44	1.66	Next to EP-9
EP-11	Beach Face	0.57	0.82	0.41	20 ft. east of EP-8
EP-12	Beach Face	1.51	-0.59	1.06	20 ft. east of EP-11
EP-13	Beach Face	0.59	0.76	0.61	20 ft. east of EP-12
EP-14	Beach Face	0.73	0.44	1.04	20 ft. east of EP-13

[1]For ripple descriptions: α = magnetic azimuth of crest
λ = crest-to-crest wave length
h = trough-to-crest wave height

[2]Groin numbers referenced to Appendix G, Falmouth BEC report, 28 December 62.

Table 3. (Continued)

Sample No.	Location	Mean Grain Size (mm)	Mean Grain Size (phi)	Standard Deviation (phi)	Remarks
EP-15	Berm	0.68	0.55	0.57	Edge of vegetation, 20 ft east of EP-14
EP-16	Beach Face	3.74	-1.90	1.90	Pebble to cobble beach covering incipient cusps
EP-17	Beach Face	0.50	1.01	0.83	Base of glacial scarp
EP-18	Beach Face	1.50	-0.58	2.18	Base of glacial scarp, 100 ft. east of EP-17
EP-20	Beach Face	0.73	0.46	1.56	West of glacial scarp
EP-21	Dune Crest	0.47	1.10	0.47	In dune field west of glacial scarp
EP-22A	Beach Face	0.80	0.31	0.73	Bay shore, Washburn I
EP-22	Beach Face	1.43	-0.51	1.92	Ocean side, Washburn I
EP-23	Beach Face	1.25	-0.32	0.98	Sand overlying pebbles, Washburn I.
EP-24	-19 ft. water depth	0.49	1.02	0.58	Ebb-oriented ripples: $\alpha = 285^{\circ}$, $\lambda = 8$ cm, $h = 2.5$ cm
EP-25	-18 ft.	0.43	1.22	0.65	Cross ripples; ebb-oriented dom., $\alpha = 285^{\circ}$, $\lambda = 19$ cm, $h = 2$ cm
EP-26	-18 ft.	0.28	1.82	1.15	Ebb-oriented ripples: $\alpha = 310^{\circ}$, $\lambda = 10$ cm, $h = 0.5$ cm
EP-27	-6 ft.	0.55	0.86	0.54	Symmetrical ripples $\alpha = 40^{\circ}$, $\lambda = 30$ cm, burrowed

(Continued)

Table 3. (Continued)

Sample No.	Location	Mean Grain Size (mm)	Mean Grain Size (phi)	Standard Deviation (phi)	Remarks
EP-28	-12 ft.	0.84	0.25	1.20	Grass on coarse sand and shell; cobbles
EP-29	-6 ft.	0.64	0.64	1.14	Gravelly, coarse sand with cobbles. Symmetrical ripples: $\alpha = 140^{\circ}$, $\lambda = 17$ cm, $h = 4$ cm
EP-30	Inlet Throat (-16 ft.)	18.12[3]	-4.18	0.96	Sandy cobbles and boulders
EP-31	N. End Channel (-10 ft.)	0.32	1.63	0.66	Grass on med. sand
EP-32	S. End Channel (-5 ft.)	1.15	-0.20	1.18	
EP-33	-8 ft.	0.57	0.80	1.01	Gravelly sand with cobbles: Burrows, cross ripples: $\alpha = 150^{\circ}$ and 165°, $\lambda = 13$ cm, $h = 6$ cm
EP-34	-6 ft.	0.67	0.59	1.77	Dense patches of eel grass on sandy gravel. Symmetrical ripples: $\alpha = 355^{\circ}$, $\lambda = 20$ cm, $h = 6$ cm
EP-35	Beach Face	1.65	-0.72	2.23	Dead Neck; east side of Waquoit Inlet
EP-36	Beach Face	2.73	-1.45	1.74	East of EP-35
EP-37	-6 ft.	1.05	-0.07	1.53	Gravelly sand; symmetrical ripples: $\alpha = 125^{\circ}$, $\lambda = 22$ cm, $h = 6$ cm
EP-40	Seapit R. (-6 ft.)	0.76	0.40	1.27	Coarse sand. Abundant marine life.

(Continued)

[3] 30% coarser than 26.7 mm (largest sieve size)

Table 3. (Concluded)

Sample No.	Location	Mean Grain Size (mm)	Mean Grain Size (phi)	Standard Deviation (phi)	Remarks
EP-41	Childs R. (-9 ft.)	0.61	0.71	0.96	Coarse sand with shells and cobbles
EP-42	Childs R. (-9 ft.)	(65% silt)		(65% silt)	Grass on silty sand
EP-43	Childs R. (-8 ft.)	0.21	2.27	2.93	Dead shell layer over silty sand. Eel grass in patches
EP-44	Eel Pond (-4 ft.)	0.57	0.82	0.91	Silty sand and shells. Eel grass
EP-45	Eel Pond (-3 ft.)	0.19	2.40	1.66	Dead shell on sandy silt. Eel grass in patches (36% silt)
EP-46	Eel Pond (-5 ft.)	(67% silt)		(67% silt)	Dense grass and algal mat over sandy silt

1. Historic Shoreline Changes

A compilation of mapped high-water shoreline positions was made by the Beach Erosion Board in 1961 (NED, 1962). Data were given for the shoreline in 1845, 1890, 1938, and 1942. These are plotted in Figure 20. Information on historic shoreline positions is also available in topographic maps published by the U.S. Geological Survey. These maps are updated and published irregularly, at a scale of 1:25,000 (USGS, 1979). Portions of maps published in 1886, 1917, 1957, and 1972, illustrating the historic evolution of Eel Pond Inlet are reproduced in Figure 21. Shoreline positions are also shown on navigation charts published by the National Ocean Survey (i.e., U.S. Department of Commerce, 1981). Caution must be exercised in using these charts, however, since updated charts frequently include earlier shoreline positions.

Shoreline changes between 1845 and 1942 have been analyzed by NED (1962). Between 1845 and 1942 erosion rates at Menauhant ranged between 1 and 3 feet per year, with maximum recession in the area of inlet formation. The entire shoreline of what is now Washburn Island eroded at a rate of 2 feet per year between 1845 and 1891. Between 1891 and 1942 the rate increased to 4 feet per year along the western end of the island, but dropped to essentially no change in the area 2,000 to 2,500 feet east of the present inlet location. East of this zone of stability, the shoreline accreted at a maximum rate of 6 feet per year at the Waquoit Bay entrance where a jetty built during 1937 impounded material.

A more detailed description of the shoreline changes since the opening of Eel Pond Inlet is given in the following analysis of aerial photography.

2. Aerial Photographs

A total of seven sets of vertical aerial photographs (from 1938 to 1975) were obtained for analysis. These were identified through a number of sources, including an inventory compiled by Barwis (1975), the CERC Coastal Imagery Data Bank (Szuwalski, 1972), and the EROS Data Center (U.S. Department of Interior, 1972). Photography was also obtained from NED and from another investigator working in the area (Cyril Galvin, Coastal Engineer, personal communication). Additional sources of aerial photography from the area have been compiled by Aubrey and Gaines (1982) and are reproduced in Appendix C.

Analysis of the available sets of photographs has revealed a number of general trends concerning shoreline changes, net longshore transport direction, and net circulation within the Eel Pond/Waquoit Bay system.

a. Shoreline Changes

A general trend of landward migration of the barrier beach immediately to the east of Eel Pond Inlet has amounted to approximately 17 feet per year since the inlet formed in 1938. The average width of the spit has doubled from approximately 100 feet to 200 feet. The shoreline on the southeastern end of Washburn Island, adjacent to the Waquoit Inlet, has accreted at a rate of approximately 4.5 feet per year. This accretion is due to the impoundment of material against the west jetty of the inlet and has slowed considerably since 1942. The fillet extends for approximately 2,000 feet to the west and amounts to an estimated 150,000 cubic yards of sediment accumulation between 1938 and 1975. Most of this sediment was impounded between 1937 and 1947.

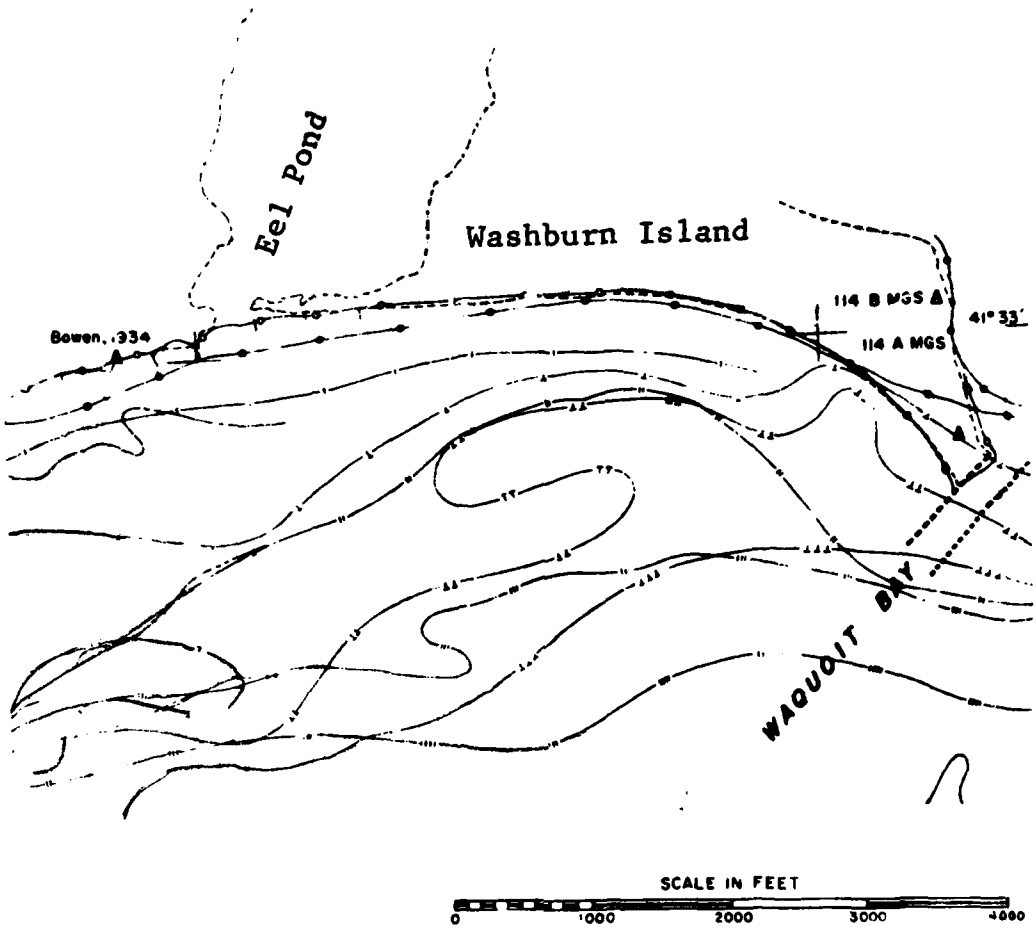

Figure 20. Shoreline and depth changes between 1845-1942 at Eel Pond

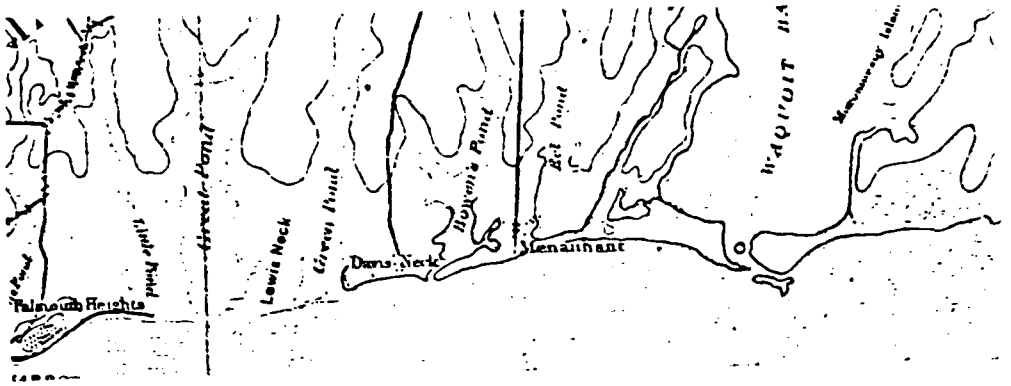

1886

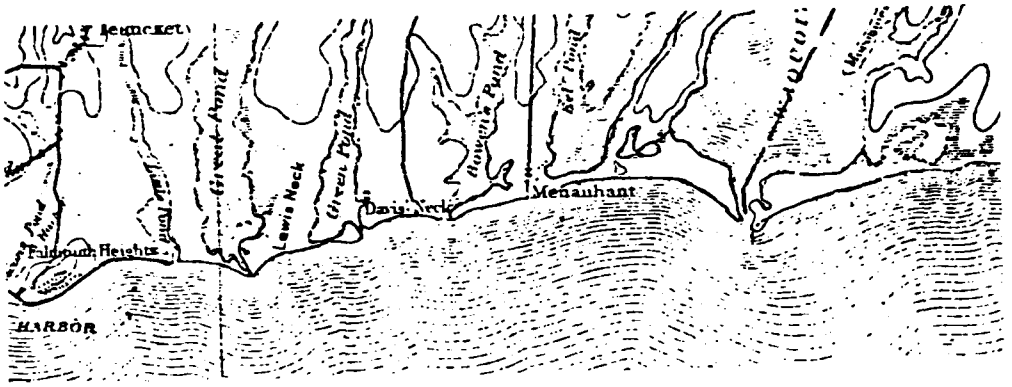

1917

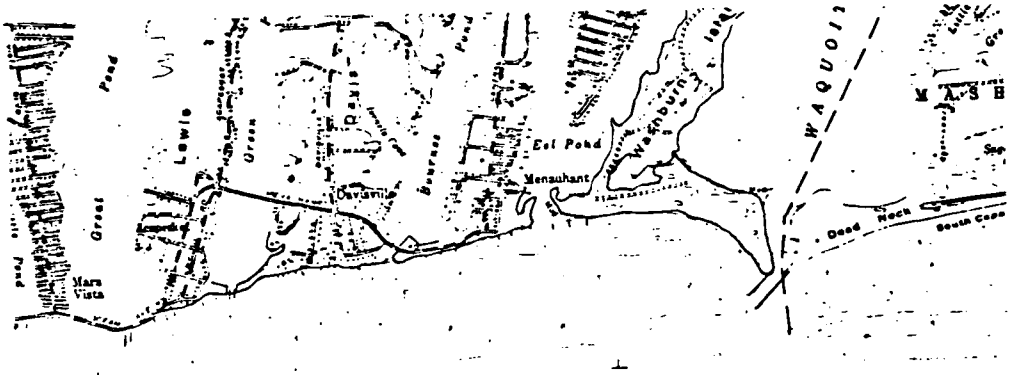

1957

1972

Figure 21. Shoreline changes as depicted by U.S.G.S. topographic maps, 1886-1972 (Mass. D.E.M., 1980)

Shoreline configurations, outlined from selected photographs and referenced to the 1971 position, are presented in Figure 22.

b. Inlet Position

With the exception of the period between 1942-1944 when it was artificially closed, all photographs reviewed for this study show the inlet to Eel Pond open, with its positions being generally at the southwest end of the pond. The initial position of the inlet, as depicted in November 1938, is very close to the Menauhant shoreline. This had been the westernmost position observed for the inlet. The inlet position in 1947 is approximately 400 feet to the east of its 1938 position. The geometry of the north shore of the barrier in 1947 suggests that the 1944 breach was even farther to the east. In October 1951 the inlet width had approximately doubled, causing the centerline to shift approximately 200 feet to the east. By November 1961 the inlet had narrowed to about 250 feet and had assumed a position very close to its present one (Figure 23). In October 1970 the inlet had reached its minimum width of approximately 100 feet, hugging the shoreline at the Menauhant Yacht Club, and has essentially maintained that position to the present (1981). Because of the increasing offset resulting from the northward-migrating barrier spit on Washburn Island, the inlet throat position has moved northward approximately 700 feet since 1938.

c. Sediment Transport

As stated earlier, all of the aerial photographs indicate a net west to east longshore transport direction. A local reversal occurs to the east of Eel Pond inlet with a nodal point of divergence located approximately 1,500 to 2,500 feet east of the Menauhant shoreline. An eroding glacial bluff, approximately 2,000 feet east of the inlet with its toe protected by a lag deposit of cobbles and boulders winnowed from the till, forms a subtle headland that may mark the nodal point. In 1938 this bluff was fronted by a natural sandy beach about 175 feet wide. Downdrift erosion from the groinfield installed in 1942(?) resulted in the removal of 75-100 feet of this beach by June 1943. By October 1947, following the reopening of the inlet, the beach in front of the bluff was essentially gone and active erosion of the bluff had begun. Large fillets on the west side of each of the four new groins in 1943 clearly indicate that the sediment transport direction was from west to east at that time and that no local reversal existed. It is apparent that the reversal was, in fact, initiated sometime after the rebreaching of the spit and subsequent flanking of the groinfield. Although it is difficult to be certain, a west to east transport direction still appeared to be predominant in October 1947, as suggested by asymmetrical scouring of the shoreline within and landward of the groinfield. The first indication of a local reversal appears in October 1951, although reversed fillets east of Green Pond suggest that this may have been a seasonal shift in direction.

The result of this local reversal in net transport direction has been a westward extension of the barrier spit and narrowing of Eel Pond Inlet. Tidal flow velocities through the inlet do not allow the inlet to become narrower than approximately 100 feet. A net flood-directed flow transports sediment into the inlet. Much of this sediment has continued to migrate around the spit and into the pond. This conveyor-belt-type movement of material has resulted in

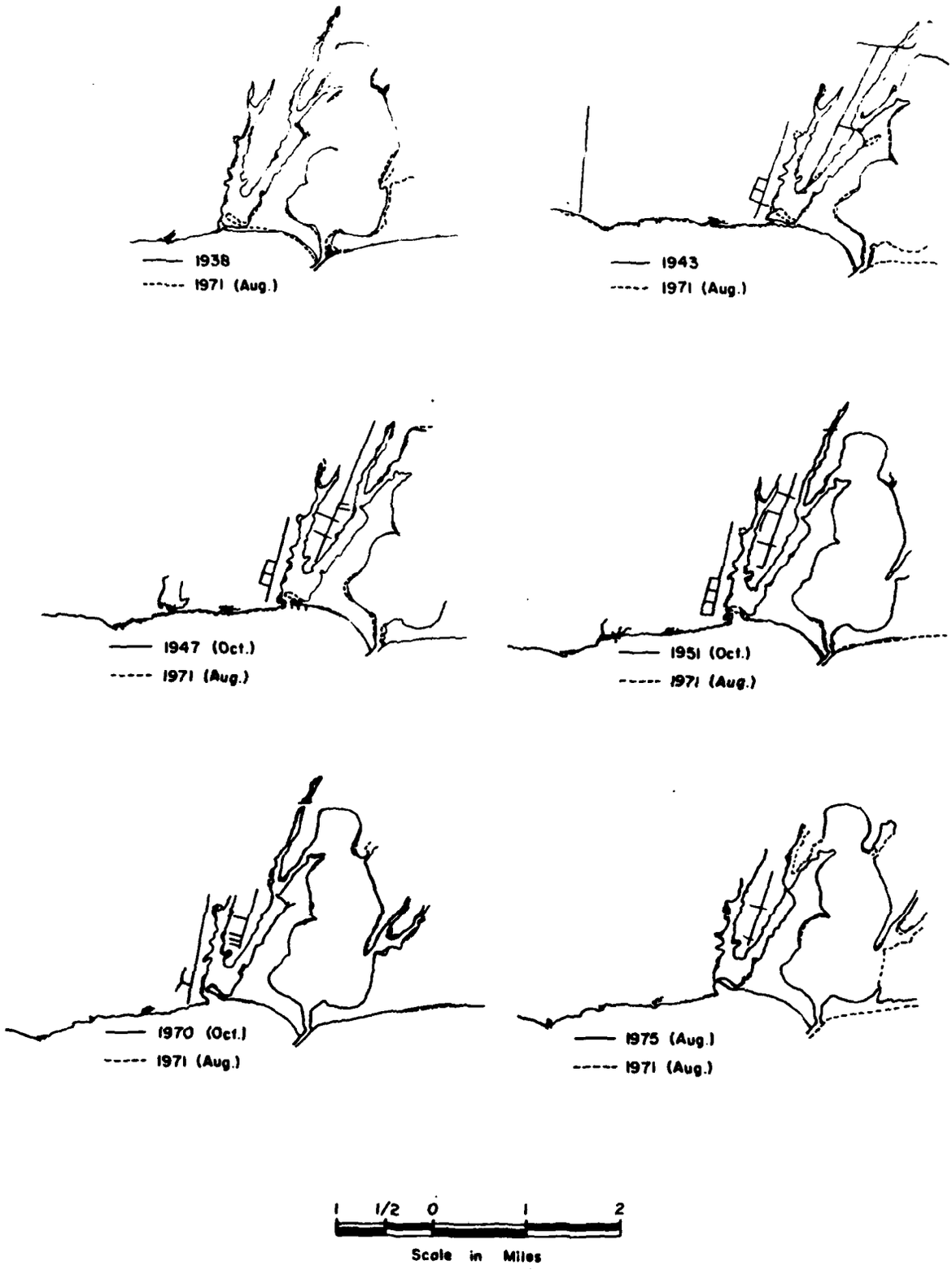

Figure 22. Shoreline configurations outlined from selected aerial photographs

Figure 23. Eel Pond inlet, 27 November 1961. Note 2 stranded groins in foreground off Washburn Island

Figure 24. Aerial photograph, 21 November 1938

the clockwise rotation of the barrier. Since more material is deposited on the pond (north) side than is removed from the sound (south) side of the spit, there has been a net increase in its width. The average width of the spit was approximately 100 feet in November 1938. In 1971 the average width of its western 800 feet was approximately 250 feet. The remaining 600 feet of the spit, to its junction with Washburn Island, was approximately 125 feet in width.

Geomorphic indicators of sediment transport within the Eel Pond/Waquoit Bay system are conflicting. A submerged flood tidal delta in Waquoit Bay indicates a flood-dominant flow, and that the inlet is acting as a sediment sink. In November 1938, Eel Pond Inlet had small ebb and flood shoals that were approximately the same size, suggesting a relatively balanced flow at that time. Since the inlet had only existed for 2 months, when the photograph was taken, it is likely that an equilibrium had not yet been reached. Northward-directed spits along the eastern shore of Eel Pond, below the Seapit River, indicate a new transport in that direction - that is, from Eel Pond toward the Seapit River. However the orientation of bedforms, visible in several photographs at the channel constriction immediately south of the Seapit River junction, indicate a southward-directed flow. This may be a reflection of higher runoff flowing through the Childs River rather than a new flow directed through the Seapit River into Waquoit Bay.

d. Aerial Photograph: 21 November 1938

This photograph was taken 2 months after the inlet to Eel Pond was formed during the hurricane of 21 September 1938 (Figure 24). As previously mentioned, small flood and ebb tidal deltas exist at either end of the inlet. The entire spit on the southwest of Washburn Island is barren sand, with little evidence of vegetation, suggesting that the barrier was subjected to massive washover during that storm. The bottom of the southern part of Eel Pond is covered with light-colored material, suggesting that a significant amount of sand was transported from Vineyard Sound and deposited in the pond. Other areas of freshly deposited sand on Washburn Island indicate overwash penetration of up to 500 feet landward of the normal shoreline.

A groin, located approximately 600 feet east of Central Avenue in Menauhant, is effectively functioning as a jetty on the west side of the inlet. Total inlet width is approximately 250 feet, although about half of the width is choked by shoals. There is a small offset to the shoreline, with the shoreline on the east side of the inlet shifted about 200 feet northward.

The west jetty at Waquoit Bay inlet has been constructed to about half of its present length. A network of three or four branching channels appears to have been recently dredged through the flood tidal delta in the bay.

e. Aerial Photograph: 24 June 1943

This photograph illustrates the extensive artificial modification undertaken during the military use of Washburn Island (Figure 25). The inlet into Eel Pond has been closed and a paved roadbed has been constructed on the barrier spit. A borrow pit approximately 500 feet wide and 600 feet long can be seen adjacent to the Menauhant Yacht Club in the area where the inlet flood tidal delta had been located in 1938. There is no indication as to how deep this borrow pit might have been, but it is clearly deeper than most other areas in the pond, where the bottom is visible in the photograph. A field of four groins, spaced approximately 400 feet apart, extends along the full length

Figure 25. Aerial photograph, 24 June 1943

of the barrier beach fronting Eel Pond.

The west jetty has been extended by about 500 feet - to its present length - and the beach to the west of this jetty has increased in width by about 100 feet since the 1938 photograph. A new channel approximately 350 feet wide and 3500 feet long has been dredged through the inlet and its flood tidal delta. Several piers - 700 to 800 feet in length - extend from the northeast shoreline of Washburn Island, and an additional access road has been constructed across the Childs River at the channel constriction to the channel. The Childs River narrows to about 150 feet at this point.

Spit growth toward the west at Bournes Pond has narrowed that inlet and resulted in a shift of its position about 200 feet westward.

f. Aerial Photograph: 6 October 1947

This photograph was taken after the inlet was reopened (Figure 26). It is assumed that this reopening occurred during the hurricane of 14-15 September 1944, although there are unconfirmed reports that the inlet was reopened artificially when Washburn Island was abandoned by the military. There is no evidence of the paved roadbed on the spit, and in most places the shoreline has eroded past its former location. The inlet width is approximately 300 feet on the Vineyard Sound side but narrows to 200 feet on the pond side. The west boundary of the inlet is offset landward by about 100 feet. The beach width on the east end of Washburn Island is essentially unchanged from its 1943 condition.

The borrow pit, described from the 1943 photograph is still apparent, with some evidence of infilling by the flood tidal shoal. Although the Vineyard Sound side of the barrier receded by about 100 feet, total barrier width was increased by 100 to 150 feet along the eastern portion. This may represent washover deposit resulting from a storm such as the 1944 hurricane. The dredged channel in Waquoit Bay is also still clearly discernible with shoaling just landward of the inlet throat. Part of this shoaling appears to be related to damage at the landward end of the east jetty, which is allowing littoral drift into the inlet from the east.

The bridge crossing the Childs River to Washburn Island has been removed. The channel width at this point is just over 100 feet. The piers on the northeast side of the island have also been removed.

g. Aerial Photograph: 22 October 1951

Between 1947 and 1951 (Figures 26 and 27) something (presumably a storm surge out of the inlet) caused the inlet to widen to many times its usual width. In the 1951 photograph Eel Pond Inlet has widened to almost 600 feet on the Vineyard Sound side, and to about 300 on the pond side (Figure 27). The inlet is also shallow with the deeper portion of the channel running along the west side. The western boundary of the inlet is still apparently controlled by the westernmost groin of the 1942 groinfield. The next groin to the east is essentially in the middle of the inlet mouth. Very little offset of the shoreline is apparent on either side of the inlet. A considerable

Figure 26. Aerial photograph, 6 October 1947

Figure 27. Aerial photograph, 22 October 1951

volume of sediment has been flushed seaward, and forms a broad shield-like shoal extending about 600 feet into Vineyard Sound, with an alongshore width of about 1000 feet. Ebb-oriented, recurved spits flank either side of the inlet in Eel Pond. The borrow pit excavated in 1942 is still discernible, although appears nearly filled. The shoreline position on the barrier to the east of the inlet has more-or-less remained unchanged or has undergone slight erosion, but the width of the barrier has increased to 250-300 feet due to continued accretion on the north side.

Four groins have either been built or rebuilt along the Menauhant shore between Eel Pond and Bournes Pond. Two of these were reportedly built in 1949 (U.S. Army Corps of Engineers, 1962). They do not appear to be trapping a significant amount of sand and give no indication of a net transport direction. The beach width to the west of the Waquoit Bay jetty has not changed appreciably since 1947. There is evidence of sand moving seaward along both jetties and either entering and/or bypassing the inlet at Waquoit Bay. A developing sand spit on the eastern side of the inlet throat indicates continued leakage through the east jetty. The dredged channel into Waquoit Bay is still discernible, although it appears to have shoaled considerably.

h. Aerial Photograph: 6 October 1970

Considerable change has occurred during the 19 years since the previous photograph (Figure 28). The inlet width has narrowed to 100 feet, or less, due to the westward growth of the barrier spit. The shoreline offset is approximately 700 feet, with the location of the inlet throat immediately adjacent to the Menauhant Yacht Club. The jetty, reportedly constructed in 1953 (U.S. Army, Corps of Engineers, 1962), is located in virtually the same position as the groin that previously controlled the western shoreline of the inlet. There is no evidence of the entrance channel reportedly dredged to a 7-foot depth two years earlier (U.S. Army Corps of Engineers, 1978). However, a dredged channel is discernible within the pond, bearing to the northeast from the inlet throat.

The width of the western 900 feet of the Washburn Island sand spit averages 250 to 300 feet. The average width of the remaining 500 feet is approximately 150 feet. The shoreline in front of the bluff just to the east of the spit, and the bluff itself, has eroded approximately 50 feet. Volume loss to the bluff alone is estimated to be approximately 11,000 cubic yards.

Twin jetties have been constructed at the entrance to Green Pond (completed in 1953; U.S. Army Corps of Engineers, 1962), and a dredged entrance channel is discernible through both the flood and ebb tidal shoals. A fillet has accumulated against the west jetty and there is evidence of a comparable erosion area to the east of this inlet.

The beach width to the west of the Waquoit Bay inlet is approximately 400 feet - essentially the same as in 1951. Shoaling just inside the channel entrance suggests that some bypassing around this inlet is occurring, although the beach immediately to the east has narrowed by about 100 feet since the 1951 photograph.

i. Aerial Photograph: 5 August 1971

Very little change has occurred since the previous photograph (Figure 29).

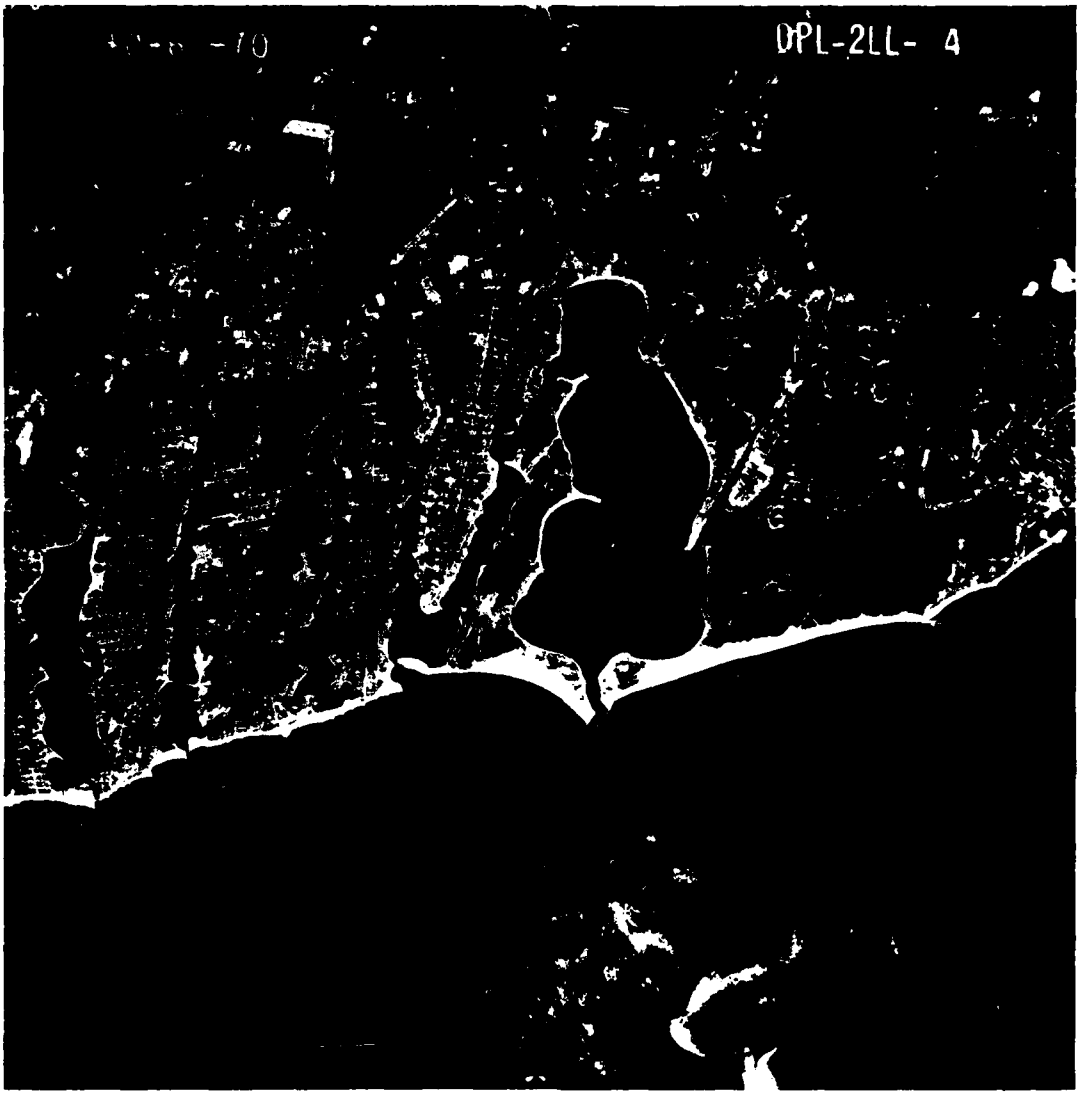

Figure 28. Aerial photograph, 6 October 1970

Figure 29. Aerial photograph, 5 August 1971

Figure 30. Aerial photograph, 20 August 1975

The inlet throat is in essentially the same position as in 1970, and has a width of approximately 100 feet. An ebb tidal delta extends from the inlet approximately 800 feet to the end of the jetty. The overall width of the barrier spit has narrowed slightly while the bluff position to the east appears unchanged. The beach width west of the Waquoit Bay jetties has not changed and material still appears to be bypassing toward the east. A shoal extending to the southeast from the seaward end of the east jetty at Waquoit Bay suggests that material bypassing the inlet does not return to shore but is diverted offshore.

j. Aerial Photograph: 20 August 1975

The shoreline and inlet positions are virtually unchanged since the 1971 photograph (Figure 30). The inlet throat is located adjacent to the Yacht Club and the width is approximately 100 feet. The ebb tidal delta has enlarged and extends beyond the seaward extent of the jetty. A linear flood shoal lies along the northwest flank of the main flood channel in the pond and is oriented to the northeast. The western tip of the Washburn Island sand spit has narrowed as a result of minor erosion of the shoreline on the Vineyard Sound side. The remainder of the Washburn Island shoreline to the Waquoit Bay jetties has remained stable. The shoal at the seaward end of these jetties does not appear to have enlarged.

3. Eolian Transport

Estimates of potential eolian sand transport rates were made in order to evaluate the contribution of this source of sediment for shoaling within Eel Pond and to evaluate the potential direct contribution of wind to the migration of the barrier spit. Using methods proposed by Bagnold (1954), Zingg (1952), and Hsu (1974), potential sand transport by wind was estimated for sand carried from Washburn Island spit and deposited either in Eel Pond or offshore. Assumptions made in these estimates included:

(1) Length of spit contributing to transport - 1000 ft.

(2) No sand stabilization by ground cover (beach grass, snow, etc.)

(3) Dry sand

(4) Mean diameter of blown sand - 0.5 mm

(5) Gradation of sand grains typical for naturally occurring sands (i.e. not uniform grain size nor gap-graded nor with an extreme range of significant grain sizes)

(6) Average spit orientation - N 68^{o} W

Wind data were taken from records for Nantucket Island for the period 1960-1969 (Figure 4). No account was taken of sand moisture. Experiments by Kadib (1964) suggest that saturated winds transport significantly less sand than dry winds (dry wind assumed in this analysis), and that a water content of 1 percent in the sand (from rain, snow, overtopping spray, etc.) would preclude sand transport by wind for the range of wind speeds in this analysis. No attempt was made to estimate the fraction of time that winds of sufficient strength to initiate sand movement

were accompanied by enough precipitation to reduce or prevent sand movement. The sand transport estimates, given below, then represent maximum expected values.

Table 4 lists the potential transport rates into Eel Pond (onshore), into Vineyard Sound (offshore), and into the inlet (onshore or offshore), computed by each of three methods. Example calculations are given in Appendix D. These data indicate that the potential contribution of windblown sand from the barrier spit to the infilling of Eel Pond could be as high as 2,400 to 5,900 cubic yards per year, and that the total potential loss from the spit ranges from 6,200 to 14,300 cubic yards per year.

A review of available aerial photographs (see preceding section) indicates that dunes on the barrier are generally covered by vegetation and that the potential eolian transport would be greatly reduced. However, following high storm surge events such as the hurricanes of 1938, 1944 and 1954, overwash has either levelled the dunes, or covered them with additional sand, as vegetation is notably absent. Until the vegetation has been reestablished, then actual eolian transport rates may approach those predicted.

4. Numerical Model

The computer program "INLET 2" was used to predict inlet velocities, discharge rates and water levels for the Eel Pond/Waquoit Bay System. This program is based on the simple spatially integrated numerical model of Seelig, Harris, and Herchenroder (1977).

The input to the model includes: 1) the geometry of the system, including inlet depths, side slopes and surface area of the bays; 2) water level fluctuations of the sea as a function of time; 3) flow nets of the inlets, including the interconnecting channel through the Seapit River; and 4) bottom friction (Manning's "n"). The program also has a provision for inflow from sources other than inlets (e.g., runoff, rivers, etc.) as a function of time. Tides may be expressed either as a sinusoidal function with a period and amplitude or they may be described by instantaneous measurements made at a constant sampling rate. Program output includes tables and plots of water elevations, velocities and discharge rate.

A complete description of the program is in Appendix E.

a. Model Setup and Calibration

Initial conditions for INLET 2 are listed in Appendix F. An ocean tidal range of 1.6 feet with a period of 12.4 hours (National Ocean Survey, 1981) was used as a sinusoidal forcing function. Bay surface areas and depths at the entrance to Waquoit Bay and the Seapit River were taken from the Falmouth topographic map (U.S. Department of Interior, 1979) and the latest navigation chart (U.S. Department of Commerce, 1981). Inlet geometry and bathymetry at Eel Pond were taken from a topographic and hydrographic survey conducted by NED in April and May 1979.

For calibration, the model was run using water elevation data obtained from Vineyard Sound during the September 1981 field trip (Figure 31). Predicted discharge velocities at the inlet throat were then compared with measured velocities. It was found that the initial calibration run underpredicted ebb-flow velocities, but overpredicted flood-flow velocities. Since the initial

Table 4. Potential Eolian Transport Rates On Washburn Spit, Falmouth Mass. (in yd^3/yr)

Sand Transport	Bagnold (1954)	Zingg (1952)	Hsu (1974)
Into Eel Pond (winds from W to SE)	4,400.	2,400.	5,900.
Into Vineyard Sound (winds from NW to E)	6,900.	3,750.	8,300.
Along Spit to Eel Pond Inlet (winds from E to SE)	425.	230.	550.
Along Spit to Washburn Island (winds from WNW)	365.	200.	485.
Total Potential Eolian Sand Loss (all directions except WNW)	11,400.	6,200.	14,300.

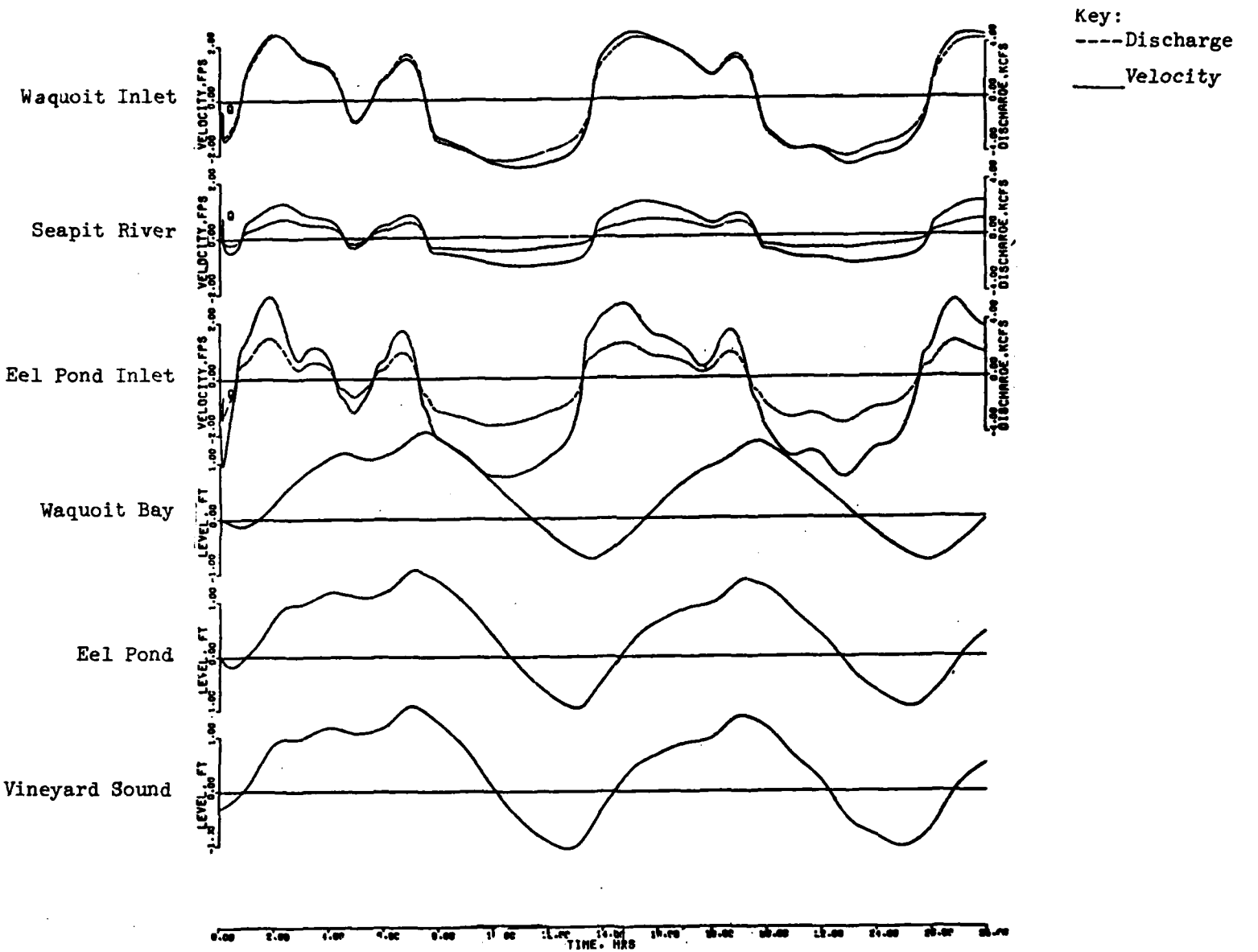

Figure 31. Calibration run of INLET 2, 500-cfs freshwater inflow

conditions did not include any freshwater inflow to the system, several runs were made varying the parameter to account for the runoff expected from the heavy rainfall that occurred during the time of field measurements. It was found that a constant inflow of 500 cubic feet per second into both Eel Pond and Waquoit Bay resulted in a reasonable calibration of the model. Therefore, no adjustments were made to the initial friction coefficient. Subsequent runs of the model, with existing and altered channel geometry, did not include the freshwater inflow parameter since this volume of runoff was not considered to represent typical conditions.

For the existing inlet geometry, the model predicts a tidal discharge volume of 2.91×10^7 cubic feet flowing through Eel Pond Inlet and 5.24×10^7 cubic feet flowing through Waquoit Bay Inlet. These values are approximately 24 percent lower for Eel Pond and 7 percent lower for Waquoit Bay than prisms predicted by O'Brien's (1931) Area vs Prism relationship. The combined prisms for both bays is 11 percent lower than those predicted using O'Brien's relationship. When compared with a total of 96 other inlets with one or no jetties, as summarized by Jarrett (1976), the tidal prisms for Eel Pond and Waquoit Bay, as predicted by INLET 2, were found to be within the 95 percent confidence limits for both Eel Pond and Waquoit Bay. The INLET 2 predictions are plotted, together with the values determined by Jarrett, for 162 other inlets in Figure 32.

The total discharge volume predicted for Eel Pond inlet by the numerical model is approximately 70 percent greater than can be accounted for by a simple computation of the tidal prism for Eel Pond alone (surface area × tide range). This indicates that the inlet is handling a significant amount of the tidal prism from Waquoit Bay. In fact, a similar computation for Waquoit Bay suggests that approximately 18 percent of the tidal prism for that bay is being channeled through Eel Pond. Flow volume predictions for the Seapit River indicate that flood flow through this interconnecting channel exceeds ebb flow by approximately 5 percent. In other words, there is a net clockwise circulation from Eel Pond into Waquoit Bay which amounts to approximately 5.62×10^5 cubic feet per tidal cycle.

The model predicts a maximum flood velocity in the Eel Pond inlet throat of 2.21 feet per second and a maximum ebb velocity of 2.11 feet per second. Further seaward, in the area of the ebb-tidal delta, maximum predicted velocities drop to less than 1.2 feet per second, with ebb velocities being somewhat higher than flood velocities.

b. Structural Changes to Inlet Hydraulics

Six combinations of possible inlet channel geometry and structures were proposed by NED for evaluation in this study. These are illustrated in Figures 33 through 38. An additional configuration that was evaluated is shown in Figure 39. Flow nets were constructed for each of these combinations, as summarized in Appendix F. The resulting INLET 2 predictions of maximum average throat velocities and discharge volumes are listed in Table 5.

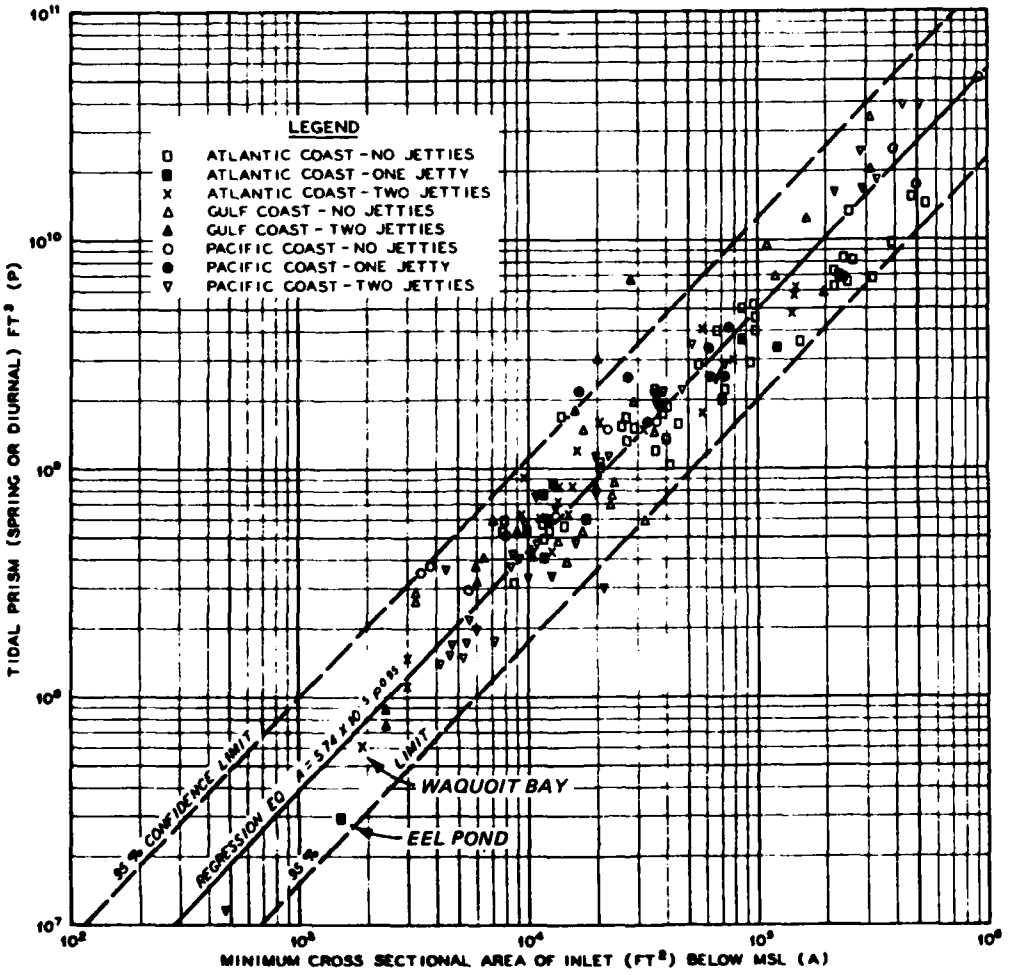

NOTE REGRESSION CURVE WITH 95 PERCENT CONFIDENCE LIMITS

Figure 32. Tidal prism versus cross-sectional area. All inlets on Atlantic, Gulf, and Pacific Coasts (after Jarrett, 1976)

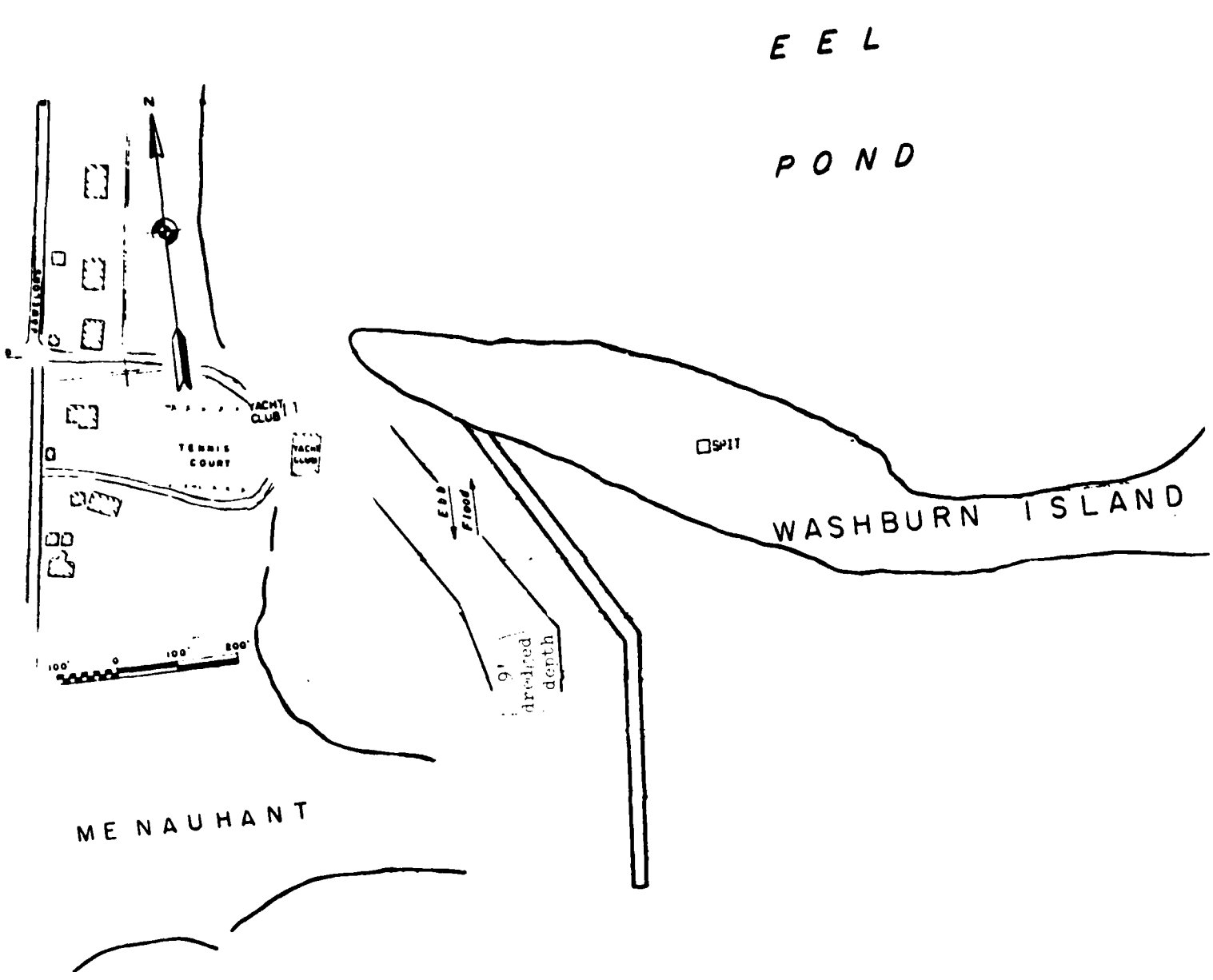

Figure 33. Proposed configuration "C1J1"

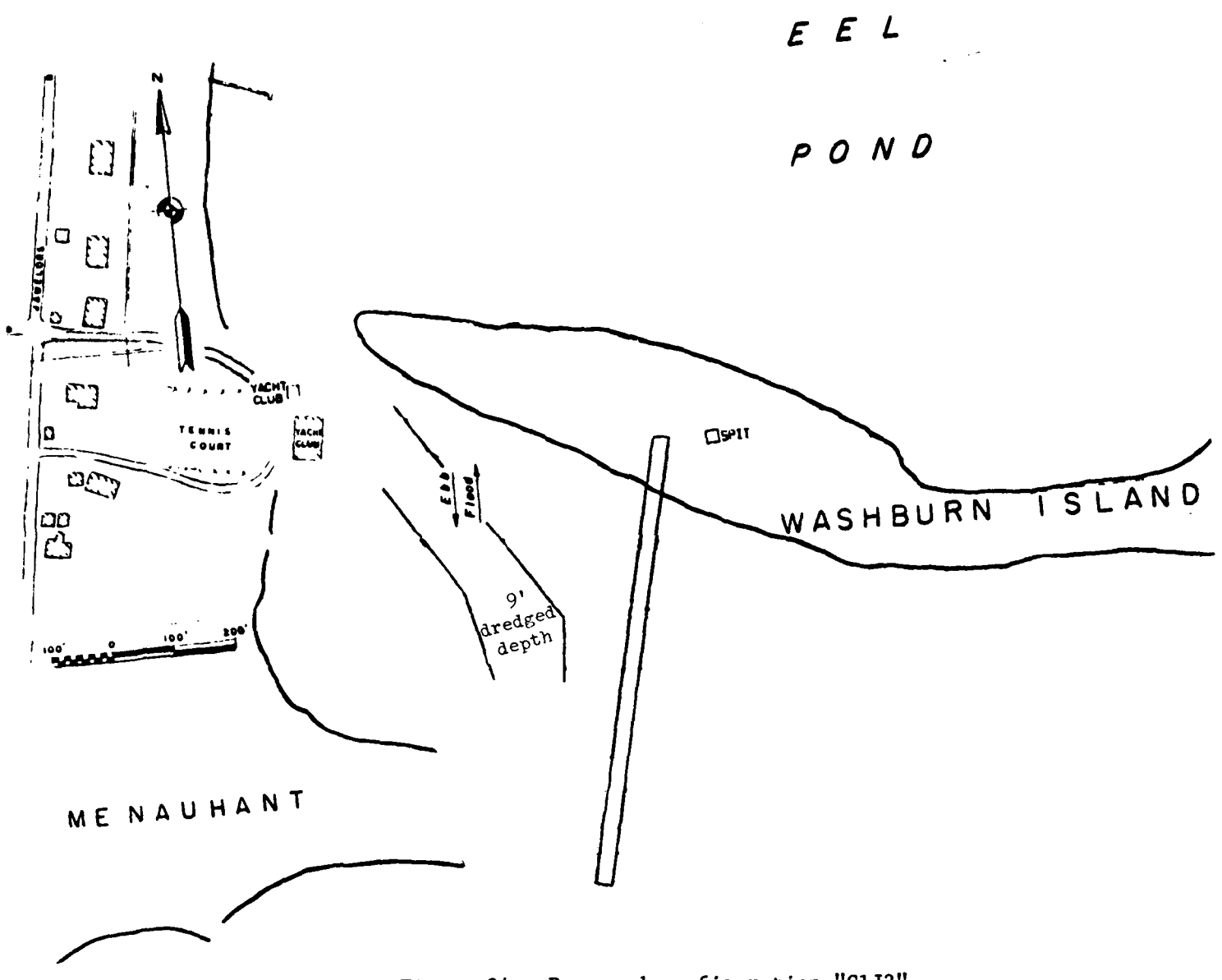

Figure 34. Proposed configuration "C1J2"

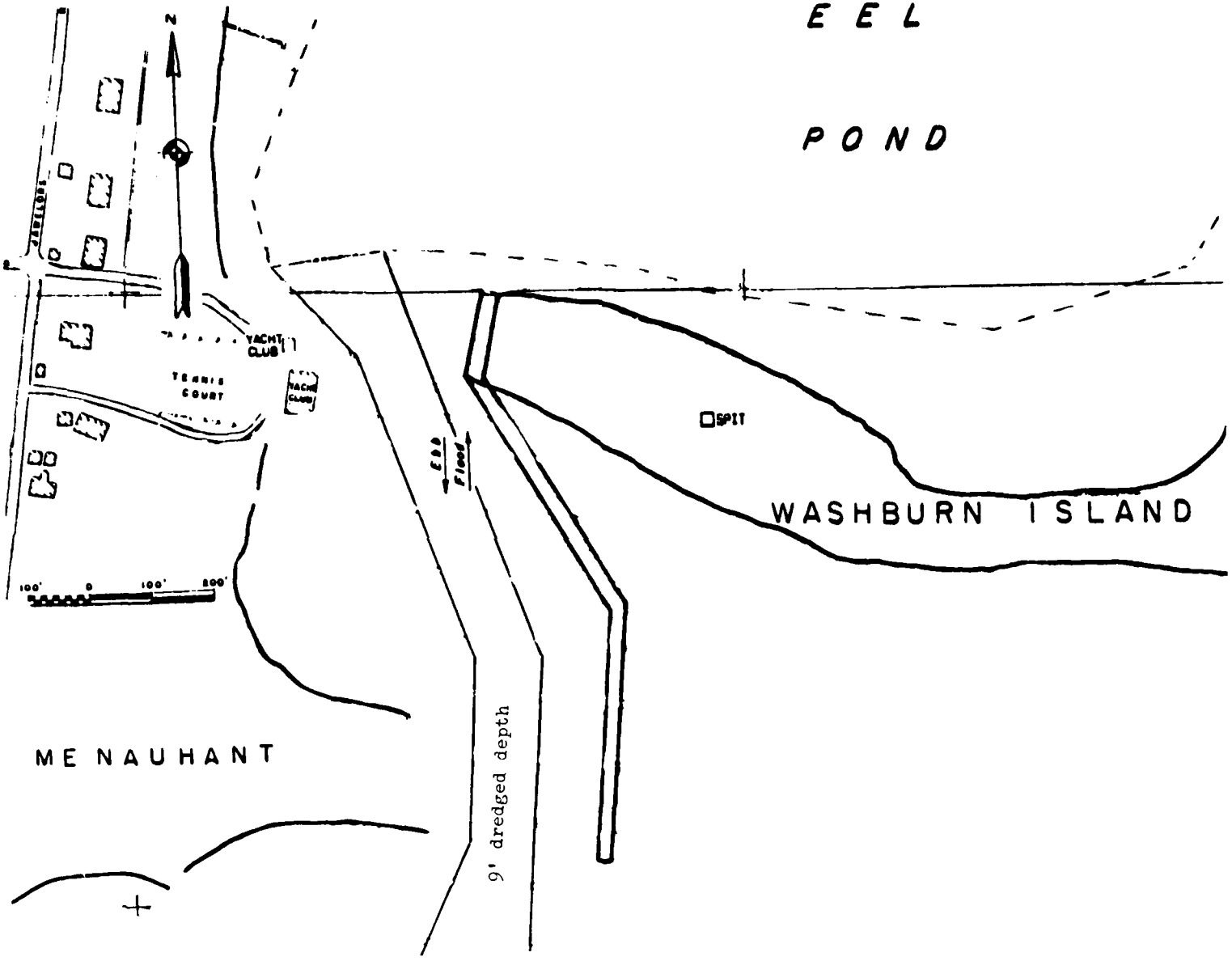

Figure 35. Proposed configuration "C2J1"

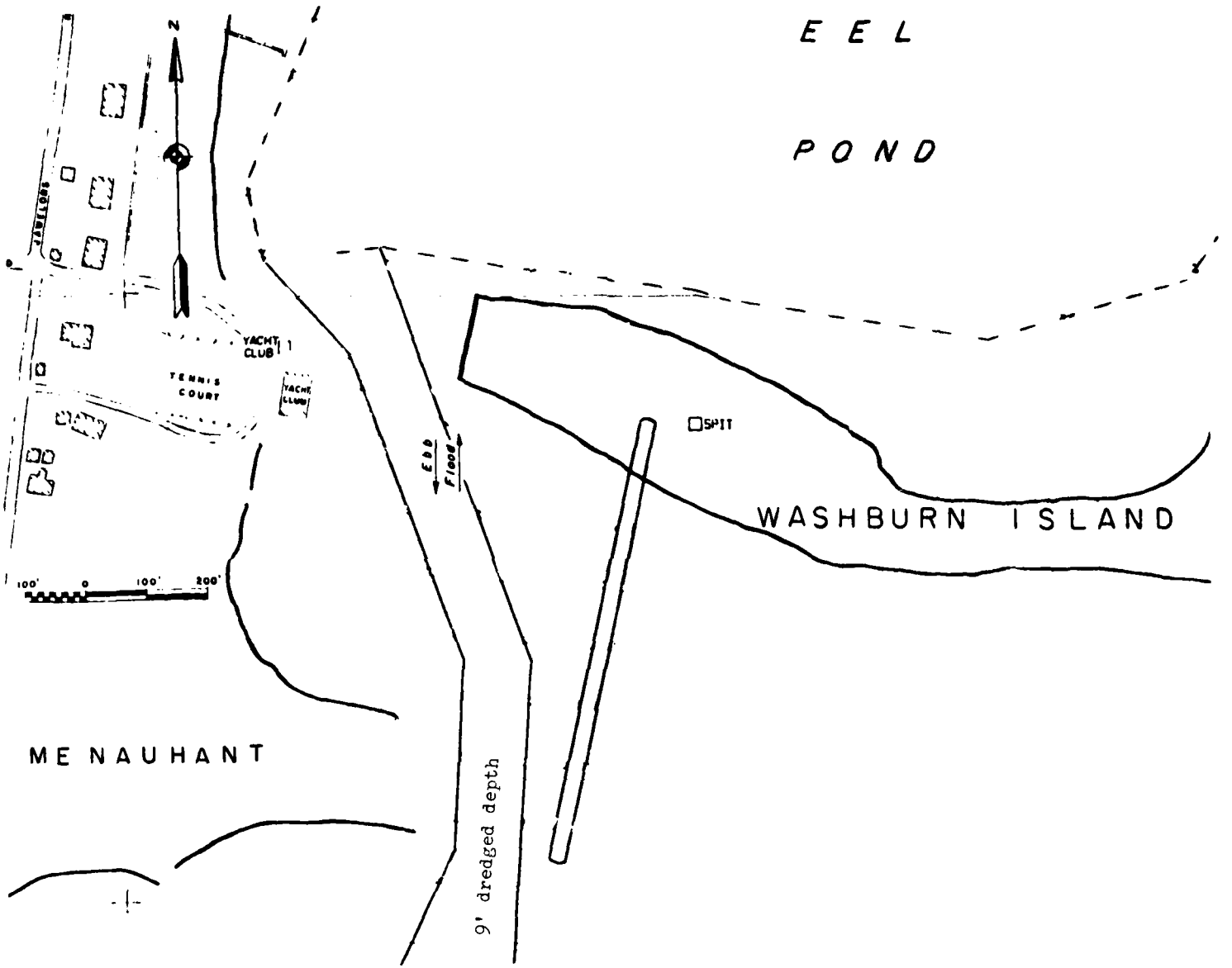

Figure 36. Proposed configuration "C2J2"

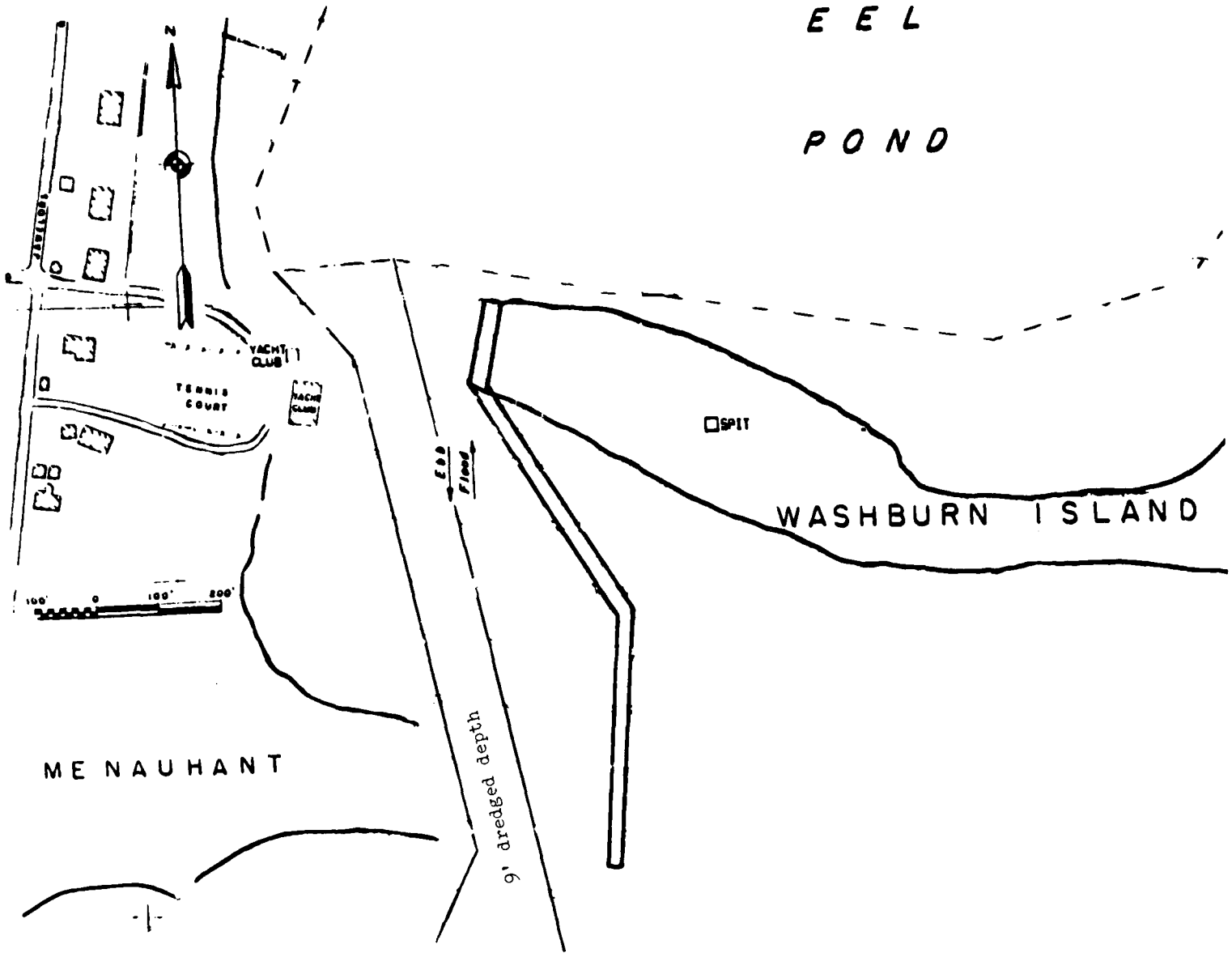

Figure 37. Proposed configuration "C3J1"

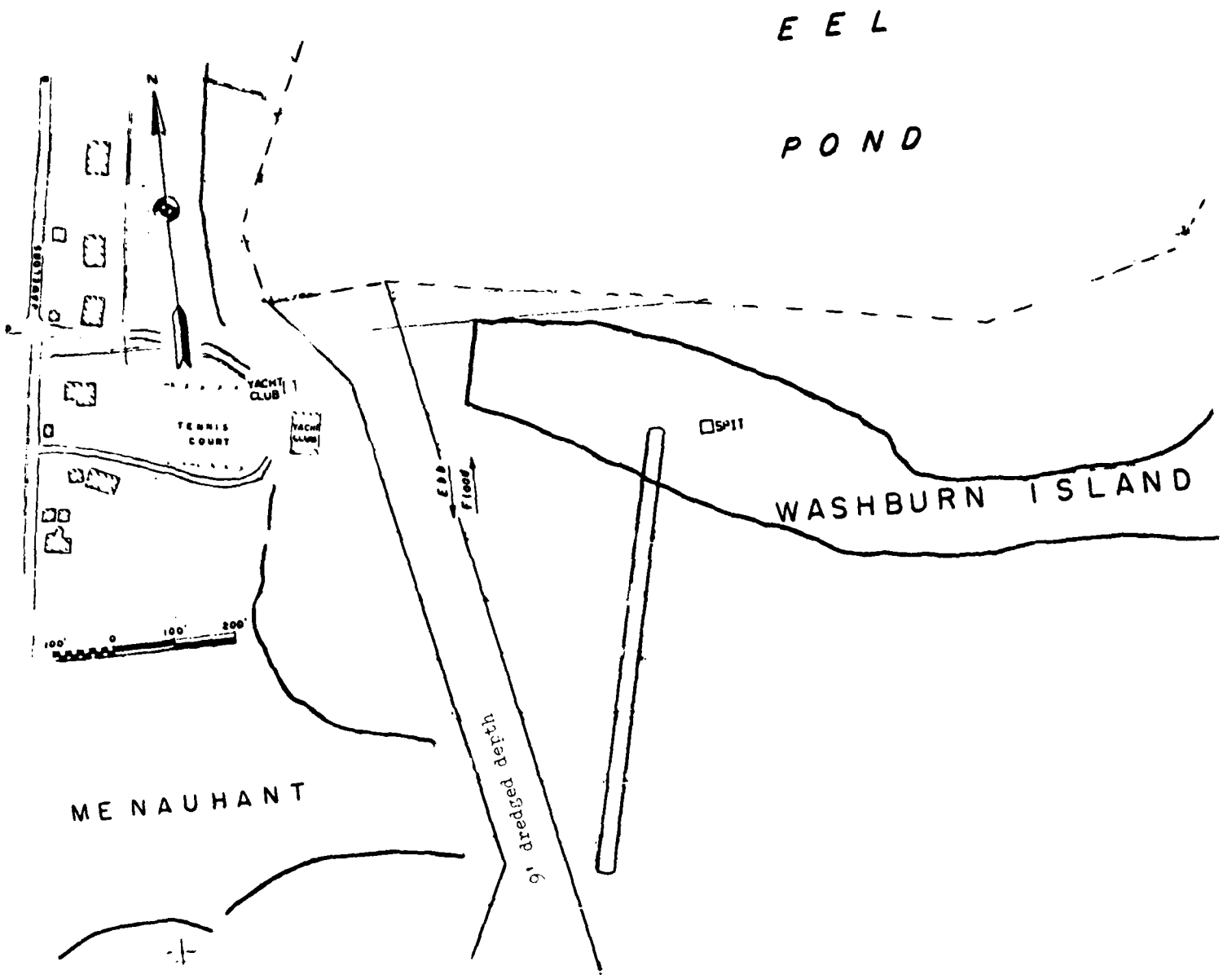

Figure 38. Proposed configuration "C3J2"

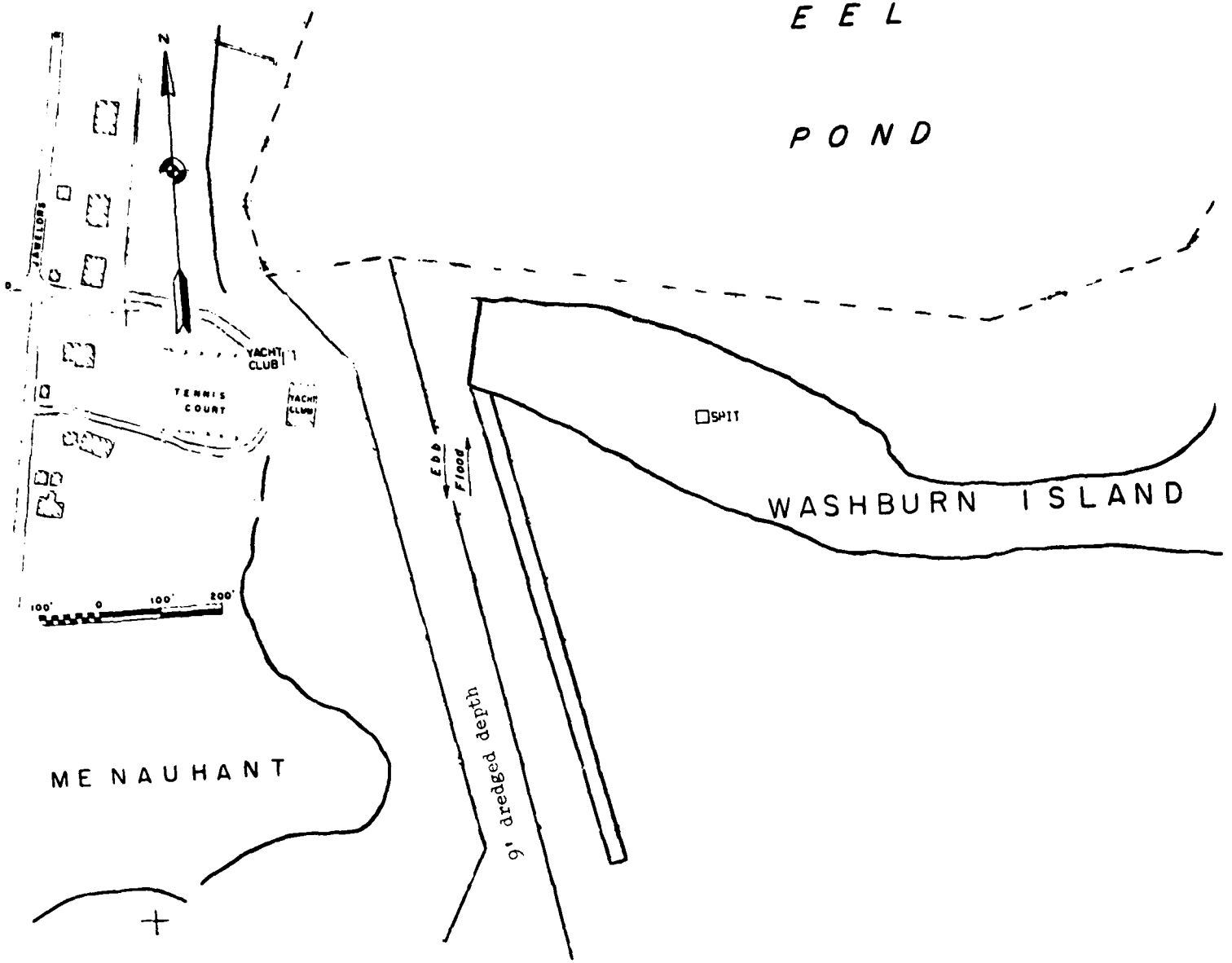

Figure 39. Proposed configuration "C3J3"

Table 5. Predicted Hydraulics of Eel Pond/Waquoit Bay

	Inlet Geometry[1]									
	Existing	C1J1	C1J2	C2J1	C2J2	C3J1	C3J2	C3J3	C2	C3
Maximum Average[2] Ebb & Flood Velocity in Eel Pond Inlet Throat (fps)	-1.51 +1.60	-1.51 +1.58	-1.65 +1.64	-1.14 +1.15	-1.18 +1.17	-1.17 +1.16	-1.24 +1.23	-1.17 +1.20	-1.15 +1.16	-1.10 +1.11
Eel Pond Inlet Average Discharge Volume ($ft^3 \times 10^7$)	2.91	2.91	2.87	3.00	3.00	3.00	3.00	2.97	3.02	3.02
Waquoit Bay Average Discharge Volume ($ft^3 \times 10^7$)	5.24	5.24	5.28	5.17	5.17	5.18	5.18	5.20	5.15	5.15
Net (Flood) Flow Volume at Eel Pond ($ft^3 \times 10^5$)	+5.62	+5.83	+5.95	+6.37	+6.46	+6.49	+6.51	+6.40	6.06	6.14
Tide Range (ft)										
Eel Pond	1.60	1.60	1.59	1.60	1.60	1.60	1.60	1.60	1.60	1.60
Waquoit Bay	1.56	1.56	1.56	1.56	1.56	1.56	1.56	1.56	1.56	1.56

Notes: 1. Refer to Figures 33 through 38 for model configurations.

2. Average maximum velocity at inlet throat during peak flow. Negative indicates ebb flow.

With the exception of channel number C1 (see Figure 33), each of the proposed changes resulted in a decrease in maximum average throat velocity and an increase in discharge volume. Channel C1, which is essentially a partially dredged channel, in combination with any of the jetties considered, actually reduces the efficiency of the existing inlet conditions. Maximum average velocity at the inlet throat remains essentially the same, or slightly increases, while predicted discharge volumes decrease. Generally, the addition of a jetty constricts the cross-sectional area of the inlet such that the "throat", the region of minimum cross-section, effectively relocated to the region near the seaward end of the jetties. This condition is particularly evident in configuration C3J3 (Figure 39). Although the maximum average velocity at the inlet throat is reduced to 1.20 feet per second, the velocity near the seaward end of the jetties increases to 1.8 feet per second.

Channel number C2, in combination with jetty number J1 (Figure 35), results in the most efficient flow characteristics of the options modelled. Maximum throat velocity is reduced by approximately 23 percent which would allow for safer navigation conditions while still maintaining sufficient velocity to scour the channel. The predicted discharge volume for this configuration increases by approximately 3 percent.

All of the proposed changes resulted in a net flood flow through Eel Pond inlet and a net ebb flow through Waquoit Bay. The combination of channel C3 and jetty J2 (Figure 38) results in the largest net flow through the system, 6.51×10^5 cubic feet per tidal cycle, which is an increase of 16 percent over existing conditions.

c. Predicted Channel Stability

An objective of this study was to predict, with some degree of confidence, the project life of a selected channel improvement scheme before additional maintenance dredging would be required. For this study, the minimum allowable depth is considered to be -6 feet, MLW. An ideal solution, obviously, would be an improved configuration that would be self-maintaining without causing detrimental effects to the adjacent shoreline. Traditional methods of predicting shoaling rates are based on hydrographic surveys and dredging records from the inlet in question, ideally, or from nearby inlets exposed to similar processes. Hayes (1982) has summarized a survey and evaluation of the currently available methods of predicting shoaling patterns in channels that cut through bars offshore of inlets. Each of the methods reviewed requires a knowledge of currents and wave climate or, at least, a good estimate of longshore transport rates. For Eel Pond none of these parameters is well-defined or documented. Very few current measurements have been made in the area, other than the few made for this study. Essentially no wave data exist, other than the limited visual observations made in 1979 and described earlier in this report.

Of the shoaling prediction methods reviewed, Galvin's (1983) was selected as the most useful for this study. Galvin derived an estimate of shoaling rates in an inlet channel based on the longshore transport rate and linear wave theory. To predict shoaling rates at dredged depths, he

derived a bypassing sediment transport ratio. The method assumes that mass transport will be the same before and after dredging and that sediment movement is a result of bottom shear due to breaking waves. Calculation of the bypassing sediment transport ratio is based on a general equation given by:

$$\text{Transport ratio} = \text{coefficient ratio} \times \text{shear ratio} \times \text{velocity ratio}$$

Assuming that the coefficient remains the same for pre- and post-dredged conditions, the transport ratio becomes:

$$\text{Transport ratio} = \text{shear ratio} \times \text{velocity ratio}$$

If the pre- and post-dredging tidal discharge remain the same, the transport ratio ultimately derives to:

$$\text{Transport ratio} = (d_1/d_2)^{5/2}$$

where d_1 = the minimum controlling depth of the ebb shoal; d_2 = the depth of the dredged channel; and $(d_1/d_2)^{5/2}$ = ratio of predredging to the post-dredging capacity of currents to transport sediment into the channel and to lift and transport it out again. For example, if the depth of the channel is doubled then the transport ratio is 0.18 and 18 percent of the littoral drift will be bypassed while 82 percent will be deposited in the channel. This quantity is assumed to be uniformly distributed along the length of the channel over an interval of time, say one month, after which a new transport ratio is computed, based on the new (shoaled) d_2. This procedure is repeated until the shoaled depth equals the original depth, d_1, or to the minimum acceptable depth for safe navigation. The number of iterations equals the number of time increments (months) required to shoal the channel.

d. Longshore Transport Estimates

A critical input to this method, as with any other method of predicting shoaling rates, is an estimate of the longshore transport rate. As is the case in most coastal areas, this is one of the most poorly documented factors. Several methods are recommended by the Shore Protection Manual (U.S. Army Corps of Engineers, 1984):

(1) estimates from dredging quantities or from impounded sediment adjacent to coastal structures,

(2) estimates made from other studies in the area,

(3) estimates using available wave data.

Dredging quantities are poorly documented for the area. Impoundment rates were estimated from analysis of aerial photographs. The fillet development to the west of the Waquoit Bay entrance was most pronounced between 1938 and 1947, and amounted to approximately 8,000 to 15,000 cubic yards per year. This represents the net west-to-east sediment transport volume. If the groin fillets, described in the June 1943 aerial photograph, developed naturally over a one-year period, then they represent a west-to-east net

transport of at least 17,000 cubic yards per year. Since each of these groins was filled and appeared to be bypassing material, this amount should be considered a minimum. The migration of the Washburn Island sand spit into Eel Pond inlet amounted to a maximum of 700 feet between 1938 and 1971. This would have required an estimated net east-to-west transport rate of approximately 4,700 cubic yards per year, assuming that sediment was transported from the seaward side of the spit, through the inlet, and deposited on the landward side of the spit.

An empirical method for estimating an upper limit of the gross longshore transport rate requires knowledge of the annual average breaker height (SPM, 1977):

$$Q_g = 2 \times 10^5 H^2$$

where H is the breaker height, in feet, and Q_g is in cubic yards per year. Using the LEO estimate of 0.54 foot as an average annual breaker height results in a predicted gross transport rate of 58,000 cubic yards per year.

A final estimate of potential net and gross transport rates was made using hindcast techniques (U.S. Army Corps of Engineers, 1981) for developing wave height and directions input for the wave energy-flux method (U.S. Army Corps of Engineers, 1977). Shallow-water wave forecasting curves were used with the 10-year wind data set from Nantucket Island. Due to the extremely complicated bathymetry in Nantucket and Vineyard Sounds, this technique is probably the least reliable. The computational procedure is presented in Appendix D. This method resulted in a computed potential gross transport rate of approximately 100,000 cubic yards per year and a net west-to-east transport rate of 30,000 cubic yards. Assuming that the empirical method of gross transport rate is a more reasonable estimate of the actual value, the transport rates computed by the wave energy flux method were reduced by 50 percent for computation of shoaling rates.

5. Shoaling Rate Prediction

Using a computed potential gross longshore transport rate of 50,000 cubic yards per year, shoaling rates were predicted for each of the three channel configurations proposed by NED. These computations assumed that all of the potential longshore drift (Q_g) will enter the channel and that the pre- and post-dredging discharge volumes will remain the same. Example computations are presented in Appendix H.

The predicted shoaling rates are listed in Table 6. These predictions show that for a dredging-only solution, the channel could potentially shoal to the minimum allowable depth within 7 months. The addition of a jetty would be expected to increase project life considerably by:

(1) Preventing littoral drift from entering the navigation channel and,

(2) increasing the flushing capacity of the tidal currents by channelizing flow.

Table 6. Predicted Shoaling Times for Selected Channel Configurations

Channel*	Dredged Depth, ft MLW	Dredged Volume, yd^3	Shoaled Depth, ft MLW	Time Interval months
C1	9	28,400	7.5	1
			6.4	2
			5.6	3
C2	9	68,300	8.3	1
			7.8	2
			7.3	3
			6.8	4
			6.4	5
			6.1	6
			5.8	7
C3	9	57,000	8.3	1
			7.7	2
			7.2	3
			6.7	4
			6.3	5
			6.0	6

* Channel as shown in Figures 33 through 38, with no jetties in place.

IV. DISCUSSION

The preceding sections of this report have discussed the detailed results developed during this study which pertain to the shoaling problem in Eel Pond inlet. The following sections will review the important results, in the perspective of alternative solutions.

1. Stability of Existing Inlet

Although historical records dating back to at least 1845 show Eel Pond inlet closed until 1938, the fact that it has remained open essentially continuously since that time suggests that the inlet probably was opened earlier as well. The location of the inlet is more or less at the convergence of two lines defined by the axes of the two arms of upper Eel Pond. Ebb flow, especially that coming through the Seapit River from Waquoit Bay, is effectively aimed toward the southwest side of the pond. Both the 1938 and 1944 breaches were on this side of the pond and the inlet has tended to hold this position. The relative stability of the inlet and spit geometry for at least 13 years since 1970 suggests that, barring a major storm, the system will remain in its state of equilibrium. A hurricane similar to those witnessed in 1938 and 1944 would probably cause the inlet to widen and migrate somewhat further east, ultimately to return to a position similar to the present one.

2. Sediment Transport

Until the wave climate in Vineyard and Nantucket Sounds is better defined, the average annual net and gross longshore transport rates can be regarded as little more than a guess. An estimate of the gross longshore transport rate, based on visual wave observations, suggests that the magnitude is less than 50,000 cubic yards per year. It should be noted that this is a maximum potential transport rate, and that limits on sediment supply would be expected to result in a lower rate. The net direction of longshore sediment transport is from west to east in the general vicinity of Eel Pond. Filling adjacent to the west jetty at Waquoit Bay and at other structures suggests that the magnitude of net transport is between 8,000 and 15,000 cubic yards per year.

Figure 40 is a summary of sediment transport patterns apparent from this study and, for the case of the westerly directed arrow to the east of Waquoit Bay, from other studies (Strahler, 1966). It is clear that, in its present configuration, Eel Pond is acting as a sediment sink. Although the net transport is directed from west to east, the bulk of the sediment presently entering the inlet is coming from the east and is probably derived from erosion of the glacial bluff on Washburn Island. The bottom current data collected just offshore of the inlet indicate a potential for onshore transport of sediment from the nearshore shelf as well. Active current-oriented ripples observed in this region also support this conclusion. An undetermined quantity of sediment is transported into Eel Pond as overwash deposits during severe storms. Eolian sand transport from the Washburn Island spit into Eel Point may also be significant, particularly following severe storms, until damaged vegetation has been reestablished.

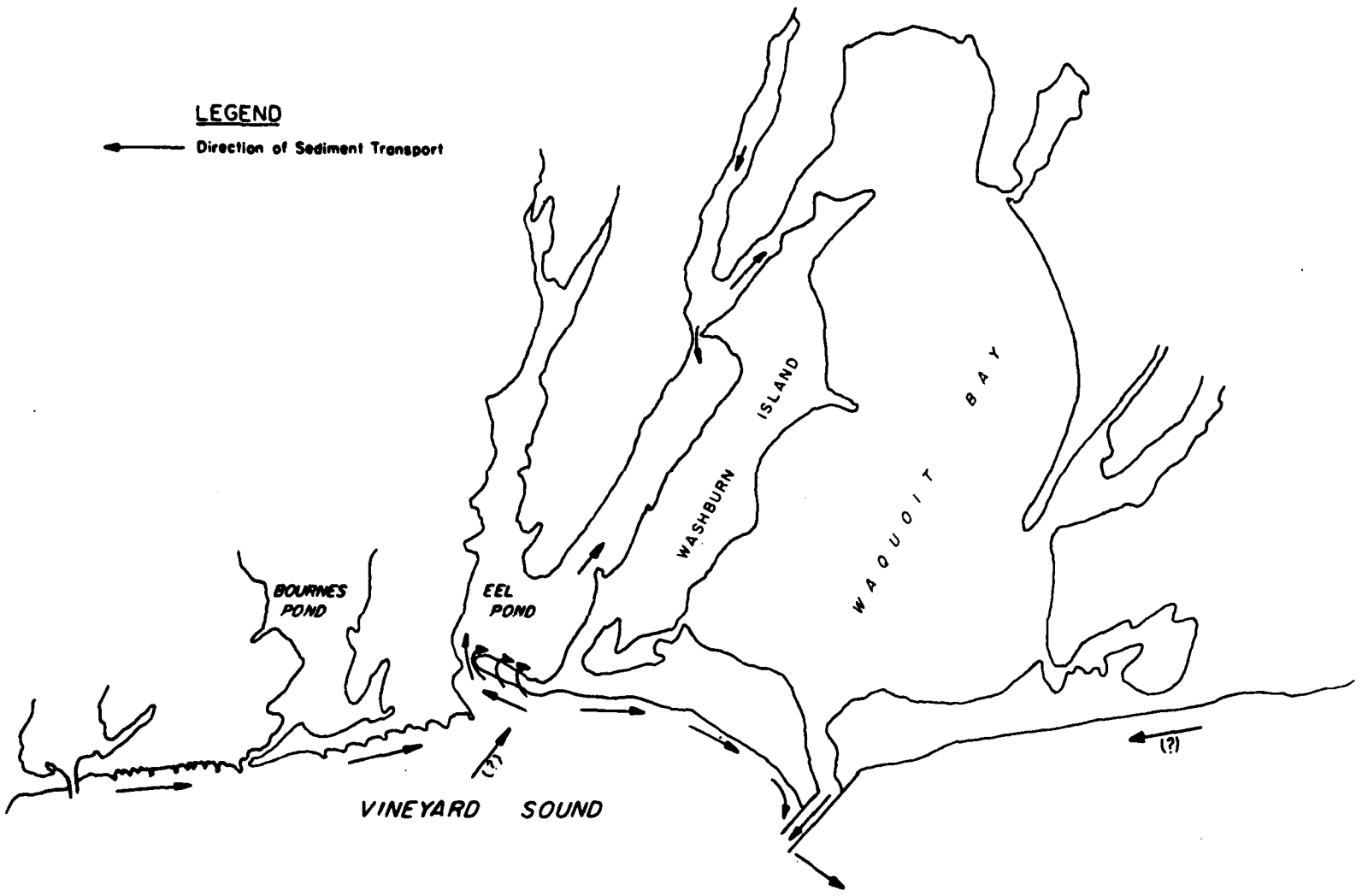

Figure 40. Sediment transport patterns, Eel Pond, Mass.

The existence of a large flood tidal delta inside Waquoit Bay inlet suggests that this inlet functions as a sediment sink also. However, the persistence of channels dredged through this delta before 1938 and in 1942 indicates that the shoal predates the 1938 opening of Eel Pond inlet, particularly in light of the strong ebb-dominant flow predicted by the numerical model. It appears that, prior to 1938, Waquoit Bay inlet was flood-dominant and developed the large ebb tidal delta. Once Eel Pond inlet was opened, a resulting net-clockwise flow pattern was established, causing a reversal in dominant flow at Waquoit.

In contrast, channels dredged through the entrance to Eel Pond rapidly fill. For example, the channel dredged in 1968 has apparently totally filled and is not discernible in the October 1970 aerial photograph.

3. Causes of Shoaling

As sediment is transported toward the entrance to Eel Pond, primarily from the east along the Washburn Island barrier spit, it is entrained by the flood tidal flow and quickly carried through the inlet throat. Once in the pond, where the current is no longer confined, flow is dispersed and sediment is dropped out of suspension. Some of this sediment is deposited in the area just to the north of the Menauhant Yacht Club, while much of it is carried around the spit to the east and deposited on the back side of the barrier. During ebb flow, some material is transported back through the inlet and deposited on an ebb shoal just seaward of the inlet throat, as the flow disperses.

At present, the sediment supply from the west of Eel Pond does not appear to be a significant factor to shoaling in the inlet. Beaches along the Menauhant shoreline are generally sand-starved and groins constructed in the late 1940's are still not filled. Much of the sediment presently on this section of beach has been placed as fill removed from Eel Pond in 1956, 1962, and 1967.

4. Recommended Improvements

It is clear that a dredge-only approach would be a temporary solution to the shoaling problem at Eel Pond. Past experience, as well as predicted shoaling rates, indicate that each of the alternative channels would be essentially filled to the minimum 6-foot depth in less than one year, as a conservative estimate. The addition of an east jetty will have the principal benefit of prohibiting material from entering the channel. This will not only greatly extend the channel life, but will also keep the bulk of the potential sediment influx out of any dredged anchorage areas planned within Eel Pond. The proposed configuration of channel C2 and jetty J1 (Figure 35) results in the most efficient hydraulic characteristics of the options modelled. This also offers the most desirable flow characteristics from a navigational standpoint. A realignment of this jetty to more closely parallel the existing jetty, such as illustrated in Figure 39, would more effectively train the flow through the inlet gorge. However, this alignment may actually increase the maximum flow velocity through the

inlet and will lengthen the distance over which this velocity is maintained.

Additionally, it is recommended that the sand-sized dredged material (which should include most of the project from the ebb tidal delta to the inlet throat and a good portion of the anchorage area in the vicinity of the flood tidal delta) be used to increase the dune elevation and spit width from the proposed jetty eastward to the eroding glacial bluff. The dune areas should then be stabilized with American beach grass (Ammophila Breviligulata, see Knutson, 1980). This will reduce the risk of overtopping of the spit and the potential for opening a new inlet in this region.

5. Effects on Net Circulation

The recommended channel improvements would increase the net circulation from Eel Pond through the Seapit River and into Waquoit Bay by an estimated 16 percent. The increased efficiency of Eel Pond inlet would result in a slight decrease (approximately one percent) in the discharge volume at Waquoit Bay inlet.

Channel improvements are not expected to have an appreciable effect on salinity levels within the pond. Salinity measurements obtained by the Washburn Island Preserve Limited Partnership (1982) indicate salinity levels in Waquoit Bay are similar to levels in Vineyard Sound.

REFERENCES CITED

AUBREY, D. G., and GAINES, A. G., Jr. 1972. "Recent Evolution of an Active Barrier Beach Complex: Popponesset Beach, Cape Cod, Massachusetts," WHOI Technical Report 82-3.

BAGNOLD, R. A. 1954. The Physics of Blown Sand and Desert Dunes, Methuen and Co., Ltd.

BARWIS, J. H. 1975. "Catalog of Tidal Inlet Aerial Photography," General Investigation of Tidal Inlets, Report 2, US Army Engineer Waterways Experiment Station, Vicksburg, Miss.

GALVIN, C. 1983. "Shoaling with Bypassing for Channels at Tidal Inlets," unpublished manuscript, PO Box 623, Springfield, Va.

HARRIS, D. L. 1963. "Characteristics of the Hurricane Storm Surge," Technical Paper No. 48, US Weather Bureau, Washington, DC.

HAYES, M. A. 1982. "Prediction of Deposition Rates in Channels Dredged Through Bars Offshore of Inlets--Review of Literature," CERC unpublished manuscript.

HICKS, S. D., DeBAUGH, H. A., Jr., and HICKMAN, L. E., Jr. 1983. "Sea Level-Variations for the United States, 1855-1980," National Ocean-Service, Rockville, Md.

HSU, S. A. 1974. "Computing Eolian Sand Transport from Routine Weather Data," Proceedings of Fourteenth Coastal Engineering Conference, ASCE.

JARRETT, J. T. 1976. "Tidal Prism-Inlet Area Relationships," General Investigation of Tidal Inlets, Report 3, US Army Engineer Waterways Experiment Station, Vicksburg, Miss.

KADIB, ABDEL-LATIF. 1964. "Sand Movement by Wind," Addendum II to CERC Technical Memorandum No. 1.

KNUTSON, P. L. 1980. "Experimental Dune Restoration and Stabilization, Nauset Beach, Cape Cod, Massachusetts," CERC Technical Paper No. 80-5.

MASSACHUSETTS DEPARTMENT OF ENVIRONMENTAL MANAGEMENT. 1980. "Washburn Island, a Landscape Analysis," Office of Planning and Program Development.

MEANY, C. C. 1949. "Mean Sea Level--a Basic Engineering Datum," Journal of the Coast and Geodetic Survey, Vol 2, pp 34-37.

NATIONAL OCEAN SURVEY. 1981. National Oceanic and Atmospheric Administration, "1981 Tide Tables, East Coast of North and South America, Including Greenland."

O'BRIEN, M. P. 1931. "Estuary Tidal Prisms Related to Entrance Areas," Civil Engineering, Vol 1, No. 8, pp. 738-739.

REDFIELD, A. C. 1980. Introduction to Tides, Marine Science International, Woods Hole, Mass.

SCHNEIDER, C. 1982. "The Littoral Environment Observation (LEO) Data Collection Program," CERC Coastal Engineering Technical Aid, No. 81-5.

SEELIG, W. N., HARRIS, D. L., and HERCHENRODER, B. E. 1977. "A Spatially Integrated Numerical Model of Inlet Hydraulics," General Investigation of Tidal Inlets, Report 14, US Army Engineer Waterways Experiment Station, Vicksburg, Miss.

SEELIG, W. N. 1977. "Stilling Well Design for Accurate Water Level Measurement," CERC Technical Paper No. 77-2.

SKIDMORE, OWINGS, and MERRILL. 1982. "Washburn Island Preserve," Draft Environmental Impact Report, EOEA 4259.

SOUTHARD, J. B. 1981. "Further Studies of Tidal-Current Sand Waves," MIT Final Technical Report No. OSP. 85979, Cambridge, Mass.

STRAHLER, A. N. 1966. A Geologist's View of Cape Cod, The Natural History Press, Garden City, N. Y.

SZUWALSKI, A. 1972. "Coastal Imagery Data Bank: Interim Report," CERC Miscellaneous Paper 3-72.

US ARMY CORPS OF ENGINEERS. 1962. "Beach Erosion Control Report of Cooperative Study of Falmouth, Massachusetts," US Army Engineer Division, New England.

US ARMY CORPS OF ENGINEERS. 1978. "Eel Pond, Falmouth, Massachusetts, Small Boat Navigation Project Reconnaissance Report, US Army Engineer Division, New England.

US ARMY CORPS OF ENGINEERS. 1981. "Revised Method for Wave Forecasting in Shallow Water," CERC Coastal Engineering Technical Note No. I-6.

US ARMY CORPS OF ENGINEERS. 1977. Shore Protection Manual, US Army Engineer Waterways Experiment Station, Vicksburg, Miss.

US DEPARTMENT OF COMMERCE. 1981. "South Coast of Cape Cod and Buzzards-Bay, Massachusetts," National Ocean Survey, Nautical Chart 13229.

US DEPARTMENT OF COMMERCE. 1982. U.S. Coast Pilot, Vol 2, Atlantic Coast: Cape Cod to Sandy Hook, National Ocean Survey.

US DEPARTMENT OF INTERIOR. 1972. "Falmouth, Massachusetts," US Geological Survey Information Pamphlet INF-72-24.

US DEPARTMENT OF INTERIOR. 1979. "Falmouth, Massachusetts," US Geological Survey Topographic Map, 7.5-Minute Series, N4130-W7070/7.5.

ZINGG, A. W. 1952. "Wind Tunnel Studies of the Movement of Sedimentary-Material," Proceedings of Fifth Hydraulics Conference.

APPENDIX A: CURRENT MEASUREMENTS FROM VINEYARD SOUND

Date: Tuesday, 15 Sep 1981

Time (EDT)	Speed (fps)	Direction (True North)
1500		316
1530	.20	312
1600	.28	298
1630	.50	243
1700	.42	235
1730	.45	239
1800	.31	200
1830	.38	62
1900	.59	65
1930	.74	66
2000	.71	74
2030	.74	69
2100	.63	67
2130	.60	63
2200	.47	59
2230	.38	63
2300	.35	65
2330	.24	66
2400	.18	49

Date: Wednesday, 16 Sep 1981

Time (EDT)	Speed (fps)	Direction (True North)
0030	.07	37
0100	.33	317
0130	.59	297
0200	.87	292
0230	.95	296
0300	.75	308
0330	.28	326
0400	.14	310
0430	.40	329
0500	.31	331
0530	.15	13
0600	.20	52
0630	.29	76
0700	.47	73
0730	.57	72
0800	.57	73
0830	.73	68
0900	.70	67
0930	.54	64
1000	.50	66
1030	.45	71
1100	.25	67
1130	.25	67
1200	.17	71
1230	.08	276
1300	.21	283
1330	.56	297
1400	.82	298
1430	.87	300
1500	.70	303
1530	.46	318
1600	.18	331
1630	.06	311
1700	.15	328
1730	.13	27
1800	.11	55
1830	.11	131
1900	.27	196
1930	.49	99
2000	.61	74
2030	.60	80
2100	.78	75
2130	.60	72
2200	.54	71
2230	.46	69
2300	.35	64
2330	.36	66
2400	.22	72

Date: Thursday, 17 Sep 1981

Time (EDT)	Speed (fps)	Direction (True North)
0030	.25	63
0100	.18	31
0130	.14	22
0200	.50	303
0230	.80	293
0300	.91	293
0330	.82	300
0400	.59	303
0430	.21	320
0500	.10	313
0530	.13	315
0600	.11	24
0630	.10	188
0700	.29	167
0730	.35	82
0800	.53	80
0830	.71	75
0900	.66	71
0930	.61	70
1000	.71	70
1030	.40	68
1100	.33	67
1130	.29	73
1200	.31	75
1230	.22	74
1300	.15	62
1330	.01	65
1400	.25	298
1430	.56	292
1500	.80	278
1530	.95	294

EEL POND, MASSACHUSETTS DATA
STATION EPC S/N 699
15 SEP 1981 - 17 SEP 1981

APPENDIX B: HOURLY TIDAL CURRENT MEASUREMENTS

Date/Time (EDT)	Station A		Station B		Station C	
	Depth (Ft, SWL)	Velocity[1] (Fps)	Depth (Ft, SWL)	Velocity[1] (fps)	Depth (Ft, SWL)	Velocity[1] (fps)
16 Sep 81/1130	9.0	1.87	14.6	1.60	7.2	1.28
	6.6	1.94	10.2	1.65	5.4	1.17
	2.2	1.58	3.4	1.35	1.8	1.24
1200	5.6	0.40	6.4	0.99	6.4	1.17
	4.2	0.40	4.6	0.76	4.6	0.58
	1.4	0.47	1.6	0.76	1.6	0.80
1300	9.6	1.54	8.8	2.13	12.2	---[2]
	7.2	1.58	6.6	2.39	8.4	2.28
	2.4	1.61	2.2	2.68	2.8	2.28
1400	10.4	1.13	9.6	0.76	6.5	0.21
	7.8	1.17	7.2	0.84	4.8	0.47
	2.6	1.13	2.4	0.62	1.6	0.62
1500	8.8	-1.72	10.4	-1.83	8.0	-1.50
	6.6	-1.35	8.4	-1.80	6.0	-2.35
	2.2	-1.24	2.8	-1.91	2.0	-2.83
1600	8.8	-3.01	13.6	-3.01	9.6	-3.38
	6.6	-2.79	10.2	-3.09	7.2	-3.31
	2.2	-1.50	3.4	-3.23	2.4	-3.09
1700	9.0	-3.97	12.8	-4.19	8.8	-4.01
	7.0	-4.08	9.6	-4.08	6.6	-4.05
	2.5	-2.50	3.2	-3.79	2.2	-3.86
1800	8.8	-4.01	12.8	-4.23	7.2	-3.71
	6.6	-3.86	9.6	-4.30	5.4	-4.16
	2.2	-2.13	3.2	-4.12	1.8	-3.90

Eel Pond - 2

Date/Time (EDT)	Station A Depth (Ft, SWL)	Station A Velocity[1] (fps)	Station B Depth (Ft, SWL)	Station B Velocity[1] (fps)	Station C Depth (Ft, SWL)	Station C Velocity[1] (fps)
1900	8.0	-3.23	10.2	-3.38	6.4	-0.34
	6.0	-3.13	8.4	-3.38	4.8	-0.35
	2.0	-1.91	2.8	-3.38	1.6	-0.36
2000	8.0	-0.91	10.4	-1.35	4.8	-0.88
	6.0	-0.95	7.8	-1.17	3.6	-0.76
	2.0	-1.02	2.6	-1.13	1.2	-0.49
2100	8.0	3.05	12.8	2.79	8.8	1.76
	6.0	3.35	9.6	3.09	6.6	2.06
	2.0	3.09	3.2	3.01	2.2	1.83
2200	7.2	3.35	13.6	3.27	12.0	1.39
	5.4	3.46	10.2	3.23	9.0	2.28
	1.8	3.31	3.4	3.27	3.0	2.90
2300	8.0	2.87	13.6	2.57	11.2	---[2]
	6.0	2.79	10.2	2.72	8.4	1.32
	2.0	2.65	3.4	2.72	2.8	1.72
2400	8.0	1.80	15.2	1.65	5.6	1.10
	6.0	1.94	11.4	1.87	4.2	1.17
	2.0	1.94	3.8	1.94	1.4	1.13
17 Sep 81/0100	10.8	1.21	12.8	1.47	8.8	0.43
	8.0	1.43	9.6	2.09	6.6	0.65
	2.7	1.50	3.2	2.09	2.2	0.51
0200	8.8	2.46	15.2	2.39	7.2	0.47
	6.6	2.65	11.4	2.57	5.6	0.62
	2.2	2.65	3.8	2.42	1.8	0.62
0300	10.4	-0.51	13.6	-1.17	8.0	-1.87
	7.8	-0.51	10.2	-1.50	6.0	-1.91
	2.8	-0.69	3.4	-1.54	2.0	-1.87

Date/Time (EDT)	Station A		Station B		Eel Pond - 3 Station C	
	Depth (Ft, SWL)	Velocity[1] (fps)	Depth (Ft, SWL)	Velocity[1] (fps)	Depth (Ft, SWL)	Velocity[1] (fps)
0400	9.6	-2.72	12.8	-2.79	7.2	-2.94
	7.2	-2.76	9.6	-2.79	5.6	-2.90
	2.4	-1.87	3.2	-2.76	1.8	-2.87
0500	9.6	-3.09	12.8	-3.60	7.2	-3.05
	7.2	-3.27	9.6	-3.71	5.4	-3.82
	2.4	-2.06	3.2	-3.71	1.8	-3.60
0600	8.8	-2.42	12.4	-4.27	6.4	-4.01
	6.6	-3.01	9.6	-4.30	4.8	-3.97
	2.2	-2.28	3.2	-4.08	1.6	-3.97
0700	8.8	-3.09	13.0	-2.98	6 4	-2.46[2]
	6.6	-3.01	9.0	-3.01	4.8	- - -[2]
	2.2	-2.90	3.0	-3.12	1.6	-2.61
0800	10.4	-1.10	12.8	-3.31	5.6	-0.29
	7.8	-1.28	9.6	-1.21	4.2	-0.29
	2.6	-0.84	3.2	-1.13	1.4	-0.36
0900	8.0	3.01	14.4	2.90	6.4	2.28
	6.0	3.12	10.8	3.16	4.8	2.35
	2.0	3.01	3.6	3.23	1.6	2.79
1030	8.0	3.64	13.6	3.20	7.2	1.39
	6.0	3.71	10.2	3.42	5.4	1.24
	2.0	3.75	3.4	3.38	1.8	0.99
1130	8.8	2.78	13.6	2.28	8.0	2.09
	6.6	2.90	10.2	2.46	6.0	2.24
	2.2	2.72	3.4	2.46	2.0	1.83
1230	9.6	1.50	12.0	1.65	9.6	0.84
	7.2	1.58	9.0	1.61	7.2	1.17
	2.4	1.61	3.0	1.58	2.4	1.43

Notes: 1. + = Flood current
- = Ebb current

2. No data.

APPENDIX C: AERIAL PHOTOGRAPHS DEPICTING THE POPPONESSET BEACH AREA

Table C1. Aerial Photographs Depicting the Popponesset Beach Area. (For Information on Depositories See Table C2) (From Aubrey and Gaines, 1982)

Date	Scale	Source	Depository	Frame Numbers[1]
21 Nov. 1938	1:24,000	USGS	NARS	95, 97, 102, 104, 106, 107, 109
18 Dec. 1940	1:20,020	USAF	NARS	13, 15, 26, 27, 38, 107
24 June 1943	1:25,000	USAF	NARS	2, 21, 20, 23, 28, 30, 5, 7, 61 110
6 Oct. 1947	1:24,500	USAF	NARS	16, 17, 19, 21, 32, 33, 34
Oct. 1949	1:18,000	LAPS	LAPS	3
19 Oct. 1949	1:40,500	USAF	NARS	3, 25, 45
22 Oct. 1951	1:20,250	USDA	WHOI (DGA)	16, 38, 40
23 Oct. 1951	1:9,800	USC&GS	NOS	66, 67, 76, 78, 80, 82
26 July 1952	1:66,200	RAS	RAS	
15 Nov. 1955	1:30,200	USC&GS	NOS	1, 15, 17, 53, 57
6 May 1960	1:63,750	USAF	NARS	30, 31, 32, 33
2 May 1960	1:7,600	TDG	TDG	26
2 May 1960	1:7,600	TDG	TDG	1581, 1705, 1576 1499, 1096, 1143 1654, 1652, 1647, 1649, 1707
12 April 1961	1:29,900	USC&GS	NOS	45, 46, 47, 48, 49, 50
11 April 1962	1:24,242	USC&GS	NOS	71, 72, 73, 74, 78, 79, 80
1 April 1965	1:40,000	LKBI	LKBI	12, 13, 14, 15, 16
13 Sept. 1969	1:120,000	NASA	EROS	8
6 Oct. 1970	1:40,000	USDA	USDA	3, 33
29 Oct. 1970	1:40,000	USDA	USDA	9, 10, 11
5 Aug. 1971	1:20,000	USDA	USDA	15, 16, 17, 24, 29, 30, 31, 32, 42, 51, 52
27 May 1972	1:40,000	LKBI	LKBI	271, 272, 406, 407, 408, 409
25 March 1973	1:22,600	USGS	EROS	15, 16, 17, 21, 22, 23, 24, 25
25 March 1973	1:132,400	KAS	KAS	
15 March 1974	1:9600	COL	COL	19, 20
7 April 1974	1:9600	COL	COL	1-2

[1]Frame numbers may vary for Eel Pond.

Table C1. (Concluded)

Date	Scale	Source	Depository	Frame Numbers
18 April 1974	1:30,200	USC&GS	NOS	22, 23, 24, 25, 26
2 May 1974	1:9600	COL	COL	6
5 March 1975	1:9600	COL	COL	3-3, 4-3, 3-5, 5-2
20 Aug. 1975	1:144,000	NASA	EROS	8754
Nov. 1976	1:11,900	REDI	REDI	30
May 1976	1:11,900	REDI	REDI	35, 38, 37A, 29
1 April 1977	1:82,000	USGS	EROS	63, 64, 66, 82
17 April 1977	1:83,000	USGS	EROS	9, 10
29 April 1978	1:18,000	(check)	ANCO	163, 164, 165, 166, 167, 168, 169, 170, 171, 172, 201, 202, 204, 205
8 May 1978	1:25,000	LMI	LMI	90, 91, 92, 109, 110, 111, 112, 113, 114
20 April 1978	1:115,000	NASA	EROS	39
21 April 1979	1:115,000	NASA	EROS	99

Table C2. Depositories of Vertical Aerial Photographs
(From Aubrey and Gaines, 1982)

A. Private

APNE	Aerial Photos of New England, Inc.	Norwood Municipal Airport Access Road,Norwood, MA 02062
AGC	Aero-Graphics Corp.	Box 248, Bohemia, NY 11716
AMS	Aero-Marine Surveys	38 Green Street, New London, CT 06320
AIT	Air Image Technology	Boxboro Road, Stow, MA 01775
ANCO	Anderson-Nichols Co.	150 Causeway Street, Boston, MA 02114
AVIS	Avis Air Map, Inc	454 Washington Street, Braintree, MA 02184
BSC	Boston Survey Consultants	263 Summer Street, Boston, MA 02210
COL	Col-East, Inc.	Harriman Airport, North Adams, MA 01247
DFS	Dutton Flying Service	239 Newton Road, Haverhill, MA 01830
FAS	Fairchild Aerial Surveys	Los Angeles, CA
RK	Mr. Richard Kelsey	20 Heritage Lane, Chatham, MA
KAS	Keystone Aerial Surveys, Inc.	North Philadelphia, PA
LKBI	Lockwood, Kessler & Bartlett, Inc	One Aerial Way, Syosset, NY 11791
LMI	Lockwood Mapping, Inc.	P.O. Box 5790, 580 Jefferson Rd., Rochester, N.Y. 14623
LAPS	Lowry Aerial Photo Service	234 Cabot Street, Beverly, MA 01915
NESS	New England Survey Service	1220 Adams Street, Box 412, Dorchester, MA 02122

(Continued)

Table C2. (Concluded)

NEAA	Northeast Airphoto Association, Inc.	29 Grafton Circle, Shrewsbury, MA 02576
REDI	Real Estate Data, Inc.	Northeast Division, 629 Fifth Avenue, P.O. Call Box D, Pelham, N.Y. 10803
RAS	Robinson Aerial Surveys	
JWS	James W. Sewall Company	West Wareham, MA 02576
TDG	Teledyne Geotronics	725 E. 3rd Street, Long Beach, CA 90802
WHOI	Data Library	Woods Hole Oceanographic Institution, Woods Hole, MA 02543
B. Government		
NED	U.S. Army Corps of Engineers	New England Division, 424 Trapelo Road, Waltham, MA 02154
USDA	U.S. Department of Agriculture	Agricultural Stabilization and Conservation Service, 2222 W. 2300 South, P.O. Box 30010, Salt Lake City, Utah 84125 and, Soil Conservation Service, Cartographic Division, Federal Center Building No. 1, Hyattsville, MD 20782
NARS	National Archives and Record Service	General Services Administration, Cartographic Archives Division Rm 2W, 8 Pennsylvania Avenue NW, Washington, D.C. 20408
NCIC	U.S. Department of Defense	Central Film Library, U.S. Geological Survey, National Cartographic Information Center, National Center, Mail Stop 507, Reston, VA 22092
EROS	U.S. Department of Interior	EROS Data Center, Sioux Falls, SD 57198
NOS	Chief, Photo Map & Imagery Section	Coastal Mapping Division, C3415, National Ocean Survey, NOAA, Rockville, MD 20852

APPENDIX D: EOLIAN SAND TRANSPORT CALCULATION PROCEDURE

U. S. Army Coastal Engineering Research Center	COMPUTATION SHEET	PAGE 1 OF 6 PAGES
		DATE 1/83
	SUBJECT: EEL POND HYDRAULIC STUDY	
COMPUTED BY: B. Danielson	COMPUTATION: Aeolian Sand Transport (Example)	NUMBER
CHECKED BY		

Symbol List:

A = a value between 0.08 and 0.1 in Bagnold's equation for U*t.

C = constant term in Bagnold's formula

$$1.5 \leq C \leq 1.8$$

In Zingg's modification, C = 0.83

d or D = average grain diameter of sand in reach.

$D_{.25}$ = average grain diameter of 0.25mm sand.

e = density of air.

g = acceleration of gravity.

ℓ_1 = length of reach perpendicular to wind direction.

q = weight of sand transported per unit width of reach perpendicular to wind direction and per unit time.

Q = total weight of sand transported per year for given study area.

t or T = period of time that wind from a particular direction blows with a given average speed.

u = average wind speed in a given direction.

u' = "focus" speed for plot of speed profiles of wind transporting sand[1/2].

U* = shear speed = $\sqrt{\tau/e}$

U*t = threshold shear speed - shear speed at which sand movement is initiated.

w = water content of sand expressed as a %

z = height at which wind speed is measured.

z' = "focus" height corresponding to u'.

γ = specific weight of air.

σ = specific weight of sand.

τ = shear stress of wind on sand.

U. S. Army Coastal Engineering Research Center	COMPUTATION SHEET	PAGE 2 OF 6 PAGES
		DATE 1/83
	SUBJECT: EEL POND HYDRAULIC STUDY	
COMPUTED BY B. Danielson	COMPUTATION: Aeolian Sand Transport (Example)	NUMBER
CHECKED BY		

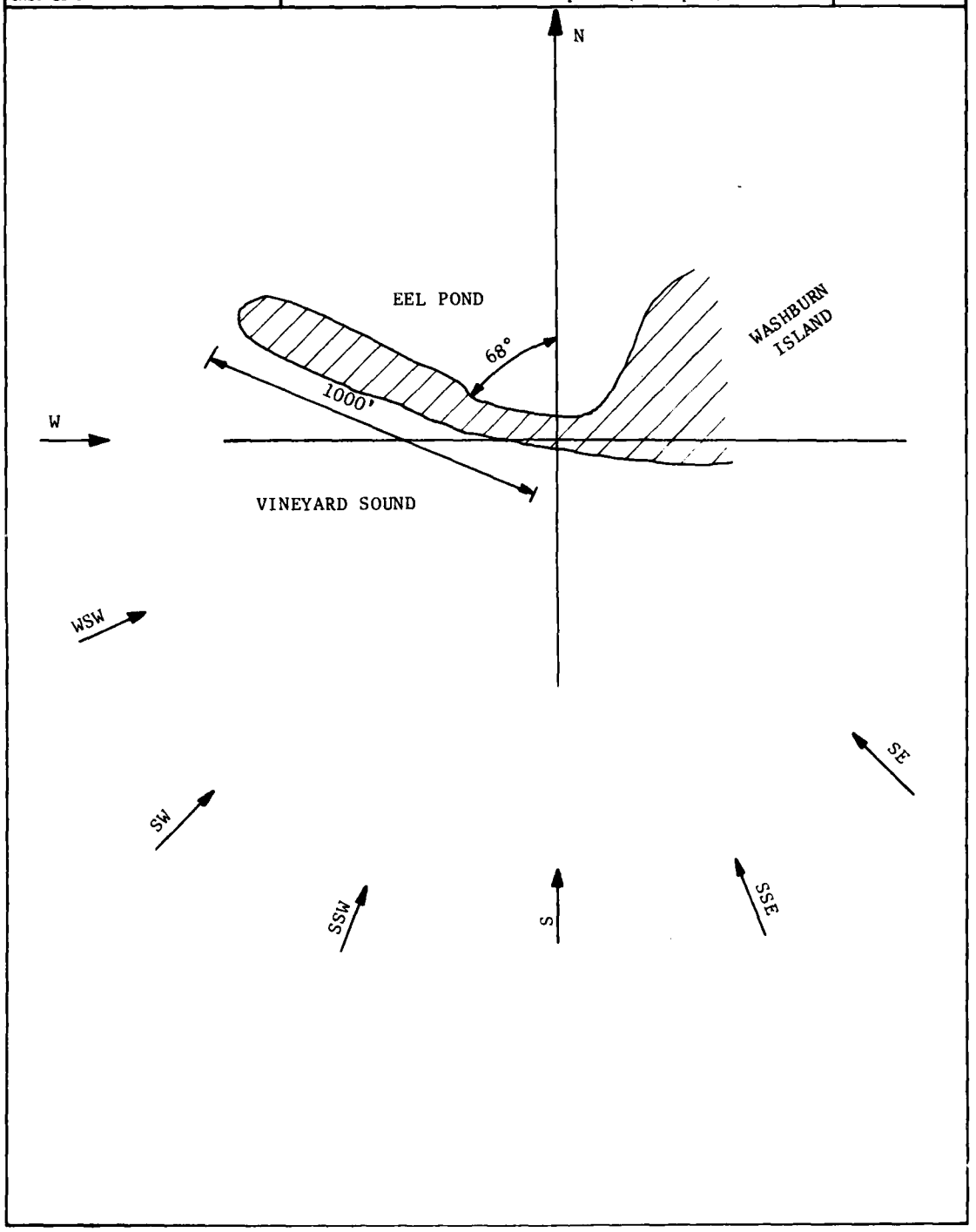

CERC Form 259-81
26 June 1981

AD-A147 548 INLET PROCESSES AT EEL POND FALMOUTH MASSACHUSETTS(U) 2/2
COASTAL ENGINEERING RESEARCH CENTER VICKSBURG MS
A E DEWALL ET AL. OCT 84 CERC-MP-84-9

UNCLASSIFIED F/G 8/3 NL

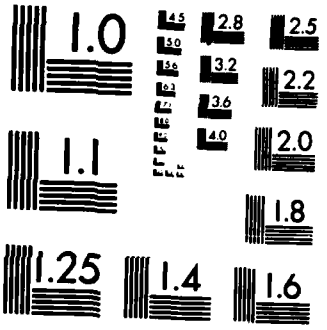
1.0
2.8
2.5
3.2
2.2
3.6
4.0
2.0
1.1
1.8
1.25
1.4
1.6

U.S. Army Coastal Engineering Research Center	COMPUTATION SHEET	PAGE 3 OF 6 PAGES
		DATE 1/83
	SUBJECT: EEL POND HYDRAULIC STUDY	
COMPUTED BY B. Danielson	COMPUTATION: Aeolian Sand Transport (Example)	NUMBER
CHECKED BY		

Bagnold's Formula:

$$Q = C \cdot \rho_L \cdot T \cdot \sqrt{D/D_{.25}} \cdot (\gamma/g) \cdot U^{*3} \qquad \text{(with D in mm)}$$

C = 1.5 for nearly uniform sand
1.8 for naturally graded sand
2.8 for sand with very wide grain diameter range

$$U^* = \frac{u - u'}{6.13 \log (z/z')} \qquad \text{(Zingg)}$$

(Zingg) $\begin{cases} z' = 10d \\ u' = 20d \end{cases}$ (u' in miles/hr., d in mm)

$$U^*t = A\sqrt{\left(\frac{\sigma - \gamma}{\gamma}\right) \cdot gd} \qquad \text{(Bagnold)}$$

Sand will not begin to move until U* exceeds U*t; therefore, the transport formulas do not apply until that condition is reached.

Zingg's Modificiation of Bagnold's Formula:

$$Q = C \cdot \rho_L \cdot T \cdot (D/D_{.25})^{3/4} \cdot (\gamma/g) \cdot U^{*3} \qquad \text{(with C = 0.83)}$$

Hsu Formula:

$$Q = K \cdot \rho_L \cdot t \cdot (gd)^{-1.5} \cdot U^{*3}$$

$\ln K = 4.97 \cdot D - 9.68$ $\begin{cases} K \text{ in gm/cm-sec} \\ D \text{ in mm} \end{cases}$

$\ln K = 4.97 \cdot D - 4.19$ $\begin{cases} K \text{ in lb/ft-hr} \\ D \text{ in mm} \end{cases}$

$U^* = 0.04u$ (average value for u measured between 2m and 10m above ground)

Kadib Effects of Moisture on U*t:

1) For wind with non-zero humidity:

$$U^*t = \left(1 + \frac{1}{2}\frac{h}{100}\right) A\sqrt{\left(\frac{\sigma - \gamma}{\gamma}\right) \cdot gd}$$ (where h = relative humidity of air in %)

i.e., threshold shear speed is increased by the factor $\left(1 + \frac{1}{2}\frac{h}{100}\right)$ relative to the Bagnold U*t formula.

CERC Form 259-81
26 June 1981

2) for sand with non-zero water content:

$$U^*t = (1.8 + 0.6 \log_{10} w) \cdot A\sqrt{\left(\frac{\sigma - \gamma}{\gamma}\right) \cdot gd}$$ (where w = water content of sand as %)

i.e., threshold shear speed is increased by the factor $(1.8 + 0.6 \log_{10} w)$ relative to the Bagnold U*t formula.

Example Calculation (Bagnold):

Wind Data - Average Hours/Year

Wind Direction	Knots 1 - 3	4 - 6	7 - 10	11 - 16	17 - 21	22 - 27	28 - 33
S	18 hr.	96 hr.	272 hr.	201 hr.	61 hr.	9 hr.	0
SW	9 hr.	114 hr.	350 hr.	333 hr.	79 hr.	9 hr.	0
Average Speed in Band (knots)	2	5	8.5	13.5	19	24.5	30.5

$$U^*t = A\sqrt{\frac{\sigma - \gamma}{\gamma} \cdot gd}$$

Let A = 0.08
σ = 125 lb/ft^3
γ = 0.075 lb/ft^3
g = 32.2 ft/sec^2
d = 0.5mm = 0.00164 ft
Then, U*t = 0.75 ft/sec

$U_t = 6.13 \log (z/z') U^* + u'$ Where z = 15 ft (wind measurement height)
U* = 0.75 ft/sec = U*t
z' = 10d = 10 . 0.00164 ft
= 0.0164 ft
u' = 20D = 20 * .5 = 10 miles/hr
= 14.67 ft/sec

$U_t = 6.13 \log (15/0.0164) \cdot 0.75 + 14.67$

Ut = 28.3 ft/sec = 16.7 knots

So no sand transport until measured wind speed exceeds 16.7 knots, disregard wind data below that speed.

U.S. Army Coastal Engineering Research Center	COMPUTATION SHEET	PAGE 5 OF 6 PAGES
		DATE 1/83
	SUBJECT: EEL POND HYDRAULIC STUDY	
COMPUTED BY B. Danielson	COMPUTATION: Aeolian Sand Transport (Example)	NUMBER
CHECKED BY		

Average u Wind Speed Knots	Feet/Second	U* Feet/Second
2	3.4	Below U*t
5	8.4	Below U*t
8.5	14.4	Below U*t
13.5	22.8	Below U*t
19	32.1	0.959
24.5	41.4	1.471
30.5	51.5	2.028

Projection of Spit Length Perpendicular to Wind Direction (with Spit Orientation N68°W):

Wind Direction	$\ell_\perp$ (ft)	Comments
S	927	$\ell_\perp = 1000 \cdot \sin 67°$ *
SW	921	$\ell_\perp = 1000 \cdot \sin 68°$ *

* Length of spit assumed to be 1000 ft.

Calculation of Sand Transport:

Wind Direction	$\ell_\perp$ (ft)	Average Wind Speed (knots / ft/sec) 19/32.1	24.5/41.4	30.5/51.1	
S	927	61/1,077,000	9/574,000	0/0	Figures are: T(hrs) / Q(lb/yr)
SW	921	79/1,386,000	9,570,000	0/0	

$$Q = C \cdot \ell_\perp \cdot T \cdot \sqrt{D/0.25} \cdot (0.075/32.2) \cdot U^{*3} \quad \text{(Bagnold)}$$

With $C = 1.8$ for naturally graded sand with $D = 0.5$mm

CERC Form 259-81
26 June 1981

U. S. Army Coastal Engineering Research Center	COMPUTATION SHEET	PAGE 6 OF 6 PAGES
		DATE 1/83
	SUBJECT: EEL POND HYDRAULIC STUDY	
COMPUTED BY B. Danielson	COMPUTATION: Aeolian Sand Transport (Example)	NUMBER
CHECKED BY		

1/ Bagnold, R. A., The Physics of Blown Sand and Desert Dunes, Methuen & Co., Ltd., London, 1954.

2/ Zingg, A. W., Wind Tunnel Studies of the Movement of Sedimentary Material, Proc. of Fifth Hydraulics Conf., 1952.

3/ Hsu, S. A., Computing Eolian Sand Transport from Routine Weather Data, Proc. of Fourteenth Coastal Engineering Conference, 1974.

4/ Kadib, Abdel-Latif, Addendum II to Technical Memorandum No. 1, U. S. Army Corps of Engineers, 1964.

CERC Form 259-81
26 June 1981

APPENDIX E: INLET 2: COMPUTER PROGRAM DESCRIPTION

INLET 2 is a computer program to predict inlet velocities, discharge, and bay levels for multiple bays, inlets, and seas interconnected in any manner (Figure E1). The program is based on the lumped parameter model of Seelig, Harris, and Herchenroder (1977).

Theory

The program predicts bay levels, inlet velocities, and discharges by marching through time and at each time step setting up a series of differential equations: one area-averaged momentum equation for each inlet channel (including temporal and convective accelerations, head, and friction) and one continuity equation for each bay. The coefficients for these equations are determined by evaluating boundary conditions (sea water levels and discharges into the bays from sources other than the inlets, such as rivers), determining the local water level throughout the inlet by interpolating levels from one end of the inlet to the other based on friction losses, and evaluating the friction loss of the inlet. Friction is determined by using a flow net for each inlet, Manning's equation, and a weighting function (a systematic method of distributing flow throughout the inlet). INLET 2 uses a weighting function to distribute flow at each cross-section in the flow net so that friction is minimized. This weighting to minimize friction is similar to the electrical problem of determining the current through a series of parallel resistors. It is solved by Ohm's law, which shows that the fraction of flow through one cell is equal to the reciprocal of the resistance of the cell divided by the sum of the reciprocal of the resistance for all cells in the cross-section. Convective acceleration is evaluated in terms of an empirical loss coefficient. Continuity is determined by dividing the total discharge of water into each bay from all sources divided by the local bay surface area.

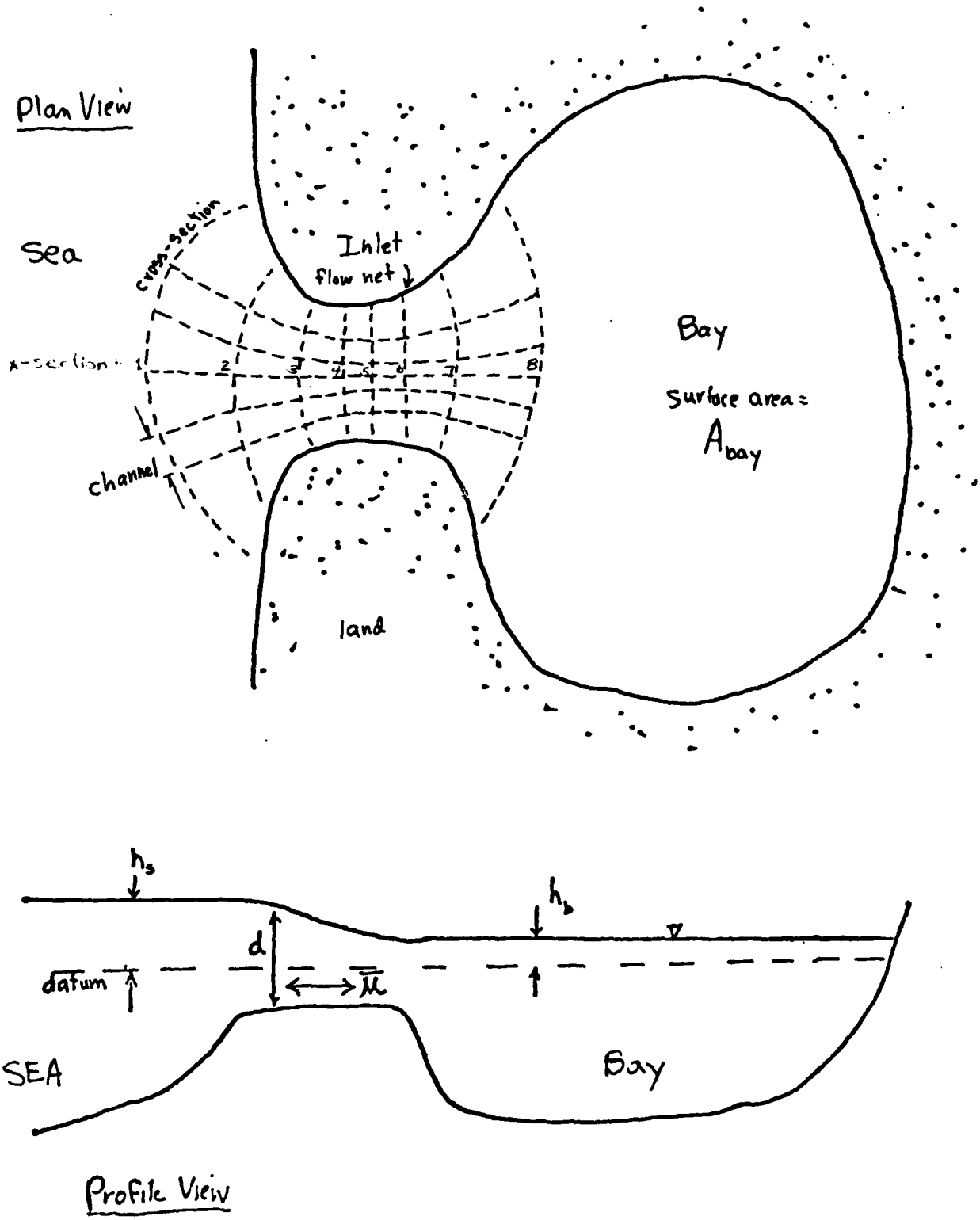

Figure E1. Inlet-bay system with one sea, one bay, and one inlet

Once this series of equations has been set up, a fourth order Runge-Kutta-Gill routine is used to solve the simultaneous equations. See Seelig, Harris, and Herchenroder (1977), for more details of the theory.

Model Use

The model is designed by systems where the water level in each bay rises and falls uniformly throughout the water level cycle. This occurs where the length of the wave in the bay is much longer than the longest axis of the bay:

$$T_F \sqrt{g\, d_{bay}} >> L_{bay}$$

where

T_F = forcing wave period

g = acceleration of gravity

d_{bay}, L_{bay} = depth and length of the bay, respectively

The seas are assumed to be much larger than the inlets and bays combined, so that any hydraulic action in the inlets and bays does not influence water level fluctuations in the sea.

Program Organization

INLET 2 is the main routine that reads in all input data, sets up the problem, and calls other routines to solve the hydraulics and output results. A flow chart of the interrelation between routines is shown in Figure E2.

RKGS is a Scientific Subroutine Package routine to solve a series of differential equations using a fourth order Runge-Kutta-Gill technique.

SETEQ is a routine called by RKGS for setting up the differential equations at each time step.

INT is a third order interpolation routine for determining sea levels of inflows into the bays. The routine is called by SETEQ and results are

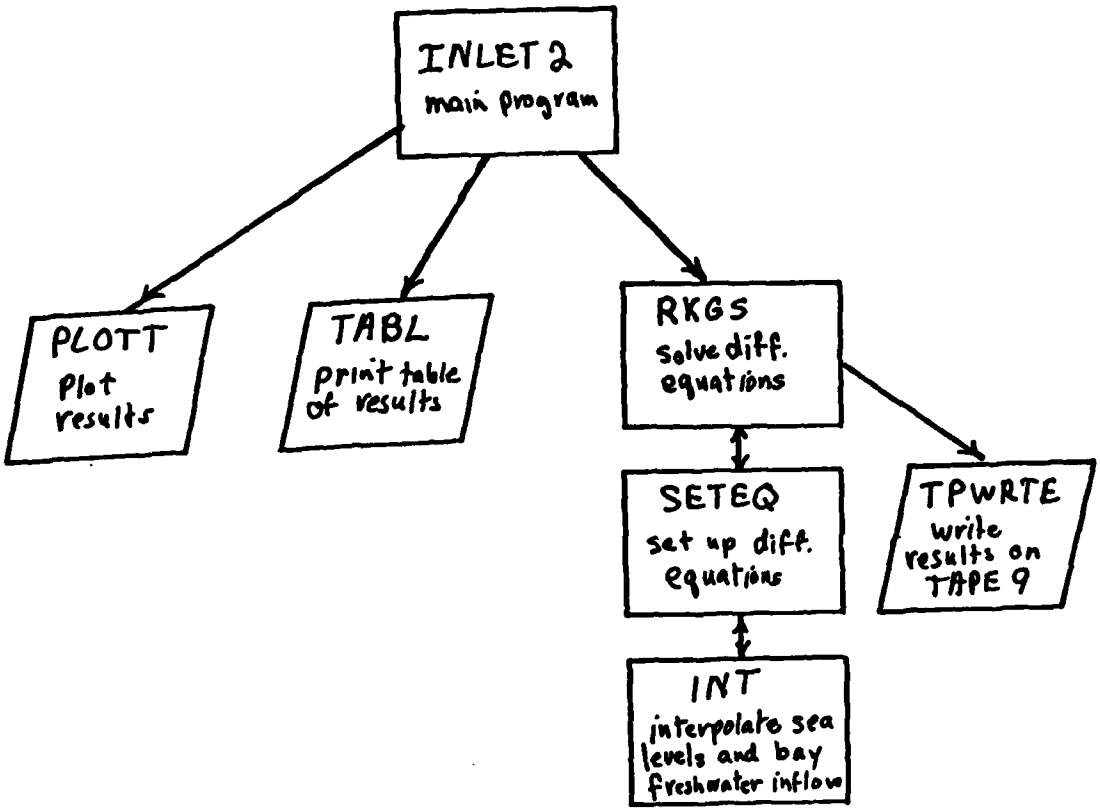

Figure E2. Program organization

used in setting up equations.

TPWRITE is called by RKGS each time results from a time stop are available. Results are written on Tape 9.

TABL outputs results in a tabular form for critical point values and at an equal time interval specified as input.

PLOTT plots results.

Procedure for Using the Computer Program

The first step is to consecutively number the inlets and major bodies of water (seas and bays) starting with the seas.

Second, evaluate the geometry of the inlets using maps, charts, hydrographic surveys, and dredging records to determine the depth of water throughout the inlets. Also measure the side slopes of the inlets at mean water level. Whenever possible obtain this information for the time of interest because inlets frequently change shape, especially during major storms.

Third, draw a flow net, a series of cross sections and channels, for each inlet (Figure E1). The flow net and inlet discharge are used to determine bottom friction throughout the inlet. The flow net is drawn by estimating the approximate path that water follows on the average for ebb and flood flows. Channel boundaries are then drawn along these paths for up to seven channels. A simple inlet with constant depth and width may be modeled with one or two channels. More complex inlets require a larger number of channels. Channels should have the smallest spacing in deep portions of the inlet where flow will be greatest. Up to seven cross sections should then be drawn perpendicular to the channels. The first cross section and the last cross section should have cross-sectional areas ten times larger than the minimum cross-sectional area. Cross sections

should be drawn with the narrowest spacing near the minimum cross-sectional area section where friction in the inlet will be high.

Fourth, measure the surface area of the bays at the mean water level, A_o , from charts or aerial photographs. For some bays the area of the bay changes as the bay water level rises and falls because sections are flooded at high water levels. If the bay area change is significant, a linear bay area variation parameter, β , is used to account for area change due to bay level variation where:

$$\beta = \frac{\text{(bay surface area at high water - bay surface area at low water)}}{A_o \text{ (high water elevation - low water elevation)}}$$

Fifth, specify the seawater level fluctuation and inflows into the bays from sources other than the inlets (i.e. rivers) as a function of time for the period of interest. Tide tables will give an estimate of the astronomical tide. Water levels can also be obtained by measuring levels using a tide gage and stilling well.* U.S. Army Corps of Engineers and U.S. National Oceanic and Atmospheric Administration gages located at numerous points along the coast may also provide the desired water level information. In this computer program the tides may either be expressed as a sinusoidal function with a period and amplitude or they may be described by instantaneous measurements made at a constant sampling rate. A cubic interpolation routine is used to smooth data specified at a constant sampling rate.

Sixth, determine the approximate time step, Δt , for the model to use in computations. As a lower limit the time step should be:

$$\Delta t = \frac{L_{in}}{\sqrt{g\ d_{max}}}$$

* Seelig, W. N. 1976. "Stilling Well Design for Accurate Water Level Measurement," CERC Technical Report.

where

L_{in} = length of the inlet

d_{max} = maximum water depth in the inlet

A much longer time step can be used for most tidal inlets and as an upper limit the time step should be one-hundredth of the forcing wave period.

Seventh, put all input data into the computer format described in Table 1, and as a first estimate, set the flood and ebb entrance and exit loss coefficients equal to one (CDF = 1.0 and CDE = 1.0). As a first approximation, Manning's n can be evaluated by the relation:

$$n = C1 - C2\ D$$

where D is the still-water depth; for depths greater than 4 feet and less than 30 feet, C1 = 0.0377 and C2 = 0.000667 ; for depths less than 4 feet, C1 = 0.0550 and C2 = 0.005 .

Eighth, calibrate the computer model by varying Manning's "n" and/or the flood and ebb loss coefficients.

The model is calibrated using short periods of field observations and by first comparing observed and predicted mean water velocities, if available, at the minimum cross-sectional area region of the inlet. If the predicted velocities are higher or lower than observed, then the value of n can be increased or decreased accordingly. When the computer model has been satisfactorily calibrated to predict inlet velocities, predicted bay water levels should be checked against measurements to assure that levels are being modeled correctly. If inlet velocities are not available, bay levels can be used to calibrate the model.

Ninth, if additional prototype data are available, it should be used tc verify or prove that the model adequately predicts inlet and bay hydraulics. Input data, output, and computations are in English units.

APPENDIX F: GEOMETRIC CHARACTERISTICS OF EEL POND/WAQUOIT BAY SYSTEM USED IN INLET 2 MODEL

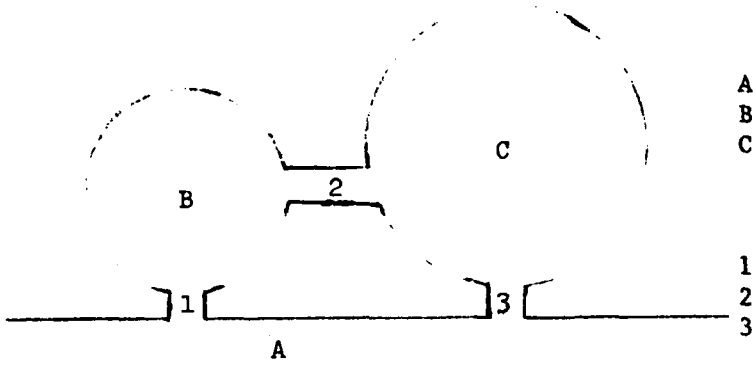

BODY OF WATER

A Nantucket Sound
B Eel Pond
C Waquoit Bay

INLET

1 Nantucket Sound/Eel Pond Inlet
2 Seapit River
3 Nantucket Sound/Waquoit Bay

WATER BODY CHARACTERISTICS

	Ocean
Tide Range (ft)	1.6
Period (hrs)	12.4

	Eel Pond	Waquoit Bay
Surface Area (ft^2)	1.10×10^7	4.2×10^7
Area Variation Parameter[1]	0.0	0.0

INLET CHARACTERISTICS

Inlet	Channel Side Slope	C1[2]	C2[2]	CDF[3]	CDE[3]
1	.15	.03770	.00067	1.0	1.0
2	0.0	.05500	.00500	1.0	1.0
3	0.0	.03770	.00067	1.0	1.0

[1]Area variation parameter = (Surface area at high water - surface area at low water)/(Surface area at mean water level)x (High water elevation - low water elevation)

[2]Manning's n: n = C1 - C2 x D, D is still water depth; for depths greater than 4 ft. and less than 30 ft., C1 = .000667 and C2 = .03770; for depths less than 4 ft., C1 = .05500 and C2 = .00500

[3]Flood and ebb entrance and exit loss coefficients

SUMMARY OF GRID CHARACTERISTICS

Section	Inlet 1	Inlet 2 Channel	Inlet 3 Channel
Area (ft^2)	(See Other Tables)	900.0	1800.0
Width (ft)		300.0	300.0
Depth (ft)		3.0	6.0
Length (ft)		2000.0	2000.0
n^1		.0400	.0337

[1]Manning's n

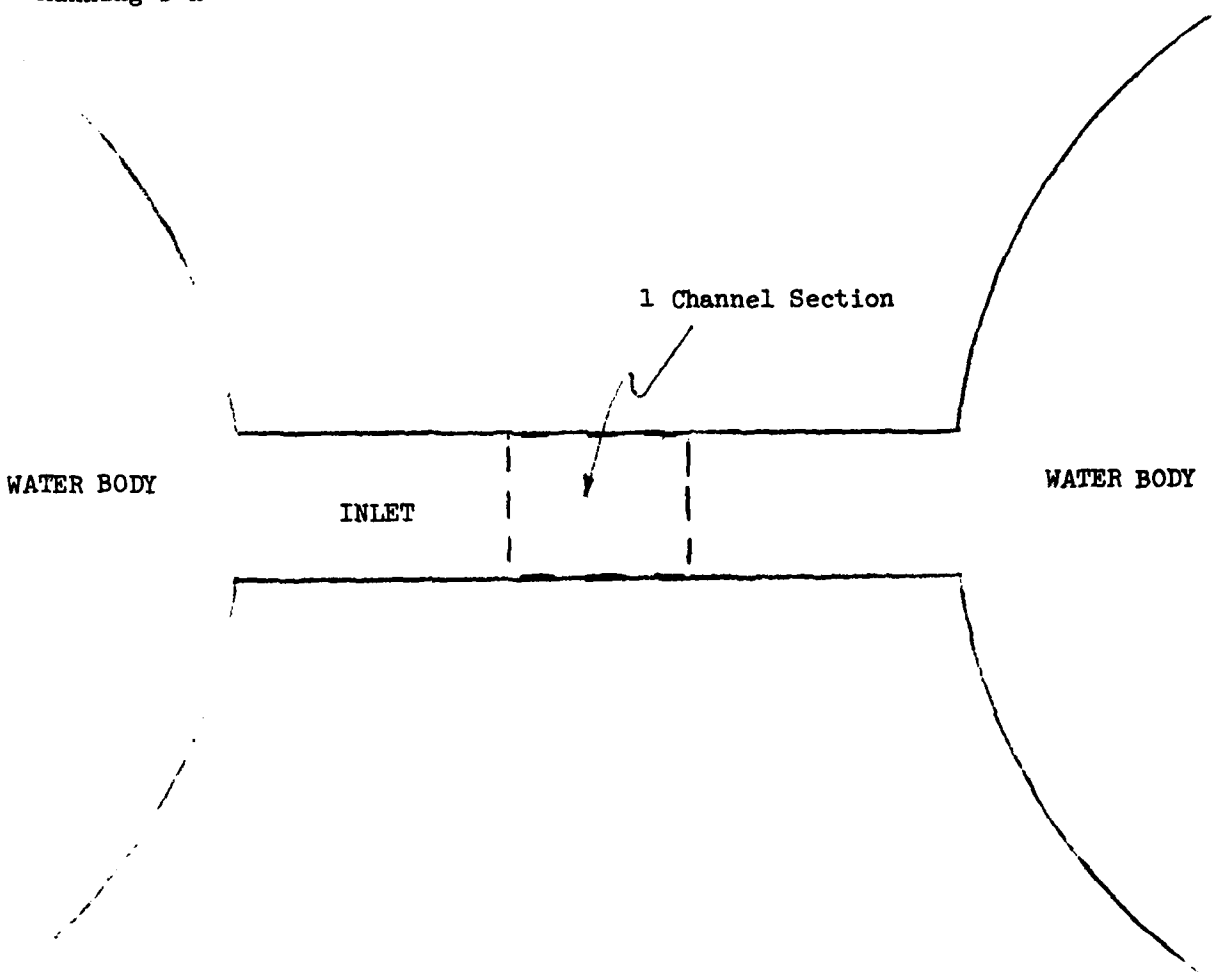

SUMMARY OF GRID CHARACTERISTICS
Inlet 1
Initial Configuration

Section 1			
Area (Ft 2)	413.8	1144.0	505.3
Width (Ft)	194.0	270.0	287.5
Depth (Ft)	2.1	4.2	1.8
Length (Ft)	255.0	264.0	266.5
n	.0363	.0349	.0365
Section 2			
Area (Ft 2)	914.3	968.5	462.8
Width (Ft)	212.5	207.5	205.0
Depth (Ft)	4.3	4.7	2.3
Length (Ft)	300.0	235.0	229.0
n	.0348	.0346	.0362
Section 3			
Area (Ft 2)	868.0	852.6	290.0
Width (Ft)	175.0	133.5	126.5
Depth (Ft)	5.0	6.4	2.3
Length (Ft)	277.5	237.5	240.0
n	.0344	.0334	.0362
Section 4			
Area (Ft 2)	556.0	570.6	192.0
Width (Ft)	55.0	67.5	61.5
Depth (Ft)	10.1	8.5	3.1
Length (Ft)	80.0	81.5	89.0
n	.0310	.0321	.0356
Section 5			
Area (Ft 2)	508.5	530.0	173.3
Width (Ft)	35.0	44.0	40.0
Depth (Ft)	14.5	12.1	4.3
Length (Ft)	77.5	81.0	81.0
n	.0280	.0297	.0348
Section 6			
Area (Ft 2)	479.0	608.0	184.4
Width (Ft)	44.0	46.5	41.5
Depth (Ft)	10.9	13.1	4.4
Length (Ft)	59.5	58.0	51.0
n	.0304	.0290	.0347

SUMMARY OF GRID CHARACTERISTICS
Inlet 1
RUN C1,J1

Section 1			
Area (Ft 2)	497.5	457.5	305.0
Width (Ft)	105.0	102.5	82.5
Depth (Ft)	4.7	4.5	3.7
Length (Ft)	250.0	250.0	242.5
n	.0345	.0347	.0352
Section 2			
Area (Ft 2)	914.5	865.0	357.5
Width (Ft)	226.0	125.0	103.5
Depth (Ft)	4.1	6.9	3.5
Length (Ft)	286.0	206.0	182.5
n	.0350	.0331	.0354
Section 3			
Area (Ft 2)	993.0	994.5	331.5
Width (Ft)	208.0	110.5	102.0
Depth (Ft)	4.6	9.0	3.3
Length (Ft)	347.5	352.5	425.0
n	.0346	.0317	.0355
Section 4			
Area (Ft 2)	520.0	617.0	231.5
Width (Ft)	56.0	63.0	76.0
Depth (Ft)	9.3	9.8	3.1
Length (Ft)	80.0	79.0	81.5
n	.0315	.0312	.0357
Section 5			
Area (Ft 2)	524.0	527.0	166.0
Width (Ft)	39.0	43.0	47.5
Depth (Ft)	13.4	12.3	3.5
Length (Ft)	82.5	95.0	100.0
n	.0287	.0295	.0354
Section 6			
Area (Ft 2)	513.0	557.0	251.0
Width (Ft)	50.0	43.0	43.0
Depth (Ft)	10.3	13.0	5.8
Length (Ft)	57.5	55.0	50.0
n	.0309	.0291	.0338

SUMMARY OF GRID CHARACTERISTICS
Inlet 1
RUN C3,J2

Section 1			
Area (Ft 2)	228.0	1183.5	359.0
Width (Ft)	48.0	131.5	77.5
Depth (Ft)	4.8	9.0	4.6
Length (Ft)	65.0	90.0	51.0
n	.0345	.0317	.0346
Section 2			
Area (Ft 2)	223.5	958.5	394.0
Width (Ft)	56.5	106.5	95.0
Depth (Ft)	4.0	9.0	4.2
Length (Ft)	197.5	207.5	200.0
n	.0351	.0317	.0349
Section 3			
Area (Ft 2)	465.0	925.0	324.0
Width (Ft)	72.0	102.5	94.5
Depth (Ft)	6.5	9.0	3.4
Length (Ft)	617.5	557.5	687.5
n	.0334	.0317	.0354
Section 4			
Area (Ft 2)	696.5	957.5	131.0
Width (Ft)	70.0	100.0	62.0
Depth (Ft)	10.0	9.6	2.1
Length (Ft)	85.0	75.0	90.0
n	.0311	.0313	.0363
Section 5			
Area (Ft 2)	548.5	1174.5	178.0
Width (Ft)	39.5	119.0	83.0
Depth (Ft)	13.9	9.9	2.1
Length (Ft)	72.5	67.5	82.5
n	.0284	.0311	.0363
Section 6			
Area (Ft 2)	299.0	1714.0	513.5
Width (Ft)	48.0	174.5	123.0
Depth (Ft)	6.2	9.8	4.2
Length (Ft)	175.0	145.0	59.0
n	.0335	.0311	.0349

SUMMARY OF GRID CHARACTERISTICS
Inlet 1
RUN C1,J2

Section 1			
Area (Ft 2)	378.0	400.5	338.5
Width (Ft)	85.0	90.0	87.5
Depth (Ft)	4.5	4.5	3.9
Length (Ft)	255.0	262.5	257.5
n	.0347	.0347	.0351
Section 2			
Area (Ft 2)	839.0	673.0	510.5
Width (Ft)	220.0	102.5	172.5
Depth (Ft)	3.8	6.6	3.0
Length (Ft)	315.0	285.0	360.0
n	.0352	.0333	.0357
Section 3			
Area (Ft 2)	925.0	814.5	479.5
Width (Ft)	207.0	90.5	171.0
Depth (Ft)	4.5	9.0	2.8
Length (Ft)	306.0	265.0	301.5
n	.0347	.0317	.0358
Section 4			
Area (Ft 2)	520.0	617.0	231.5
Width (Ft)	56.0	63.0	76.0
Depth (Ft)	9.3	9.8	3.1
Length (Ft)	80.0	79.0	81.5
n	.0315	.0312	.0357
Section 5			
Area (Ft 2)	524.0	527.0	166.0
Width (Ft)	39.0	43.0	47.5
Depth (Ft)	13.4	12.3	3.5
Length (Ft)	82.5	95.0	100.0
n	.0287	.0295	.0354
Section 6			
Area (Ft 2)	513.0	557.0	251.0
Width (Ft)	50.0	43.0	43.0
Depth (Ft)	10.3	13.0	5.8
Length (Ft)	57.5	55.0	50.0
n	.0309	.0291	.0338

SUMMARY OF GRID CHARACTERISTICS
Inlet 1
RUN C2,J2

Section 1			
Area (Ft 2)	222.5	1075.5	357.0
Width (Ft)	49.0	119.5	80.5
Depth (Ft)	4.5	9.0	4.4
Length (Ft)	59.5	64.5	48.0
n	.0347	.0317	.0347
Section 2			
Area (Ft 2)	480.0	954.0	307.5
Width (Ft)	105.0	106.0	80.5
Depth (Ft)	4.6	9.0	3.8
Length (Ft)	255.0	320.5	343.0
n	.0347	.0317	.0352
Section 3			
Area (Ft 2)	725.0	949.5	224.0
Width (Ft)	122.5	105.5	80.0
Depth (Ft)	5.9	9.0	2.8
Length (Ft)	570.0	451.0	541.0
n	.0338	.0317	.0358
Section 4			
Area (Ft 2)	704.0	927.5	76.5
Width (Ft)	71.5	102.5	55.0
Depth (Ft)	9.9	9.1	1.4
Length (Ft)	80.5	79.0	78.5
n	.0311	.0317	.0368
Section 5			
Area (Ft 2)	349.0	1214.0	145.0
Width (Ft)	39.0	119.0	80.0
Depth (Ft)	14.1	10.2	1.8
Length (Ft)	80.0	82.5	62.5
n	.0283	.0309	.0365
Section 6			
Area (Ft 2)	295.0	1724.5	611.5
Width (Ft)	50.0	166.5	132.5
Depth (Ft)	5.9	10.4	4.6
Length (Ft)	145.0	117.5	130.0
n	.0338	.0308	.0346

SUMMARY OF GRID CHARACTERISTICS
Inlet 1
RUN C2,J1

Section 1			
Area (Ft 2)	232.5	1057.5	502.0
Width (Ft)	48.5	117.5	115.0
Depth (Ft)	4.8	9.0	4.4
Length (Ft)	58.0	62.5	52.5
n	.0345	.0317	.0348
Section 2			
Area (Ft 2)	494.0	945.0	413.0
Width (Ft)	102.5	105.0	107.5
Depth (Ft)	4.8	9.0	3.8
Length (Ft)	252.5	310.0	320.0
n	.0345	.0317	.0351
Section 3			
Area (Ft 2)	723.0	945.0	224.0
Width (Ft)	117.5	105.0	80.0
Depth (Ft)	6.2	9.0	2.8
Length (Ft)	570.0	449.0	481.5
n	.0336	.0317	.0358
Section 4			
Area (Ft 2)	704.0	927.5	76.5
Width (Ft)	71.5	102.5	55.0
Depth (Ft)	9.9	9.1	1.4
Length (Ft)	80.5	79.0	78.5
n	.0311	.0317	.0368
Section 5			
Area (Ft 2)	549.0	1214.0	145.0
Width (Ft)	39.0	119.0	80.0
Depth (Ft)	14.1	10.2	1.8
Length (Ft)	80.0	82.5	62.5
n	.0283	.0309	.0365
Section 6			
Area (Ft 2)	295.0	1724.5	611.5
Width (Ft)	50.0	166.5	132.5
Depth (Ft)	5.9	10.4	4.6
Length (Ft)	145.0	117.5	130.0
n	.0338	.0308	.0346

SUMMARY OF GRID CHARACTERISTICS
Inlet 1
RUN C3,J1

Section 1			
Area (Ft 2)	219.5	1124.0	494.0
Width (Ft)	46.0	125.0	121.0
Depth (Ft)	4.8	9.0	4.1
Length (Ft)	64.0	79.0	75.0
n	.0345	.0317	.0350
Section 2			
Area (Ft 2)	258.0	900.0	514.5
Width (Ft)	55.0	100.0	139.0
Depth (Ft)	4.7	9.0	3.7
Length (Ft)	200.0	210.0	205.0
n	.0346	.0317	.0352
Section 3			
Area (Ft 2)	502.0	902.5	365.0
Width (Ft)	71.0	100.0	111.0
Depth (Ft)	7.1	9.0	3.3
Length (Ft)	615.0	548.5	593.5
n	.0330	.0317	.0355
Section 4			
Area (Ft 2)	696.5	957.5	131.0
Width (Ft)	70.0	100.0	62.0
Depth (Ft)	10.0	9.6	2.1
Length (Ft)	85.0	75.0	90.0
n	.0311	.0313	.0363
Section 5			
Area (Ft 2)	548.5	1174.5	178.0
Width (Ft)	39.5	119.0	83.0
Depth (Ft)	13.9	9.9	2.1
Length (Ft)	72.5	67.5	82.5
n	.0284	.0311	.0363
Section 6			
Area (Ft 2)	299.0	1714.0	513.5
Width (Ft)	48.0	174.5	123.0
Depth (Ft)	6.2	9.8	4.2
Length (Ft)	175.0	145.0	125.0
n	.0335	.0311	.0349

SUMMARY OF GRID CHARACTERISTICS
Inlet 1
RUN C3, J3

Section 1			
Area (Ft. 2)	212.3	1057.5	248.3
Width (Ft.)	44.0	117.5	57.0
Depth (Ft.)	4.83	9.0	4.36
Length (Ft.)	53.0	58.0	55.0
n	.0345	.0317	.0348
Section 2			
Area (Ft. 2)	231.5	900.0	235.2
Width (Ft.)	52.5	100.0	56.0
Depth (Ft.)	4.41	9.0	4.2
Length (Ft.)	203.5	215.0	220.0
n	.0348	.0317	.0349
Section 3			
Area (Ft. 2)	487.0	902.5	177.2
Width (Ft.)	71.0	100.0	55.0
Depth (Ft.)	6.86	9.03	3.22
Length (Ft.)	610.0	532.5	547.5
n	.0331	.0317	.0356
Section 4			
Area (Ft. 2)	696.5	957.5	131.0
Width (Ft.)	70.0	100.0	62.0
Depth (Ft.)	9.95	9.58	2.11
Length (Ft.)	85.0	75.0	90.0
n	.0311	.0313	.0363
Section 5			
Area (Ft. 2)	548.5	1174.5	178.0
Width (Ft.)	39.5	119.0	83.0
Depth (Ft.)	13.89	9.87	2.14
Length (Ft.)	72.5	67.5	82.5
n	.0284	.0311	.0363
Section 6			
Area (Ft. 2)	299.0	1714.0	513.5
Width (Ft.)	48.0	174.5	123.0
Depth (Ft.)	6.23	9.82	4.17
Length (Ft.)	175.0	145.0	125.0
n	.0335	.0311	.0349

APPENDIX G: INLET 2 PREDICTIONS OF INLET HYDRAULICS

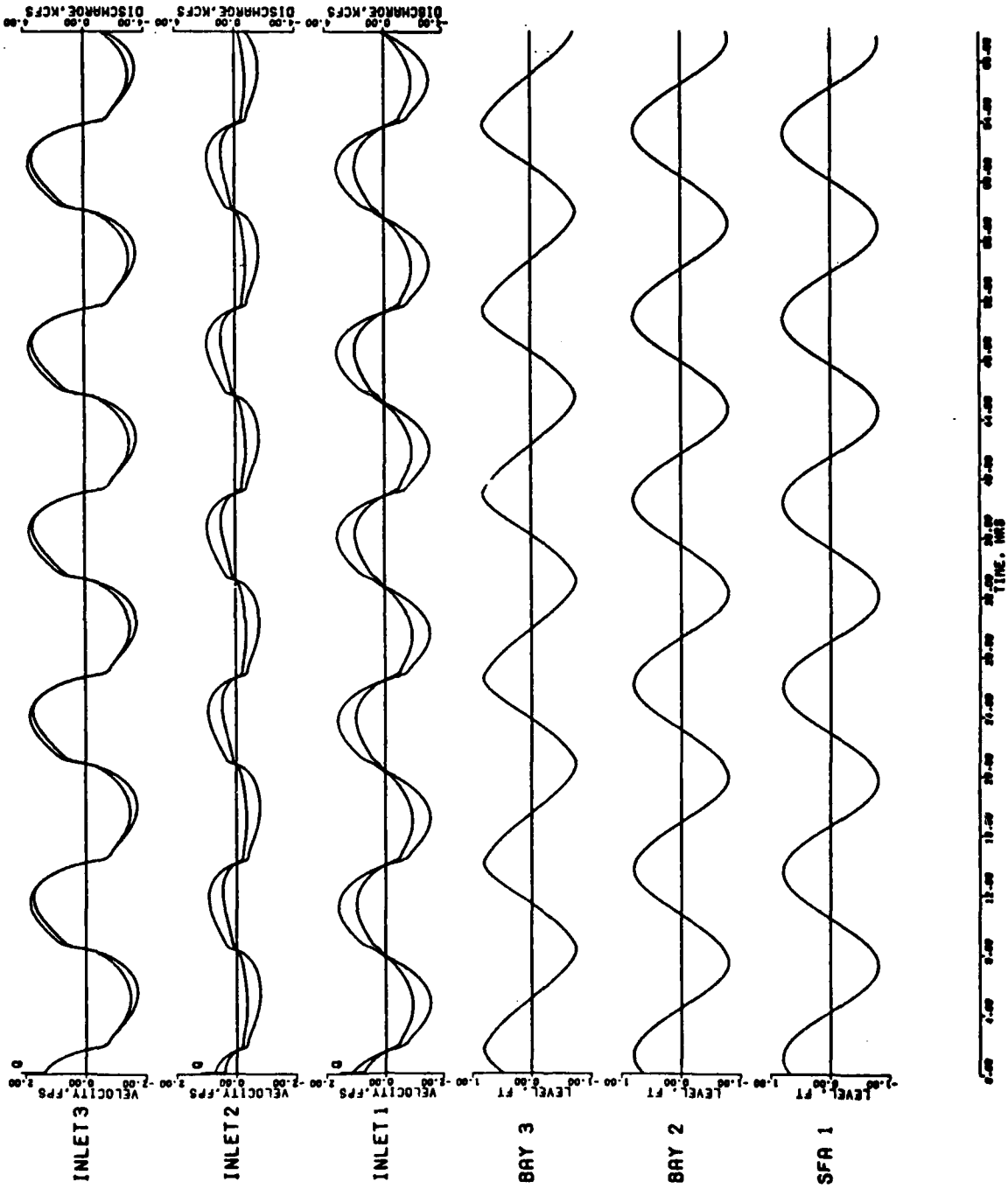

Figure G1. Present configuration

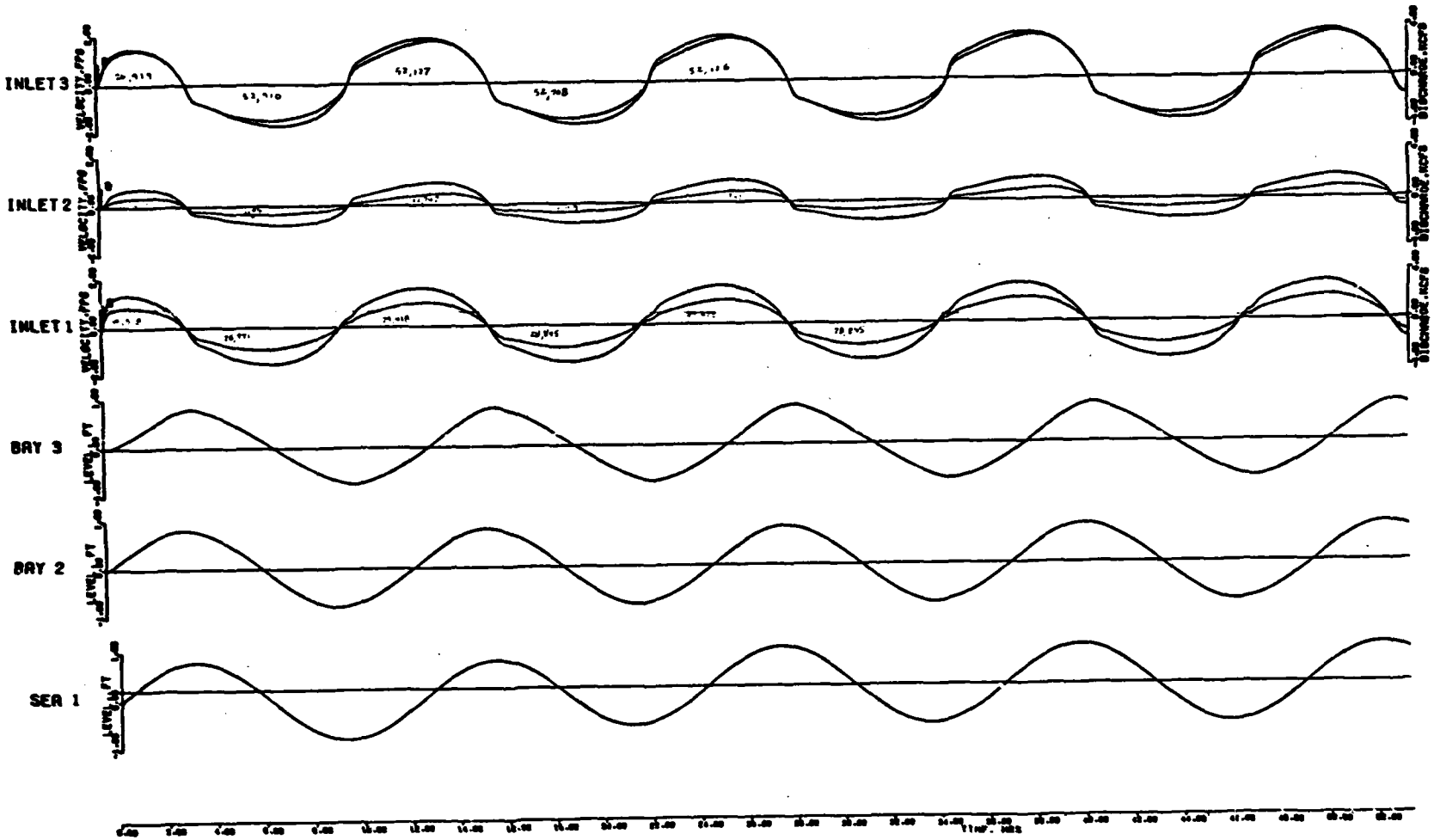

Figure G2. Configuration C1J1

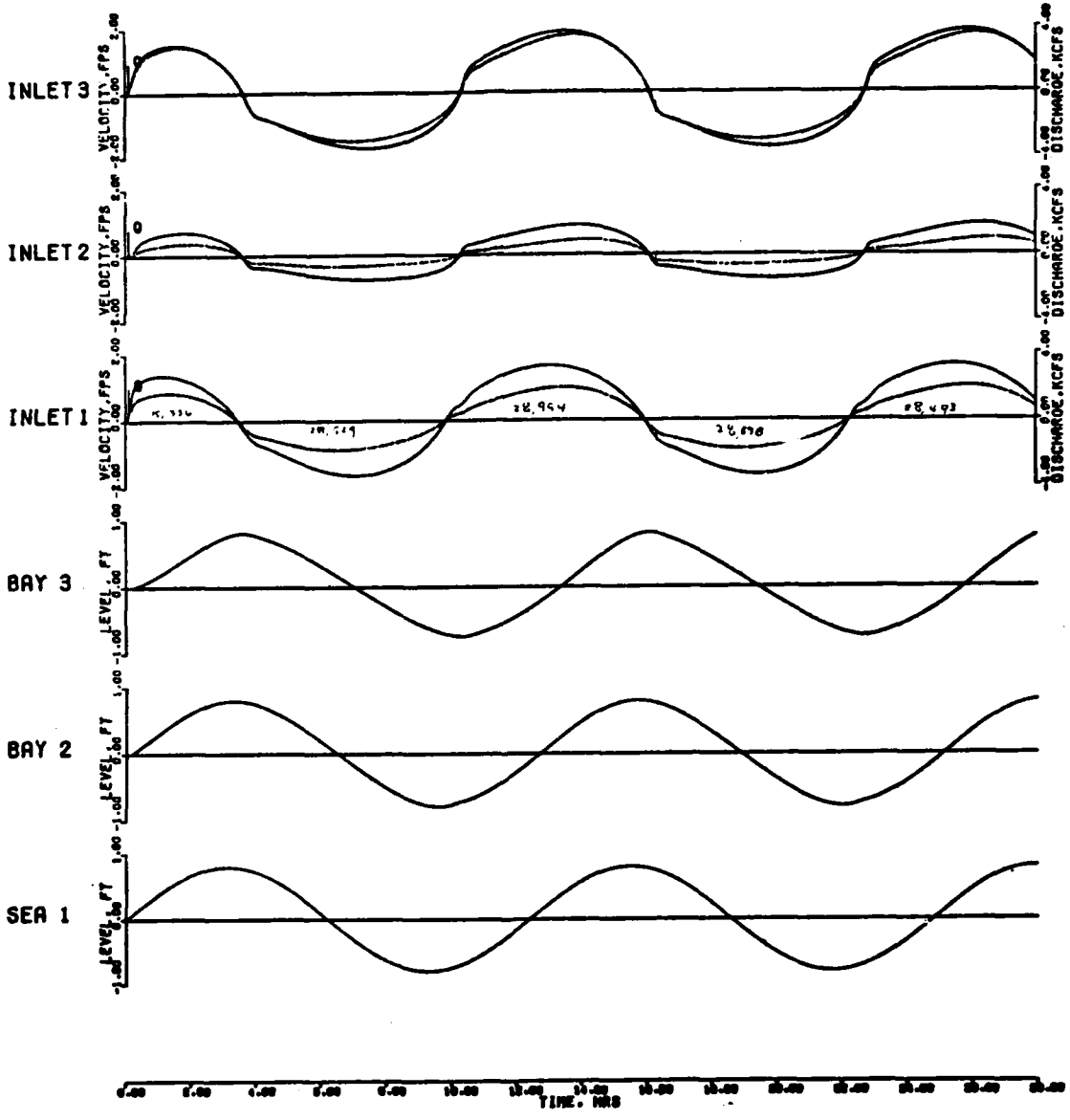

Figure G3. Configuration C1J2

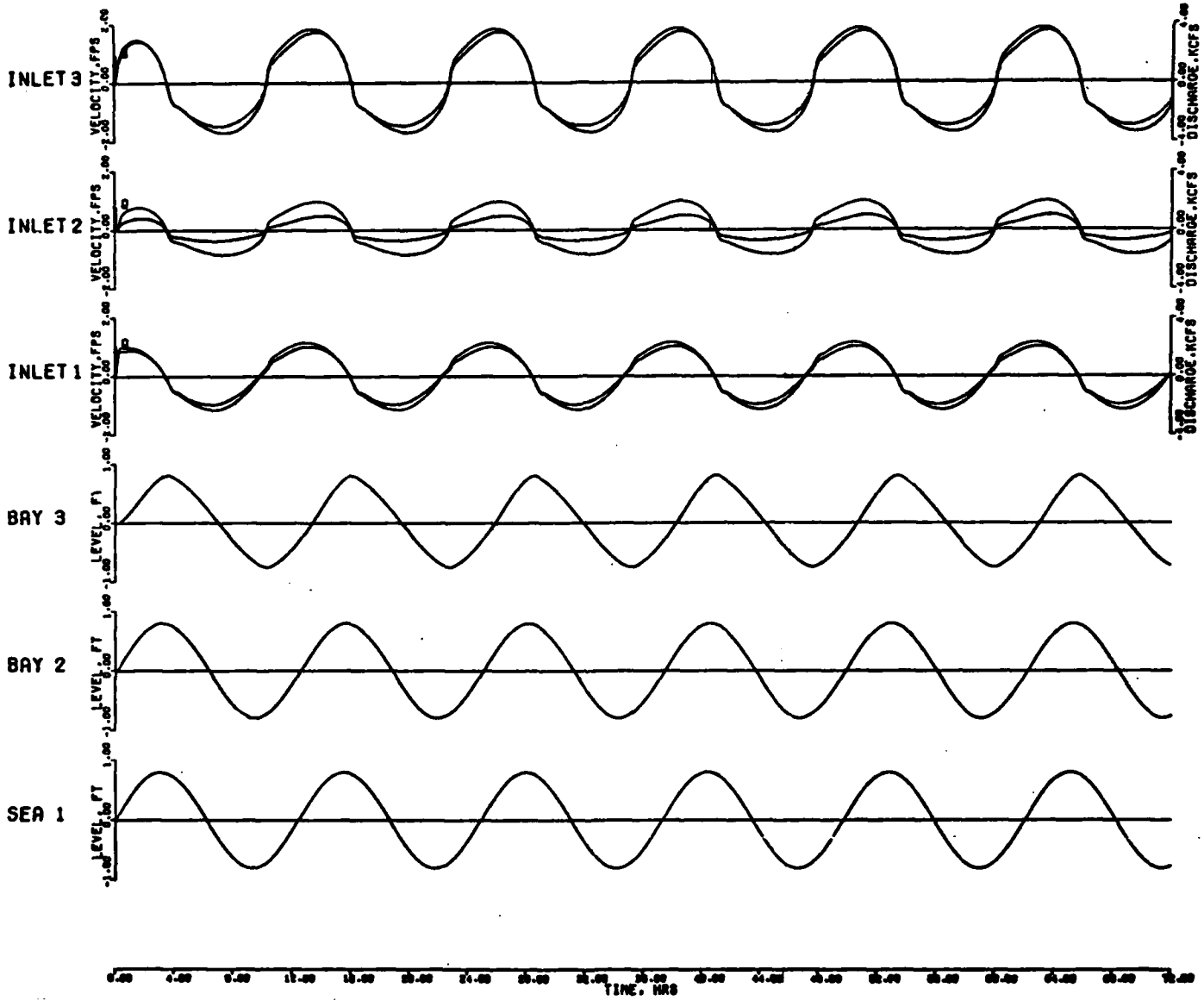

Figure G4. Configuration C2J1

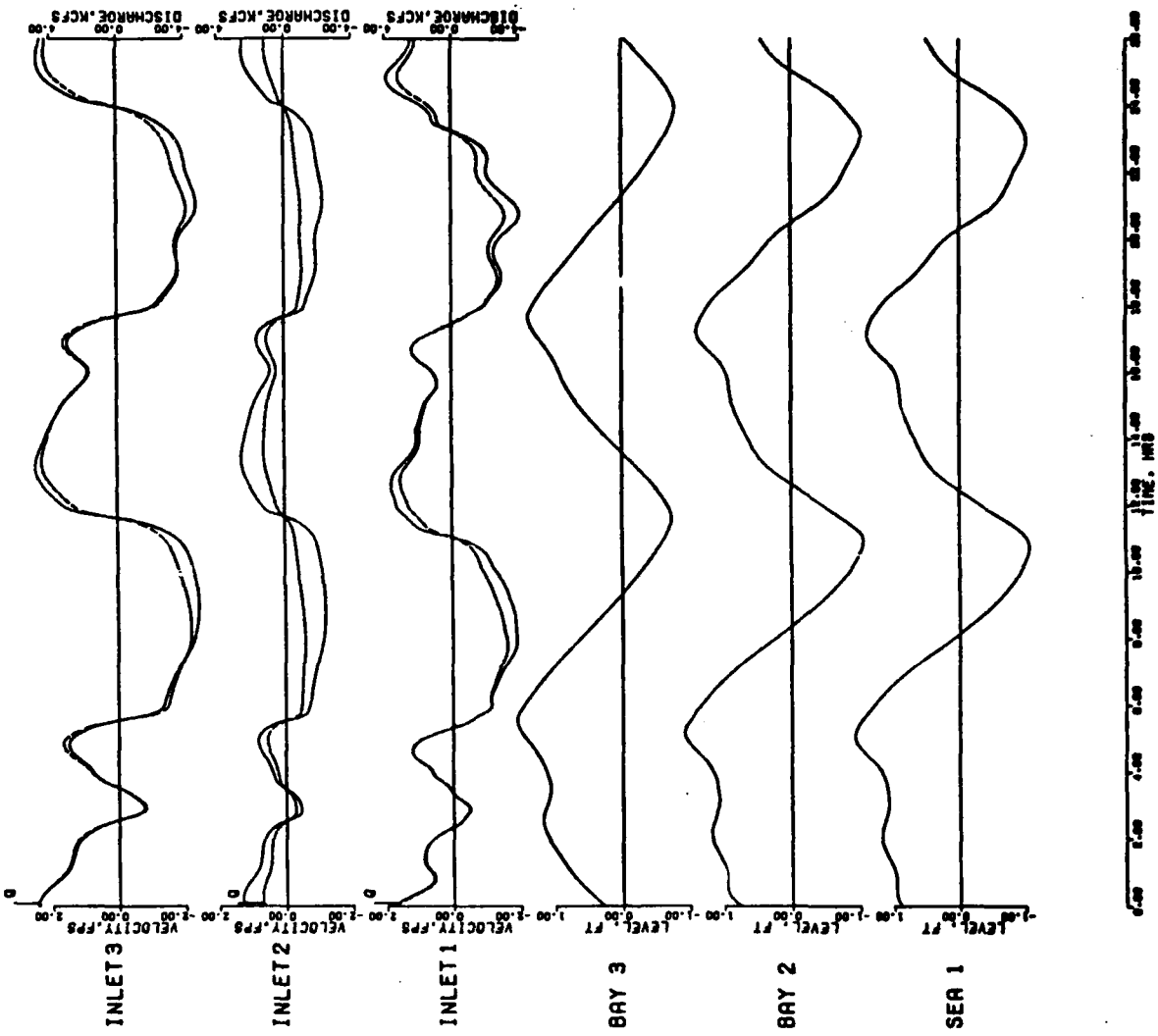

Figure G5. Configuration C2J2

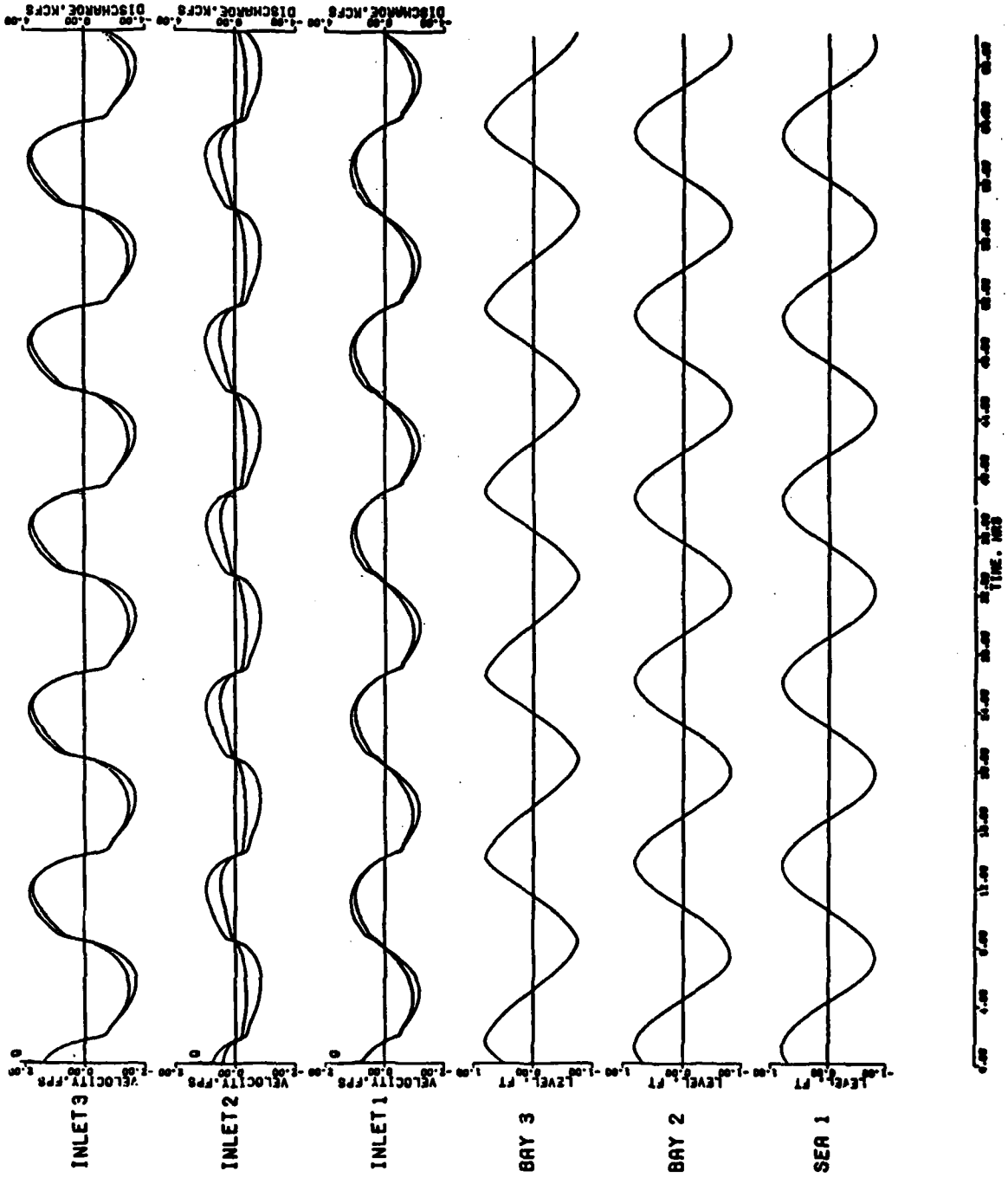

Figure G6. Configuration C3J1

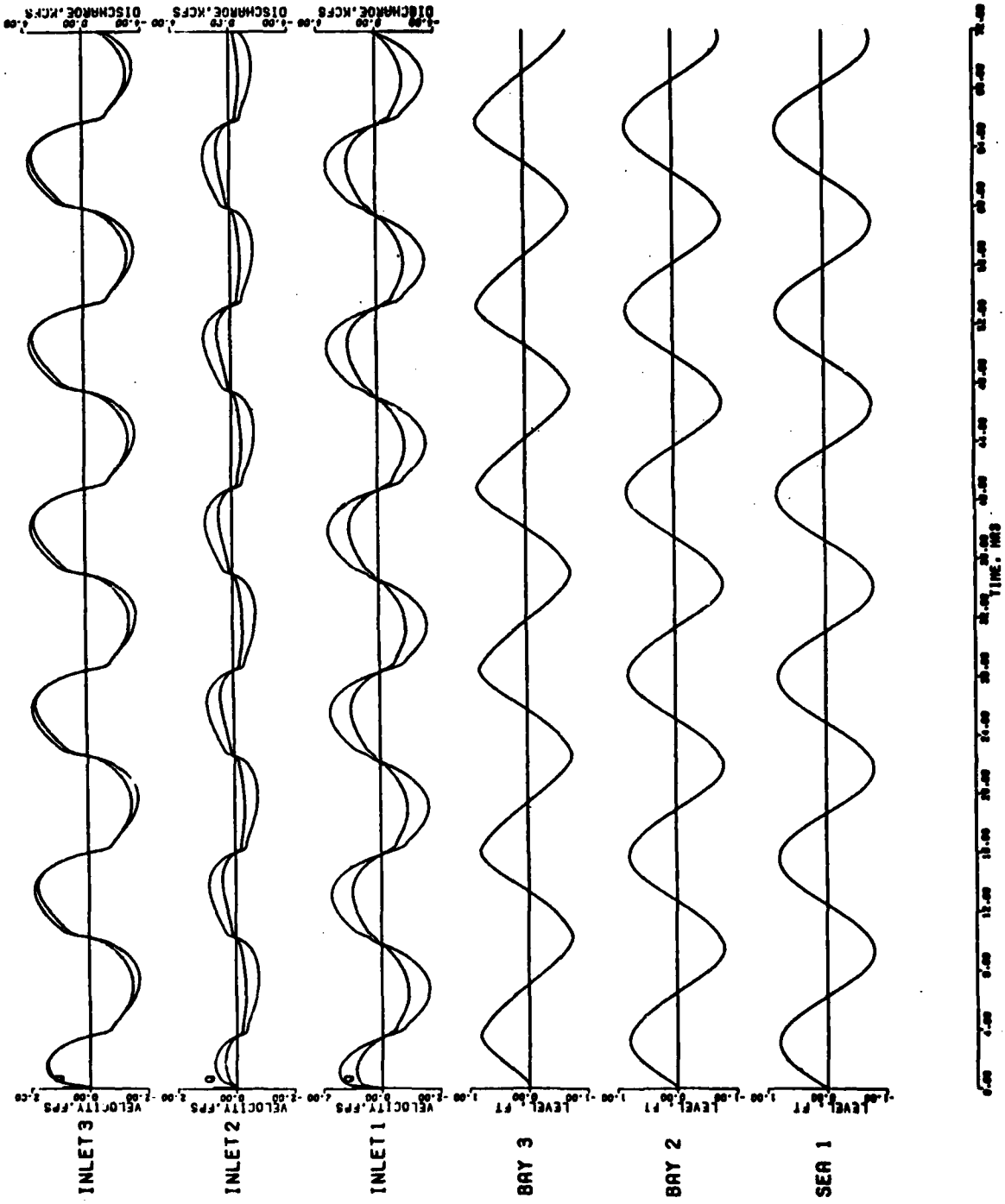

Figure G7. Configuration C3J2

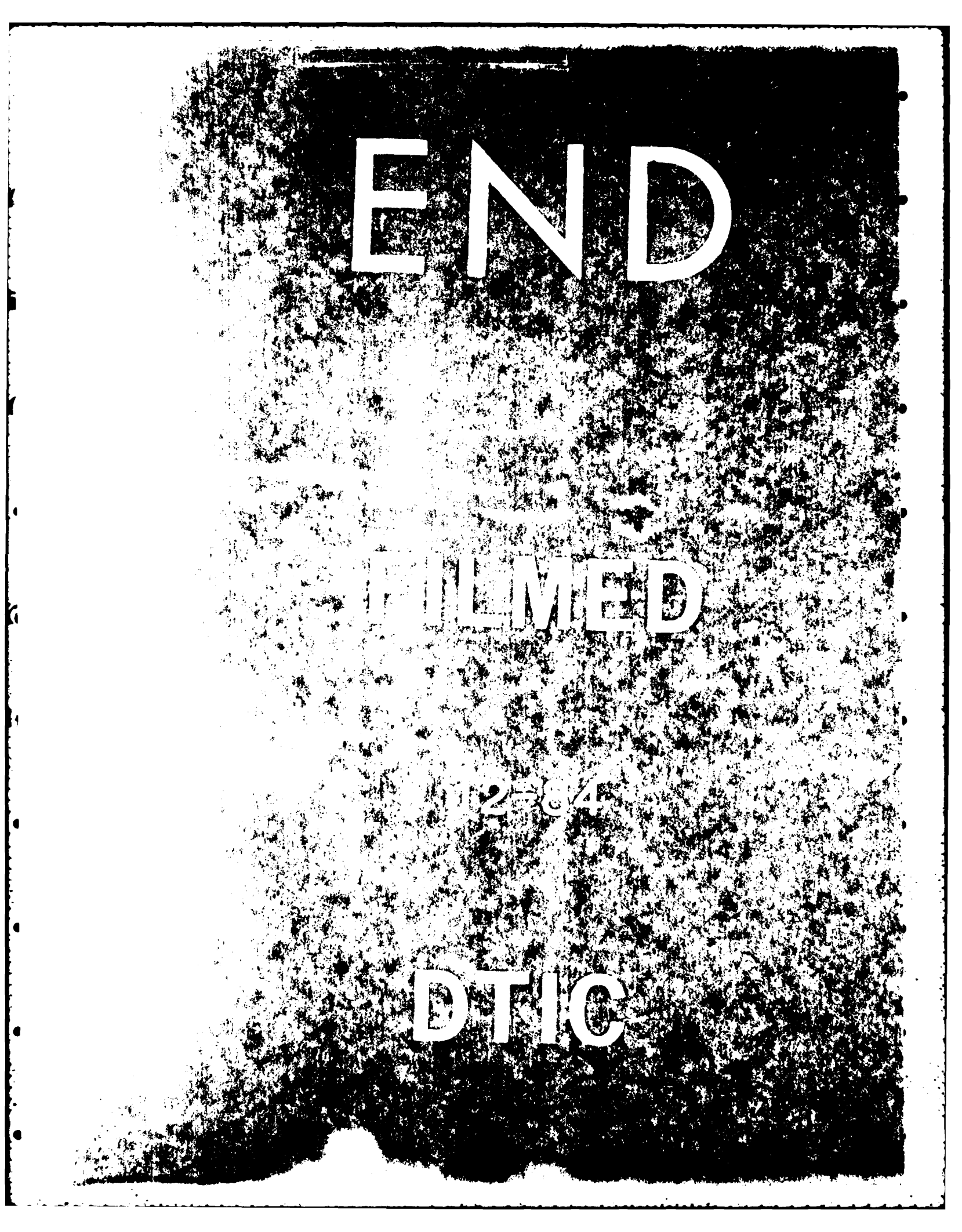
END
LMED
DTIC